



MSU

OVERDUE FINES ARE 25¢ PER DAY
PER ITEM

Return to book drop to remove
this checkout from your record.

--

© 1979

INACIO MARIA DAL FABBRO

ALL RIGHTS RESERVED

STRAIN FAILURE OF APPLE MATERIAL

By

Inacio Maria Dal Fabbro

A DISSERTATION

Submitted to
Michigan State University
in partial fulfillment of the requirements
for the degree of

DOCTOR OF PHILOSOPHY

Department of Agricultural Engineering

1979

ABSTRACT

STRAIN FAILURE OF APPLE MATERIAL

By

Inacio Maria Dal Fabbro

The objective of this work was to define a failure criteria for apple material. Cylindrical apple specimens were tested under uniaxial and triaxial state of stress and stress rate controlled uniaxial loading. Cubic apple specimens were subjected to uniaxial, biaxial and triaxial states of stress.

Linear elastic and viscoelastic material properties were used to calculate the stress and strain components within the apple flesh.

Uniaxial loading of cylindrical specimens showed that normal stress at failure varied for different strain rates. This eliminated the maximum normal stress failure criteria. Triaxial loading of cylindrical specimens indicated that maximum shear stress and normal stress at failure vary for different levels of cylindrical stress. Failure was also observed at zero maximum shear stress, which excludes the maximum shear stress failure criteria. Uniaxial, biaxial and rigid die loading of cubic and cylindrical specimens also excluded the maximum normal stress failure criteria.

Stress rate controlled uniaxial loading showed significant variations of normal stress at failure which again discarded the maximum normal stress failure criteria. Experimental results from these tests indicated that the maximum normal strain at failure remained relatively constant for all the loading situations. Total strain energy and its spherical and deviatoric components obtained from stress and strain values calculated from the linear elastic and viscoelastic theories exhibit significant variations. This eliminates the strain energies failure criterium.

A non-linear viscoelastic formulation was proposed for apple material based on the convected derivative representation for the time derivative appearing in the linear viscoelastic equations.

The most significant conclusion of this research is that apple material fails when the normal strain reaches a critical value.

Approved Larry Segerlind
Major Professor

Approved E.R. Haldeman
Department Chairman

ACKNOWLEDGMENTS

The author sincerely appreciates the kindly cooperation and guidance of Dr. Larry J. Segerlind (Agricultural Engineering) during the development of this research work.

Appreciation is extended to Professor Ernest H. Kidder, Dr. George E. Merva, Dr. Haruhiko Murase (Agricultural Engineering), and Dr. Jayaraman Krishnamurthy (Chemical Engineering) for suggestions and particular discussions.

The author is particularly indebted to the Department of Agricultural Engineering for assistance and for the general cooperation of its faculty, staff, and graduate students.

Special sincere gratitude to Dr. Joalice M. G. Bueno Dal Fabbro (my wife) and her parents whose efforts made this work possible.

To my parents, brothers, and sisters, I leave my deepest gratitude.

TABLE OF CONTENTS

	Page
LIST OF TABLES.	vi
LIST OF FIGURES	x
LIST OF SYMBOLSxii
 CHAPTERS	
I INTRODUCTION.	1
II LITERATURE REVIEW	3
2.1 General Remarks.	3
2.2 Elastic Behavior of Vegetative Material.	3
2.3 Linear Viscoelastic Behavior of Vegetative Material.	5
2.4 Failure Criteria	7
2.5 Summary.	10
III FAILURE THEORIES.	11
3.1 General Remarks.	11
3.2 The Haigh-Westergaard Hyper-space.	12
3.3 Stress Conditions.	17
3.3.1 Maximum normal stress theory.	17
3.3.2 Maximum shear stress theory	18
3.3.3 Modified maximum shear stress theory.	18
3.3.4 Internal friction theory.	19
3.4 Strain Conditions.	19
3.4.1 Maximum strain theory	19
3.4.2 Maximum shearing strain theory.	20
3.5 Energy Conditions.	20
3.5.1 Constant total strain energy theory.	20
3.5.2 Energy of distortion theory	20
3.5.3 Combined total strain energy and distortion energy theory.	21
3.5.4 Modified energy of distortion theory.	21

CHAPTER	Page
IV BASIC THEORY.	24
4.1 General Remarks.	24
4.2 The Strain Energy Stored in an Apple Specimen for Different Loading Situations	24
4.3 Maximum Shear Stress Conditions.	26
4.4 The Linear Elastic Model	27
4.5 The General Viscoelastic Model	28
4.6 Stress Controlled Uniaxial Loading	32
4.7 The Non-linear Viscoelastic Formulation for Apple Material	32
4.7.1 The convected derivative of a covariant strain tensor	34
V EXPERIMENTAL PROCEDURE.	36
5.1 General Remarks.	36
5.2 Apple Selection and Storage.	38
5.3 Specimen Preparation	38
5.4 Uniaxial Loading of Cylindrical Specimens at Different Strain Rates.	38
5.5 Uniaxial Loading of Cylindrical Specimens of Different Height at a Constant Strain Rate.	39
5.6 Triaxial Loading of Cylindrical Specimens at a Constant Strain Rate, and Different Radial Stresses.	39
5.7 Rigid Die Loading of Cylindrical Apple Specimens.	41
5.8 Uniaxial Loading of Cubic Specimens at a Constant Strain Rate	43
5.9 Biaxial Loading of Cubic Specimens at a Constant Strain Rate	43
5.10 Rigid Die Loading of Cubic Specimens	45
5.11 Stress Rate Controlled Loading of Cylindrical Specimens of Red Delicious.	45
VI RESULTS AND DISCUSSION.	47
6.1 General Remarks.	47
6.2 Uniaxial Loading of Cylindrical Specimens at Different Strain Rates.	48
6.3 Triaxial Loading of Cylindrical Apple Specimens.	54
6.4 Uniaxial, Biaxial and Rigid Die Loading of Cubic Specimens. Uniaxial and Rigid Die Loading of Cylindrical Specimens.	60
6.5 Stress Controlled Loading of Cylindrical Specimens of Red Delicious	70

CHAPTER	Page
6.6 The Non-linear Viscoelastic Formulation for Apple Material	70
6.7 Summary.	73
VII SUMMARY AND CONCLUSIONS	75
VIII SUGGESTIONS FOR FUTURE RESEARCH	77
REFERENCES.	79
APPENDICES.	87

LIST OF TABLES

Table	Page
5.1 Tests carried on apple material. Imposed strain rates and radial stresses. Shape and dimensions of the specimens	37
6.1 Uniaxial loading of cylindrical apple specimens for different strain rates. Average values and standard deviations of stress, strain and time at failure	49
6.2 Uniaxial loading of cylindrical specimens of red delicious at different strain rates. strain energy components obtained from experimental values of σ_{11} and ϵ_{11} and calculated values of ϵ_{22} . Maximum shear stress obtained from experimental data and values of ϵ_{22} calculated from the elastic and viscoelastic theories	50
6.3 Triaxial loading of cylindrical apple specimens for different radial stresses and constant strain rate. Average values of time, axial stress and strain at failure.	55
6.4 Triaxial loading of cylindrical specimens of Red Delicious at different radial stress. Strain energy components obtained from experimental values of σ_{11} and calculated values of ϵ_{22} . Maximum shear stress obtained from experimental data and values of ϵ_{22} calculated from elastic and viscoelastic theories	56
6.5 Rigid die loading of cylindrical (1) and cubic (4) specimens, uniaxial (2) and biaxial (3) loadings of cubic specimens of apple values. Average and standard deviations of stress, strain and time at failure.	61

6.6	Uniaxial (1), biaxial (2) and rigid die loadings (3) of cubic specimens. Rigid die loading of cylindrical specimens (4). Axial stress and strain, lateral or radial stress and strain and energy components obtained from elastic and viscoelastic theories. . . .	62
6.7	Creep loading of cylindrical specimens of Red Delicious. Calculated values strain energy components and experimental values of axial stress. Strain and maximum shear stress at failure	63
6.8	Uniaxial loading of cylindrical apple specimens. Average values and standard deviations of deformation at $\sigma_{11} = -0.11$ Mpa .	64
6.9	Uniaxial loading of cylindrical apple specimens of different height. Axial strain and stress at $\sigma_{11} = -0.11$ MPa for McIntosh (1), Jonathan (2), and Red Delicious (3)	65
A1	Stress, strain and time at failure for uniaxial loading of cylindrical specimens of apple. $\dot{\epsilon}_{11} = -0.002 \text{ sec}^{-1}$. . .	87
A2	Stress, strain and time at failure for uniaxial loading of cylindrical specimens of apple. $\dot{\epsilon}_{11} = -0.007 \text{ sec}^{-1}$. . .	87
A3	Stress, strain and time at failure for uniaxial loading of cylindrical specimens of apple. $\dot{\epsilon}_{11} = -0.017 \text{ sec}^{-1}$. . .	88
A4	Stress, strain and time at failure for uniaxial loading of cylindrical specimens of apple. $\dot{\epsilon}_{11} = -0.035 \text{ sec}^{-1}$. . .	88
A5	Stress, strain and time at failure for uniaxial loading of cylindrical specimens of apple. $\dot{\epsilon}_{11} = -0.069 \text{ sec}^{-1}$. . .	89
A6	Stress, strain and time at failure for uniaxial loading of cylindrical specimens of apple. $\dot{\epsilon}_{11} = -0.173 \text{ sec}^{-1}$. . .	89
A7	Stress, strain and time at failure for uniaxial loading of cylindrical specimens of apple. $\dot{\epsilon}_{11} = -0.345 \text{ sec}^{-1}$. . .	90

Table	Page
A8 Stress, strain and time at failure for triaxial loading of cylindrical specimens of apple. $\dot{\epsilon}_{11} = -0.007 \text{ sec}^{-1}$, $\sigma_{22} = 0.000 \text{ MPa}$	90
A9 Stress, strain and time at failure for triaxial loading of cylindrical specimens of apple. $\dot{\epsilon}_{11} = -0.007 \text{ sec}^{-1}$, $\sigma_{22} = -0.069 \text{ MPa}$	91
A10 Stress, strain and time at failure for triaxial loading of cylindrical specimens of apple. $\dot{\epsilon}_{11} = -0.007 \text{ sec}^{-1}$, $\sigma_{22} = -0.138 \text{ MPa}$	91
A11 Stress, strain and time at failure for triaxial loading of cylindrical specimens of apple. $\dot{\epsilon}_{11} = -0.007 \text{ sec}^{-1}$, $\sigma_{22} = -0.207 \text{ MPa}$	92
A12 Stress, strain and time at failure for triaxial loading of cylindrical specimens of apple. $\dot{\epsilon}_{11} = -0.007 \text{ sec}^{-1}$, $\sigma_{22} = -0.276 \text{ MPa}$	92
A13 Stress, strain and time at failure for triaxial loading of cylindrical specimens of apple. $\dot{\epsilon}_{11} = -0.007 \text{ sec}^{-1}$, $\sigma_{22} = -0.395 \text{ MPa}$	93
A14 Stress, strain and time at failure for loading in rigid die of cylindrical apple specimens. $\dot{\epsilon}_{11} = -0.007 \text{ sec}^{-1}$	93
A15 Stress, strain and time at failure for uniaxial loading of cubic apple specimens. $\dot{\epsilon}_{11} = -0.007 \text{ sec}^{-1}$	94
A16 Stress, strain and time at failure for biaxial loading of cubic apple specimens. $\dot{\epsilon}_{11} = -0.007 \text{ sec}^{-1}$	94
A17 Stress, strain and time at failure for loading in rigid die of cubic apple specimens. $\dot{\epsilon}_{11} = -0.007 \text{ sec}^{-1}$	95
A18 Uniaxial compression of cylindrical specimens of McIntosh. Axial deformation values at $\sigma_{11} = -0.11 \text{ MPa}$ for five specimen height. $\dot{\epsilon}_{11} = -0.007 \text{ sec}^{-1}$	96

A19	Uniaxial compression of cylindrical specimens of Jonathan. Axial deformation values at $\sigma_{11} = -0.11$ MPa for five specimen height. $\dot{\epsilon}_{11} = -0.007 \text{ sec}^{-1}$. . .	97
A20	Uniaxial compression of cylindrical specimens of Red Delicious. Axial deformation values TA $\sigma_{11} = -0.11$ MPa for five specimen height. $\dot{\epsilon}_{11} = -0.007 \text{ sec}^{-1}$	98

LIST OF FIGURES

Figure	Page
3.1 The Haigh-Westergaard hyper-space	14
3.2 Yield locus for an isotropic material which does not exhibit Bauschinger effect (Hill, 1964)	16
5.1 Triaxial loading device, showing the longitudinal cross-sectional view (a) and top view (b).	40
5.2 Top (a) and longitudinal cross-sectional view (b) of the device for loading of cylindrical specimens in rigid die.	42
5.3 Exploded view of the device used for biaxial and rigid loading of cubic specimens.	44
5.4 Creep loading apparatus	46
6.1 Stress at failure versus strain rate for uniaxial loading of cylindrical apple specimens	51
6.2 Strain at failure versus strain rate for uniaxial loading of cylindrical apple specimens	52
6.3 Time versus strain rate for uniaxial loading of cylindrical apple specimens.	53
6.4 Axial stress at failure versus radial stress for triaxial loading of cylindrical apple specimens	57
6.5 Strain at failure versus radial stress for triaxial loading of cylindrical apple specimens	58
6.6 Time at failure versus radial stress for triaxial loading of cylindrical apple specimens	59

Figure	Page
6.7 Stress at failure for controlled stress rate loading of cylindrical specimens of Red Delicious.	66
6.8 Strain at failure versus stress rate for controlled stress rate of Red Delicious . . .	67
6.9 Deformation values of cylindrical apple specimens of different height at constant axial stress value during uniaxial loading.	68
6.10 Strain values of cylindrical apple specimens of different height at constant stress values during uniaxial loading.	69

LIST OF SYMBOLS

A	Cross sectional area	mm ²
D	Diameter	mm
L	Side	mm
H	Height	mm
σ_{ij}	Stress tensor	MPa
ϵ_{ij}	Strain tensor	mm/mm
U_1	Deformation vector	mm
$\dot{\epsilon}_{ij}$	Strain rate tensor	sec ⁻¹
X_i	Cartesian coordinate system	
$v_{,i}^k$	Gradient velocity along X_i axis	mm/mm sec
v^k	Velocity along X_i axis	mm/sec
$\partial/\partial t$	Partial derivative with respect to time	
D/Dt	Convected derivative with respect to time	
$\dot{\epsilon}_{ij}^*$	Convected strain rate tensor	sec ⁻¹
t	Time	sec
S_{ij}	Deviatoric stress tensor	MPa
e_{ij}	Deviatoric strain tensor	mm/mm
U	Total strain energy	Joules
Ud	Deviatoric component of the strain energy	Joules

U_s	Spherical component of the strain energy	Joules
τ_{\max}	Maximum shear stress	MPa
σ_{III}	Maximum absolute value of the principal stress tensor	MPa
σ_I	Minimum absolute value of the principle stress tensor	MPa
$\dot{\sigma}_{ij}$	Stress rate tensor	MPa/sec
$\dot{\sigma}$	Constant of the linear stress rate function	
E	Modulus of elasticity	MPa
K	Bulk modulus	MPa
G	Shear modulus	MPa
ν	Poisson's ratio	
λ	Lame's constant	
s	Laplace parameter	
$F(\sigma_m)$	Function of mean stress	
σ_m	Mean stress	MPa
$G_1(t)$	Time dependent shear modulus	MPa
$G_2(t)$	Time dependent bulk modulus	MPa
$E(t)$	Uniaxial relaxation function	MPa
$X(t)$	Constrained relaxation function	MPa
$\nu(t)$	Time dependent Poisson's ratio	
ψ	Lode's parameter	
σ_{ot}	Tensile yielding stress	MPa
σ_{oc}	Compression yielding stress	MPa
σ_o	Yielding stress	MPa

J_2, J_3	Invariants of the stress deviator	MPa
c, b	Constants of proportionality	
ϵ_{II}	Medium absolute value of the principal strain tensor	mm/mm
ϵ_I	Minimum absolute value of the principal strain tensor	mm/mm
ϵ_m	Mean strain	mm/mm

CHAPTER I
INTRODUCTION

Bruising is a major problem in the development of new machines for the mechanical harvesting and handling of large quantities of fruits. Bruising is the rupture of the tissue and consequent exposure of the cell sap. The oxidation of the cell sap gives a darkened color to the softened tissue. This undesirable phenomenon is somehow related to the mechanical loading of the fruit. The knowledge of the fruit tissue response to known loadings may provide the basis of bruise prediction when the fruit is subjected to other loading conditions.

Many investigators have studied the mechanical properties of apple tissue through a very broad theoretical formulation bringing about non-specific results. It would be reasonable to say that the overall objective of the majority of the research work conducted on apple tissue was to identify its mechanical behavior.

Little of the relevant work on the mechanical properties of apples has been directed toward establishing the failure parameters of apple tissue. The failure phenomenon is believed to be an indicator of bruise occurrence. It means that a bruise is the result of a tissue failure. This

implies that bruises can be predicted in terms of failure parameters. Before this problem can be solved, it is necessary to define failure. Failure by yielding or by fracture may occur beyond the elastic limit for common engineering materials (Juvinall, 1967). Vegetative materials exhibit a rupture point close to the elastic limit, which has been referred to as the bio-yielding point (Mohsenin, 1970). The parameters correlated to the bio-yielding point of apple flesh can be studied by imposing different loading conditions on apple specimens.

The specific objective of this study was to establish the parameters involved in the failure of apple material.

CHAPTER II

LITERATURE REVIEW

2.1 General Remarks

Research on the mechanical behavior of vegetative material has as one objective the minimization of bruise damage. Material property determination and a stress-strain analysis seem to be the steps toward complete information on failure parameters. Vegetative material has been generally considered either as an isotropic continuous medium or as a multi-phase medium (Akyurt, 1969; Brusewitz, 1969; Gustafson, 1974; Murase, 1977). Elastic and viscoelastic models had been used to represent the mechanical response to a variety of loading conditions. Mohsenin (1971) cites ample literature on the importance of mechanical properties of agricultural products and the need for study and research in this area.

2.2 Elastic Behavior of Vegetative Material

Determination of elastic constants is a frequent subject of research due to the need for basic information on material properties. Modulus of elasticity, bulk modulus, and elastic Poisson's ratio have been determined on cylindrical and whole specimens of potato by uniaxial and hydrostatic compression (Finney, 1963; Finney and Hall, 1968). Modulus of elasticity

can also be determined by radial compression of cylindrical specimens (Sherif et al., 1976). Bulk compression tests directly obtaining the bulk modulus and the calculation of Poisson's ratio yielded reliable results for fruits (White and Mohsenin, 1967). Elastic Poisson's ratio and elastic uniaxial modulus can be simultaneously determined from elastic bulk modulus and Boussinesq solution for cylindrical plunger on a half-space (Morrow, 1965). Elastic Poisson's ratio can also be determined by comparing the axial force-deformation on free and restrained cylindrical specimens of apple (Hughes and Segerlind, 1972). Results from radial compression loading of cylindrical specimens can be interpreted using Hertz contact theory to obtain values for the modulus of elasticity (Snobar, 1973). Bulk modulus of a whole-apple specimen can be determined by considering the principle of buoyancy (Chen and Lam, 1975).

The stress and strain distribution in an elastic body is also of practical interest for further study on bruise location. Plate and plunger tests have been conducted on whole specimens of peaches and pears correlating deformation and stress distributions with those predicted by elastic models (Fridley et al., 1968). Stress and strain distributions on apples under static axi-symmetric load are similar to those in an elastic sphere subjected to the same conditions (Apaclla, 1973). Potatoes have been considered a nearly incompressible non-linear elastic material to analyze the stress distribution in hemi-spherical

specimens (Sherif, 1976).

In recent years a more complex approach has started to replace the elastic theory for describing fruits and vegetables. Vegetative material is now considered as a multi-phase medium, having gas, solid, and liquid components (Akyurt, 1969; Gustafson, 1974). A finite element method is then used to obtain strain and stress distributions in spherical bodies under axisymmetric conditions (Gustafson, 1974). Potato tissue was viewed as an interacting combination of solid and liquid phases in determining material properties (Brusewitz, 1969). Cellular and intercellular spaces were interpreted as porous and solid-liquid media (Murase, 1977). Linear elastic stress and strain constitutive equations were then derived, analogous to Duhamel's relations (Murase, 1977).

2.3 Linear Viscoelastic Behavior of Vegetative Material

Many experimental investigations have indicated a time dependency of the mechanical behavior of plant tissue. Strain rate affects the response to an impact test in biological materials (Zoerb, 1958). The mechanical damage of potatoes subjected to compressive loads is highly affected by strain rate (Finney, 1963). Non-linear viscoelastic behavior of apples was reported by Morrow and Mohsenin (1966) who approximated it by linear constitutive relations. The stress dependence of material properties of apple material made it impossible to accept a linear approximation (Chappell and Hamann, 1968). Further works have dealt with the

non-linear behavior of apple tissue, but the results were interpreted by linear viscoelastic relations (Hamann, 1967, 1970). Tensile tests conducted on apple skin suggested a viscoelastic behavior (Clevenger and Hamann, 1968). The viscoelastic Poisson's ratio can be determined indirectly from the elastic Poisson's ratio constant by the correspondence principle (DeBaerdemaeker, 1975). Time dependence of Poisson's ratio was directly noted by measuring lateral and axial displacement of cylindrical specimens (Chappell and Hamann, 1968). Similar results have been reported from tests carried out on sweet potatoes (Hammerle and McClure, 1970).

Relaxation functions can be determined by bulk and uniaxial loading (Morrow and Mohsenin, 1966). Similarly, creep functions were determined by applying hydrostatic loads to whole specimens (Morrow, 1965, and Sharma, 1970). Uniaxial loading of cylindrical specimens was reported to yield reliable results for relaxation functions (Finney, 1963; Chappell and Hamann, 1968; Morrow et al., 1971; Hammerle et al., 1971). Bulk and shear relaxation functions were experimentally determined for apple tissue and the results were used in a viscoelastic sphere loaded by a flat surface (DeBaerdemaeker, 1975). Rumsey and Fridley (1974) assumed constant bulk modulus and time dependent shear relaxation function. Dynamic methods had also been used to determine viscoelastic properties of biological material (Morrow and Mohsenin, 1968).

The parameters of a generalized Maxwell model have been experimentally determined for several different fruits and vegetables (Mohsenin, 1970; Hammerle and Mohsenin, 1970; Chen and Fridley, 1972). Results from bulk loading of apples were compared with a simple Kelvin model to obtain an expression for the creep function. The relationship between the complex moduli and the relaxation functions can be used to calculate the dynamic relaxation and shear relaxation functions from experimental results (Hamann, 1969). Force and deformation dependence on strain rate was reported by Mohsenin et al. (1963).

Creep behavior of papaya was determined under dead load conditions imposed by parallel plates (Wang and Chang, 1969). A viscoelastic stress-strain analysis is the next step once the basic time dependent properties have been determined. A simple Maxwell model can be used to represent the response of two viscoelastic spheres falling onto one another (Hamann, 1970). The viscoelastic sphere subjected to a contact load can be experimentally studied and numerically simulated (DeBaerdemaeker, 1975). Vibration analysis in a non-uniform viscoelastic beam has been used to predict the stress-strain distribution in tomato blossoms subjected to similar conditions (De Tar, 1971).

2.4 Failure Criteria

One objective of research conducted on the mechanical behavior of vegetative material is to minimize bruise occurrence. Determination of elastic constants and viscoelastic

functions is performed to obtain the constitutive laws for the material. The material properties are needed in order that the stress resulting when external loads are applied to the fruit can be calculated.

Impact testing has been used to determine whether a bruise occurs because of the maximum energy absorbed, the maximum stress applied, or the maximum deformation (Mattus et al., 1960). In this sense it was found that the energy required for bruising was greater under impact conditions than under quasi-static loading conditions (Mohsenin and Gohlich, 1962; Mohsenin et al., 1965; Nelson et al., 1968; Fridley et al., 1964) for apples and peaches. However, for pears and sweet potatoes, it requires more bruising energy under quasi-static loading (Wright and Splinter, 1968; Fridley and Adrian, 1966). Apple-limb impact and its influence in the bruising of apples was investigated by David and Rehkugler (1971). The impact of apples on cushioning material was studied by Hammerle and Mohsenin, 1966; Simpson and Rehkugler, 1972. Results from impact tests on whole specimens did not reveal any dominance of the force or energy parameter (Fluck and Ahmed, 1972). Analysis of bruise location indicates a strong possibility of bruise occurrence at maximum shear stress (Fridley and Adrian, 1966). Bruising in peaches due to impact loading can be modeled by applying similar conditions to an elastic sphere (Horsfield et al., 1972). The problem of potato cracking during handling was experimentally studied using tensile tests (Huff, 1967).

However, impact tests had been extensively carried out (Finney, 1963; Park, 1963). Flat plate loading of hemispherical specimens of apple and potato have indicated the existence of maximum shear stress near the contact region as well as a tensile stress at the circular boundary of the contact region (DeBaerdemaeker, 1975; Sherif, 1976). There is also indication of a maximum tensile stress or combination of this and shear stress near the center of the white potato (Sherif, 1976). Bruises in peaches may occur at the maximum shear stress on the axis of symmetry (Sherif, 1976). White potatoes and peaches did not fail until large displacements had taken place (Sherif, 1976). Failure strength of apples, referred to as the bio-yield point, have been determined by indenter test as well as by plunger and uniaxial ramp-loading of cylindrical specimens (Van Lancker et al., 1975). Bruise energy of peaches and apples can be evaluated by measuring the rebounding force in an impact test (Diener et al., 1977). Attempts have been made in correlating bruise occurrence location to mechanical, thermal, and electrical properties of apples (Holcomb et al., 1977). Tensile strength of potato and apple tissues increases with increasing water potential levels. The compressive strength of these products, however, decreases with increasing water potential (DeBaerdemaeker et al., 1978).

Maximum shear stress was reported to be the failure parameter of apple flesh (Miles, 1971). Cylindrical specimens of apple were subjected to several levels of hydrostatic

stress superimposed on a uniaxial loading. Failure depended on loading rate and confining pressure; those parameters, however, act independently (Miles, 1971).

2.5 Summary

Material properties and stress-strain analysis have been used to characterize the mechanical behavior of vegetative bodies. The literature discloses a significant amount of research starting from simple assumptions such as a continuous isotropic medium and linear elastic behavior, extending into multi-phase medium, linear viscoelastic, and non-linear elastic behavior. Nevertheless, the failure parameters for a vegetative material have not yet been determined.

The triaxial loading of cylindrical specimens (Miles, 1971) can be considered the best attempt toward the determination of failure criteria. In spite of time dependent non-linearities that had been noticed (Hamann, 1967, 1970), no investigation had been reported which assumed non-linear viscoelastic behavior.

CHAPTER III

FAILURE THEORIES

3.1 General Remarks

The limit of the elastic behavior of a body is determined by the existing state of stress, as well as by its material properties. Beyond this limit the material may suffer permanent deformations or fail by fracture. It is commonly agreed that vegetative materials have a rupture point very close to the elastic limit without experiencing any plastic deformations (Mohsenin, 1970). In such conditions, failure, yielding, or rupture would have nearly identical meanings.

Earlier investigators have attempted to formulate generic yield criteria for metals assuming homogeneous and isotropic condition (Prager, 1942). Some of those theories predict failure under hydrostatic stress conditions (Nadai, 1950). Loading tests conducted on specimens of solid material under high hydrostatic stress did not result in failure (Nadai, 1950). The assumption that hydrostatic loads do not cause failure has a purely experimental basis (Mendelson, 1965). Theories which do not assume failure under pure hydrostatic loads have been modified to fit experimental data from triaxial loading of soil specimens

(Bishop and Henkel, 1962). Those extended theories assume a contribution of hydrostatic stresses on failing soil specimens (Terzaghi and Peck, 1967).

Non-homogeneous materials can exhibit different values for tensile yield stress and compressive yield stress. Under that condition the difficulties in obtaining tensile yield stress values for vegetative materials is the major obstacle in making full use of theories which can account for differences between compressive and tensile yield values.

Existing failure criteria by yielding can be formulated in terms of stress, strain, or energy considerations.

The theories of failure mentioned and their discussion in this chapter by no means exhaust the available literature. Only those topics pertinent to the present study are included.

3.2 The Haigh-Westergaard Hyper-space

Failure theories can be generalized by considering the complete state of stress at a point. Since the stress tensor is symmetric, it is possible to describe yielding as a function of the six independent stress components (Mendelson, 1965). For a material specimen loaded to yield, this function can be written as follows (Prager, 1942):

$$F(\sigma_{ij}) = 0 \quad (3.1)$$

Equation (3.1) represents a hypersurface in the six-dimensional stress space formed by yield points. In other words, any point inside of this solid figure represents an elastic state and all the points located on the surface

represent the beginning of the plastic deformation or failure (Nadai, 1931). If isotropy is assumed, the rotation of axis will not affect yielding and equation (3.1) would be written in terms of principal stresses, as

$$F(\sigma_{11}, \sigma_{22}, \sigma_{33}) = 0 \quad (3.2)$$

Furthermore, since hydrostatic stresses do not affect yielding, the yielding function can be expressed in terms of stress deviators. Since the stress deviators can be written in terms of the invariants, the yielding function can also be expressed in terms of invariants of the stress deviator, as follows

$$F(J_2, J_3) = 0 \quad (3.3)$$

Equation (3.3) is symmetric in the principle axis which indicates that all principle stresses are equally important to the yield condition (Mendelson, 1965). Thus, whatever yield function is proposed it should be symmetric in the principal axis (Hill, 1964). The geometry of the yield surface in the Haigh-Westergaard stress-space is a cylinder whose main axis is the hydrostatic axis. Any point P_n ($\sigma_{11}, \sigma_{22}, \sigma_{33}$) on this surface will have the same deviatoric stress components and different spherical components. Figure 3.1 represents the Haigh-Westergaard yield surface, showing the points P_1 and P_2 representing state of stress decomposed into spherical parts A_1 and A_2 and deviatoric parts B_1 and B_2 , respectively. Plane π is the $(\sigma_{11} + \sigma_{22} + \sigma_{33}) = 0$ plane where the hydrostatic stress equals zero.

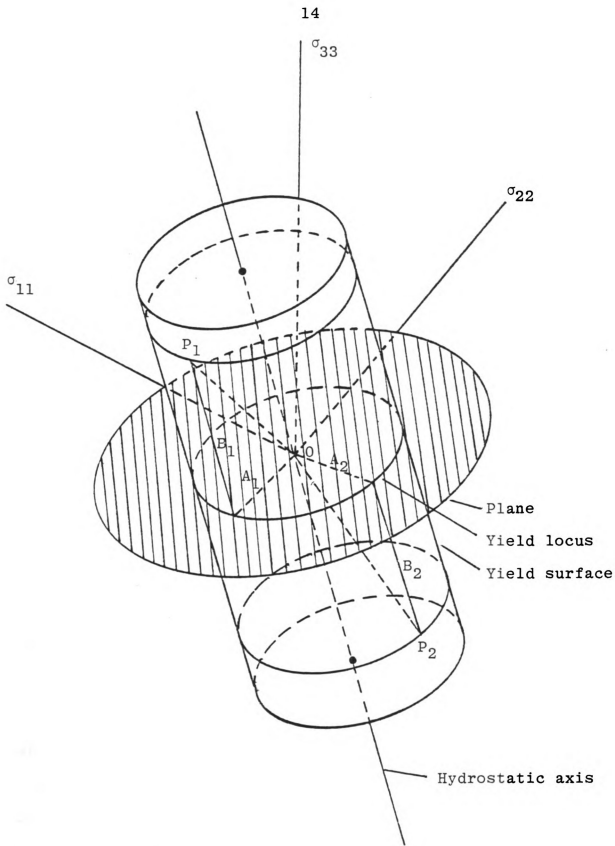


Figure 3.1. The Haigh-Westergaard hyper-space.

The intersection of the yield cylinder with any plane perpendicular to it will produce the same curve. This curve is called yield locus (Mendelson, 1965). Yield locus will be sufficient to study the yielding conditions since it is known that hydrostatic stresses do not contribute to failure. The yield locus then can be taken on the plane π . The projections of the principal stress axis on the plane π are lines 60° apart from each other, as shown on Figure 3.2. Since the material is isotropic, the locus is symmetrical about QQ' , RR' , and SS' . In other words, the yield criteria is a function of the invariants J_2 and J_3 . Similarly, the yield locus will be symmetric about the orthogonal lines to the stress axis projections passing through the origin (Hill, 1964). If the Bauschinger effect is neglected, any line representing unloading, drawn from the locus through the origin, will meet the locus again at the same distance from the origin. This is equivalent to saying that it is only necessary to analyze one of the twelve segments. It is very helpful to think in terms of Lode's parameter ψ ,

$$\psi = \frac{2\sigma_{33} - \sigma_{11} - \sigma_{22}}{\sigma_{11} - \sigma_{22}} = -3 \tan \theta \quad (3.4)$$

Where θ is the angle which defines the stress vector \overline{OP} . Stress locus can be completely determined by applying stress states such that ψ varies from zero to -1 or θ varies from zero to $\pi/6$ radians (Hill, 1964).

Existing failure theories do not always agree with the Haigh-Westergaard yield surface. Also, experimental data can

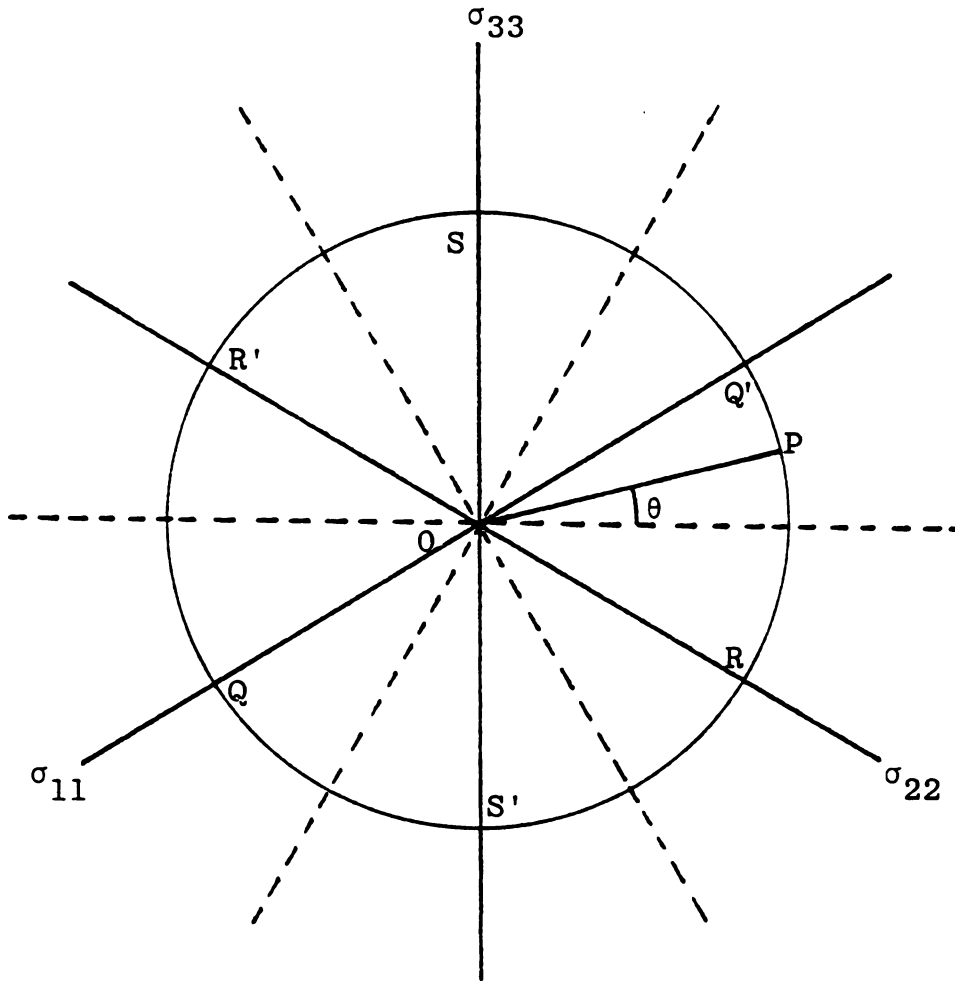


Figure 3.2. Yield locus for an isotropic material which does not exhibit Bauschinger effect (Hill, 1964).

show yield points whose locus is not symmetric with respect to the axes of principal stresses.

3.3 Stress Conditions

3.3.1 Maximum normal stress theory

The literature contains famous names from early times associated with this theory. Galileo Galilei and Leibniz were the first scientists to propose the failure criteria based on the maximum normal stress value (Prager, 1942). Later on, L. Navier, G. Lamé, B. P. E. Clapeyron, and Rankine each presented a mathematical formulation for this condition. This theory assumes that yield occurs when the largest of the principal stresses reaches the value of the tensile yield stress σ_{ot} or the yield stress value σ_{oc} . For a three-dimensional compressive stress configuration, the theory is formulated as:

$$\begin{aligned}\sigma_{11} &= \sigma_{oc} \\ \sigma_{22} &= \sigma_{oc} \\ \sigma_{33} &= \sigma_{oc}\end{aligned}\tag{3.5}$$

depending on which one of the principal stresses is the largest. For a tensile stress state, equation (3.5) can be written as:

$$\begin{aligned}\sigma_{11} &= \sigma_{ot} \\ \sigma_{22} &= \sigma_{ot} \\ \sigma_{33} &= \sigma_{ot}\end{aligned}\tag{3.6}$$

3.3.2 Maximum shear stress theory

The names of Tresca and Coulomb are related to this theory (Marin, 1953, and Mendelson, 1965). This condition assumes that yielding occurs when the maximum shear stress in the body reaches the shear stress value associated with yielding in simple tension, σ_{ot} . Mathematically, this theory can be expressed as:

$$\begin{aligned}\sigma_{11} - \sigma_{22} &= \pm\sigma_{ot} \\ \sigma_{22} - \sigma_{33} &= \pm\sigma_{ot} \\ \sigma_{33} - \sigma_{11} &= \pm\sigma_{ot}\end{aligned}\tag{3.7}$$

This condition does not predict failure under hydrostatic loading conditions (Hill, 1964).

3.3.3 Modified maximum shear stress theory

This theory is a generalization of the maximum shear stress condition, formulated by Mohr. Tresca and Mohr's criteria assume that only the largest and smallest principal stresses influence failure. While the first states that the largest principal circle on the Mohr diagram should have constant radius, the latter assumes that this radius should be a function of the normal stress. The failure will be defined by the envelope of all circles representing yield at different states of stress (Nadai, 1950). This can be analytically expressed as:

$$(\sigma_{11} - \sigma_{22})/2 = F[(\sigma_{11} + \sigma_{22})/2]\tag{3.8}$$

If the envelope lines are parallel and horizontal, equation (3.8) will be transformed back into equation (3.7), which

represents the maximum shear stress condition.

3.3.4 Internal friction theory

This condition is related to the names of Mohr, Coulomb, Guest, and Duguet. It can be considered as a special case of Mohr's theory in which the envelopes are two straight lines equally inclined to the normal stress axis (Marin, 1962). In other words, the limiting shear stress can be expressed as a linear function of the normal stress, written as:

$$\frac{\sigma_{11} - \sigma_{33}}{2} = \frac{\sigma_{ot} - \sigma_{oc}}{\sigma_{ot} + \sigma_{oc}} + \frac{\sigma_{ot}\sigma_{oc}}{\sigma_{ot} + \sigma_{oc}} \frac{\sigma_{11} + \sigma_{33}}{2} \quad (3.9)$$

It can be observed that when $\sigma_{oc} = \sigma_{ot}$, this condition is reduced to the maximum shear stress theory.

3.4 Strain Conditions

3.4.1 Maximum strain theory

This condition was independently proposed by Saint Venant and Poncelet (Prager, 1942). In a case of combined stress, yielding starts when the maximum value of the principal strains equals the value of the compressive or tensile yielding strain. The analytical expression of this statement can be expressed as:

$$\begin{aligned} \sigma_{11} - \nu(\sigma_{22} + \sigma_{33}) &= \pm\sigma_o \\ \sigma_{22} - \nu(\sigma_{33} + \sigma_{11}) &= \pm\sigma_o \\ \sigma_{33} - \nu(\sigma_{11} + \sigma_{22}) &= \pm\sigma_o \end{aligned} \quad (3.10)$$

where $\sigma_o = \sigma_{oc} = \sigma_{ot}$ and ν is the Poisson's ratio. This yield condition does not predict failure under hydrostatic stress

state.

3.4.2 Maximum shearing strain theory

This condition was proposed by G. Sandel (Prager, 1942). The maximum shearing strain is assumed to be a linear function of the mean strain. The analytical expression for this theory is:

$$\epsilon_I - \epsilon_{II} = c^2 - b^2 \epsilon_m \quad (3.11)$$

3.5 Energy Conditions

3.5.1 Constant total strain energy theory

This condition was proposed by Beltrami (Mendelson, 1965). Elastic strain energy is the factor impeding failure. In terms of principal stress it can be expressed as:

$$\sigma_{11}^2 + \sigma_{22}^2 + \sigma_{33}^2 - 2G(\sigma_{11}\sigma_{22} + \sigma_{22}\sigma_{33} + \sigma_{33}\sigma_{11}) = \sigma_o^2 \quad (3.12)$$

This condition predicts failure under hydrostatic stress conditions. The representation of the yield surface in stress space is an ellipsoid of revolution whose main axis is coincident with the hydrostatic axis (Prager, 1942).

3.5.2 Energy of distortion theory

This condition appears related to the names of Hencky, Von Mises, Hueber, and Maxwell, and it is also known as maximum octahedral stress theory (Juvinal, 1967). This theory assumes that yielding begins when the distortion energy equals the distortion energy at yield in simple tension or compression. Analytically it can be stated in

terms of principal stresses as:

$$\frac{1}{2}[(\sigma_{11} - \sigma_{22})^2 + (\sigma_{22} - \sigma_{33})^2 + (\sigma_{33} - \sigma_{11})^2] = \sigma_o^2 \quad (3.13)$$

where $\sigma_o = \sigma_{ot} = \sigma_{oc}$. This condition does not predict failure under hydrostatic stress states. The failure surface in three-dimensional stress space is a circular cylinder whose main axis is coincident with the hydrostatic axis.

3.5.3 Combined total strain energy and distortion energy theory

This condition was proposed by Huber (Prager, 1942). It is assumed that yielding will occur when the energy of distortion reaches the value of the energy of distortion at uniaxial loading when $\sigma_m < 0$ or when the total strain energy reaches the value of the total strain energy at uniaxial loading for $\sigma_m > 0$. In terms of principal stresses it is stated as:

$$\frac{1}{2}[(\sigma_{11} - \sigma_{22})^2 + (\sigma_{22} - \sigma_{33})^2 + (\sigma_{33} - \sigma_{11})^2] = \sigma_o^2$$

for $\sigma_m < 0$ (3.14)

$$\begin{aligned} \sigma_{11}^2 + \sigma_{22}^2 + \sigma_{33}^2 &= 2G(\sigma_{11}\sigma_{22} + \sigma_{22}\sigma_{33} + \sigma_{33}\sigma_{11}) \\ &= \sigma_o^2 \quad \text{for } \sigma_m > 0 \end{aligned} \quad (3.15)$$

The failure surface for this condition is represented by a cylinder prolonged by an ellipsoid.

3.5.4 Modified energy of distortion theory

This condition assumes that the energy of distortion level which causes failure is also a function of σ_m (Nadai, 1950). This modification was proposed by R. Von Mises and

F. Schleicher (Prager, 1942). The mathematical expression for this condition can be written in terms of principal stresses as:

$$\frac{1}{2}[(\sigma_{11} - \sigma_{22})^2 + (\sigma_{22} - \sigma_{33})^2 + (\sigma_{33} - \sigma_{11})^2] = F(\sigma_m) \quad (3.16)$$

Depending on the function $F(\sigma_m)$, equation (3.16) can represent a circular cone or a paraboloid of revolution (Nadai, 1950).

Figure 3.2 shows the projection of some failure surfaces on the $\sigma_{11} - \sigma_{22}$ plane.

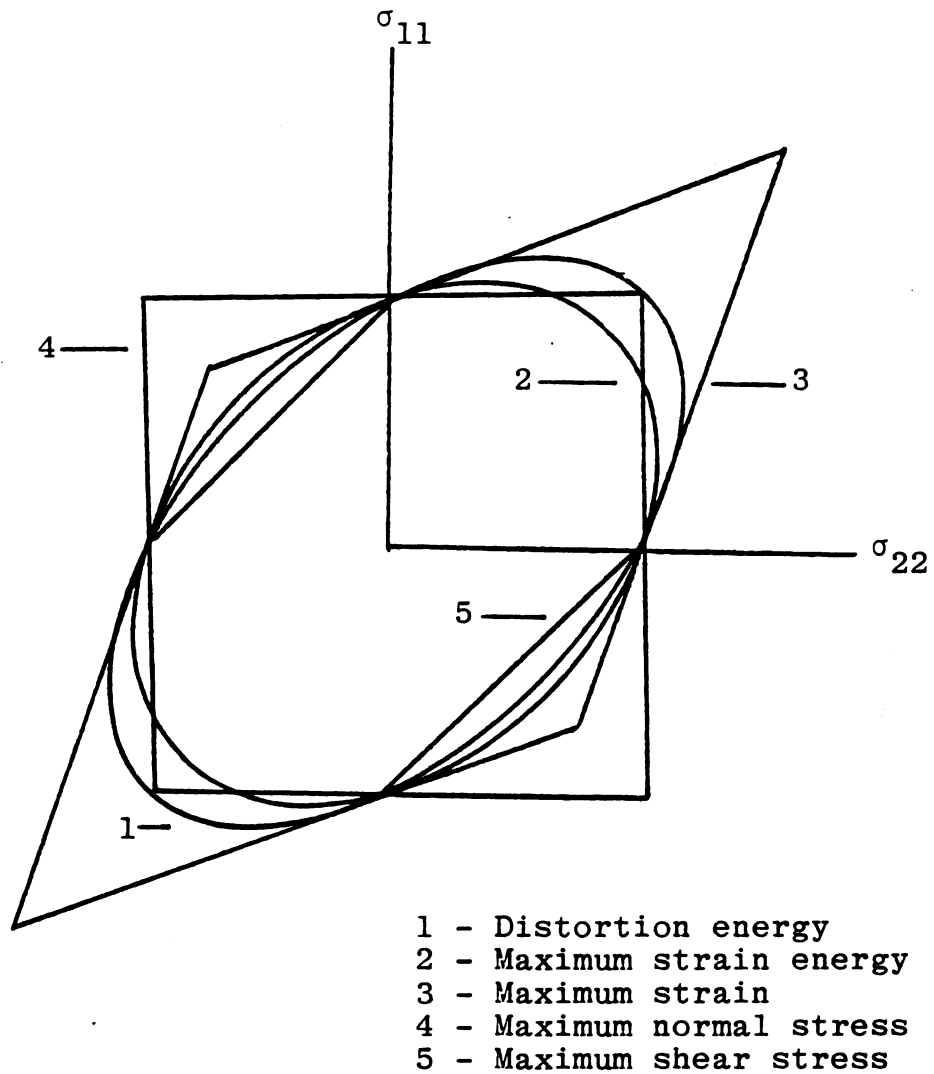


Figure 3.3. Comparison of failure surfaces as viewed on the $\sigma_{11} - \sigma_{22}$ plane.

CHAPTER IV
BASIC THEORY

4.1 General Remarks

In the preceding chapter the failure theories were classified by the parameters, stresses or strains, which are considered to produce a failure. The experimental data, however, must be combined with constitutive equations in order to obtain values for these parameters. Both elastic and viscoelastic equations have been used to represent the mechanical behavior of a vegetative material.

The objective of this chapter is to outline the calculation of the stress and strain components and the strain energy stored in the apple flesh for different types of experimental loads. The equations for the triaxial, rigid die, biaxial, and uniaxial tests are presented, first assuming a linear elastic material and then assuming a linear viscoelastic material.

4.2 The Strain Energy Stored in an Apple Specimen for Different Loading Situations

It is known from the theory of mechanics of continuous medium (Malvern, 1969) that the deviatoric stress and strain tensors are

$$S_{ij} = \sigma_{ih} - (1/3) \delta_{ij} \sigma_{kk} \quad (4.1)$$

$$\text{and } e_{ij} = \varepsilon_{ij} - (1/3) \delta_{ij} \varepsilon_{kk} \quad (4.2)$$

where σ_{ij} is the stress tensor, ε_{ij} is the strain tensor, σ_{kk} and ε_{kk} are the spherical components of the total stress and strain tensors, respectively, and δ_{ij} is the Kronecker's delta.

If a body in equilibrium is deformed by the action of external forces, so that none of the work done goes into kinetic energy, then this work is stored as strain energy of deformation. The total strain energy can be expressed as the summation of the distortional energy and spherical energy components, as

$$U = U_d + U_s \quad (4.3)$$

or in terms of strain and stress tensors

$$U = (1/2) \sigma_{ij} \varepsilon_{ij} \quad (4.4)$$

Equations (4.1), (4.2), (4.3), and (4.4) can be combined to yield the following expression for the energy of distortion

$$U_d = S_{ij} e_{ij}/2 \quad (4.5)$$

which can be developed into

$$\begin{aligned} U_d = (1/4) [& (\sigma_{11} - \sigma_{22}) (\varepsilon_{11} - \varepsilon_{22}) \\ & + (\sigma_{11} - \sigma_{33}) (\varepsilon_{11} - \varepsilon_{33}) \\ & + (\sigma_{22} - \sigma_{33}) (\varepsilon_{22} - \varepsilon_{33})] \end{aligned} \quad (4.6)$$

Similarly the expression the spherical component of strain energy becomes

$$U_s = \sigma_{11} \varepsilon_{ij}/6 \quad (4.7)$$

which yields

$$U_s = (\sigma_{11} + \sigma_{22} + \sigma_{33}) (\varepsilon_{11} + \varepsilon_{22} + \varepsilon_{33})/6 \quad (4.8)$$

In a stress state in which $\sigma_{22} = \sigma_{33}$ and $\epsilon_{22} = \epsilon_{33}$,
(4.6) and (4.8) reduce to

$$U_d = (1/2) (\sigma_{11} - \sigma_{22}) (\epsilon_{11} - \epsilon_{22}) \quad (4.9)$$

$$U_s = (1/6) (\sigma_{11} + 2\sigma_{22}) (\epsilon_{11} + 2\epsilon_{22}) \quad (4.10)$$

If the conditions $\sigma_{22} = \sigma_{33} \neq 0$ and $\epsilon_{22} = \epsilon_{33} = 0$ hold,
(4.6) and (4.8) yield

$$U_d = (1/2) (\sigma_{11} - \sigma_{22}) \epsilon_{11} \quad (4.11)$$

$$U_s = (1/6) (\sigma_{11} + 2\sigma_{22}) \epsilon_{11} \quad (4.12)$$

For the biaxial state of stress in which $\sigma_{22} \neq 0$,
 $\sigma_{33} = 0$, $\epsilon_{22} = 0$, $\epsilon_{33} \neq 0$, $\sigma_{11} \neq 0$, and $\epsilon_{11} \neq 0$

$$U_s = (1/6)(\sigma_{11} + \sigma_{22})(\epsilon_{11} + \epsilon_{33})$$

$$U_d = (1/4) [(\sigma_{11} - \sigma_{22})\epsilon_{11} + (\epsilon_{11} - \epsilon_{33})\sigma_{11}] \quad (4.13)$$

When a uniaxial loading is applied, the conditions
 $\sigma_{11} \neq 0$, $\epsilon_{11} \neq 0$, $\sigma_{22} = \sigma_{33} = 0$ and $\epsilon_{22} = \epsilon_{33} \neq 0$ define the
state of stress. When this occurs, the equations for U_d and
 U_s are

$$U_d = (1/2) (\epsilon_{11} - \epsilon_{22}) \epsilon_{11} \quad (4.14)$$

and
$$U_s = (1/6) \sigma_{11} (\epsilon_{11} + 2\epsilon_{22}) \quad (4.15)$$

4.3 Maximum Shear Stress Conditions

The loading tests described in Chapter V develop only
normal stresses within the material. For this type of stress
state, the maximum shear stress is given by Timoshenko (1970)
as

$$\tau_{\max} = \sigma_{III} - \sigma_I / 2 \quad (4.16)$$

where σ_{III} and σ_I are the maximum and minimum values of the
principle stresses, respectively.

4.4 The Linear Elastic Model

The stress and strain tensors given in (4.1) and (4.2) can be related to each other through a linear material law known as generalized Hooke's law. The stress and strain tensors are related by

$$S_{ij} = 2G e_{ij} \quad (4.17)$$

$$\sigma_{kk} = 3K \epsilon_{kk} \quad (4.18)$$

$$\sigma_{ij} = \lambda \epsilon_{kk} \delta_{ij} + 2G \epsilon_{ij} \quad (4.19)$$

The bulk modulus K and shear modulus G are related to the Lamé constant λ , the modulus of elasticity E and Poisson's ratio ν as

$$K = E/3(1-2\nu) \quad (4.20)$$

$$K = (3\lambda + 2G)/3 \quad (4.21)$$

$$E = 9GK/(3K + G) \quad (4.22)$$

In a triaxial loading test in which the state of stress is characterized by holding $\sigma_{22} = \sigma_{33}$, $\epsilon_{22} = \epsilon_{33}$ and imposing σ_{11} and ϵ_{11} . Equations (4.1), (4.2), (4.18), and (4.19) yield

$$\sigma_{11} = E\epsilon_{11} + 2\nu\sigma_{22} \quad (4.23)$$

and
$$\epsilon_{22} = (1/E) [\delta_{22} - \nu\sigma_{22} - \nu\sigma_{11}] \quad (4.24)$$

In a rigid die loading, the strains ϵ_{22} and ϵ_{33} are zero and the expressions for σ_{11} and σ_{22} are

$$\sigma_{11} = \frac{E(1-\nu)}{(1+\nu)(1-2\nu)} \epsilon_{11} \quad (4.25)$$

$$\sigma_{22} = (K + \frac{2}{3} G)\epsilon_{11} \quad (4.26)$$

In a biaxial state of stress, σ_{11} and ϵ_{11} are imposed while $\sigma_{22} \neq 0$, $\sigma_{33} = 0$, $\epsilon_{22} = 0$, $\epsilon_{33} \neq 0$. The expressions

for σ_{11} and σ_{22} in this situation become

$$\sigma_{11} = (E/(1-\nu^2)) \epsilon_{11} \quad (4.27)$$

$$\epsilon_{33} = (-\nu/(1-\nu)) \epsilon_{11} \quad (4.28)$$

$$\sigma_{22} = \frac{2\nu G}{1-\nu} \epsilon_{11} \quad (4.29)$$

The state of stress which describes the uniaxial loading of a specimen ($\sigma_{11} \neq 0$, $\epsilon_{11} \neq 0$, $\sigma_{22} = \sigma_{33} = 0$, $\epsilon_{22} = \epsilon_{33} \neq 0$) combined with equations (4.1), (4.2), (4.17), and (4.18) yield

$$\sigma_{11} = E \epsilon_{11} \quad (4.30)$$

$$\epsilon_{22} = (-\nu/E) \epsilon_{11} \quad (4.31)$$

4.5 The General Viscoelastic Model

The stress and strain tensors formulated by the equations (4.1) and (4.2) can be also related to each other through the relaxation functions $G_1(t)$ and $G_2(t)$ (Christensen, 1971). The function $G_1(t)$ is the deviatoric relaxation function or the function appropriate to the state of shear while the function G_2 is the bulk relaxation function. If a body is in equilibrium and there is no load applied before the time $t = 0$, the stress and strain relationship can be written as

$$S_{ij} = \int_0^t G_1(t-\tau) \frac{d e_{ij}(\tau)}{d\tau} d\tau \quad (4.32)$$

and

$$\sigma_{kk} = \int_0^t G_2(t-\tau) \frac{d \epsilon_{kk}}{d\tau} d\tau \quad (4.33)$$

Functions $G_1(t)$ and $G_2(t)$ can be related to each other by the Laplace transform operation as (Christensen, 1971, and Flugee, 1975):

$$\bar{E} = (3\bar{G}_1\bar{G}_2)/(\bar{G}_1+2\bar{G}_2) \quad (4.34)$$

$$\text{and } \bar{X} = (2\bar{G}_1+\bar{G}_2)/3 \quad (4.35)$$

where the bar indicates that the function is expressed in terms of the Laplace parameter s instead of time t . The function $E(t)$ is called uniaxial relaxation function and $X(t)$ is called constrained relaxation function. Experimental determination of $E(t)$ was carried out in conditions where $\sigma_{22} = \sigma_{33} = 0$, corresponding to a uniaxial loading of cylindrical specimens. In similar situations $X(t)$ is determined by holding $\epsilon_{22} = \epsilon_{33} = 0$. The functions $E(t)$ and $X(t)$ are expressed as a summation of exponential terms as given in the generalized Maxwell model relaxation function

$$E(t) = \sum_{j=0}^n E_j e^{-\alpha_j t} \quad (4.36)$$

Experimental values of $E(t)$ and $X(t)$ have been determined for Red Delicious apples and are given by an experimental series representation (DeBaerdemaeker, 1975) as

$$E(t) = 0.744 \text{ EXP}(-4.152t) + 2.863 \text{ EXP}(-0.029t) \quad (4.37)$$

$$X(t) = 2.011 \text{ EXP}(-4.630t) + 3.325 \text{ EXP}(-0.028t) \quad (4.38)$$

Discrete values for G_1 and G_2 were obtained from the relaxation functions $X(t)$ and $E(t)$ (DeBaerdemaeker, 1975). Those values were modeled by an exponential representation as follows (in all those equations t is minutes)

$$G_1(t) = 2.554 \text{ EXP}(-0.318t) \quad (4.39)$$

$$\text{and } G_2(t) = 10.665 \text{ EXP}(-0.27t) \quad (4.40)$$

The time dependent Poisson's ratio determined by DeBaerdemaeker (1975) can also be represented by a similar equation

$$\text{as } v(t) = 0.330 \text{ EXP}(-0.27t) \quad (4.41)$$

The convolution integrals (4.32) and (4.33) can be expressed in terms of the Laplace transform parameter s , as (Christensen, 1971)

$$\bar{S}_{ij} = S \bar{G}_1 \bar{e}_{ij} \quad (4.42)$$

$$\text{and } \bar{\sigma}_{kk} = S \bar{G}_2 \bar{\epsilon}_{kk} \quad (4.43)$$

The triaxial loading case expressed by the equations (4.23) and (4.24) can be derived from those equations by the correspondence principle or directly from (4.1), (4.2), (4.42), and (4.43). In either case, the resulting expressions for σ_{11} and ϵ_{22} in the Laplace domain are (Fodor, 1965):

$$\bar{\sigma}_{11} = S \bar{E} \bar{\epsilon}_{11} + 2 \bar{\nu} \bar{\sigma}_{22} \quad (4.44)$$

$$\text{and } \bar{\epsilon}_{22} = [3/S^2(2\bar{G}_2 + \bar{G}_1)] \sigma_{22} - \bar{\nu} \bar{\epsilon}_{11} \quad (4.45)$$

Equations (4.44) and (4.45) can be expressed in the time domain as follows

$$\begin{aligned} \sigma_{11}(t) = & \dot{\epsilon}_{11} [98.903 - 0.179 \text{ EXP}(-4.152t) \\ & - 98.724 \text{ EXP}(-0.029t)] \\ & + 0.660 \text{ EXP}(-0.270t) \sigma_{22} \end{aligned} \quad (4.46)$$

$$\begin{aligned} \epsilon_{22} = & [0.126 + 0.103t] \sigma_{22} \\ & - 1.222 [1 - \text{EXP}(-0.27t)] \dot{\epsilon}_{11} \end{aligned} \quad (4.47)$$

The state of stress described by (4.25) and (4.26) for loading in a rigid die can be used to obtain its viscoelastic counterpart, resulting in the following expression for σ_{11} and σ_{22}

$$\bar{\sigma}_{11} = (1/S) \bar{X} \dot{\epsilon}_{11} \quad (4.48)$$

$$\bar{\sigma}_{22} = (1/35)(\bar{G}_1 + \bar{G}_2) \dot{\epsilon}_{11} \quad (4.49)$$

The inversion of $\bar{\sigma}_{11}$ and $\bar{\sigma}_{22}$ results in

$$\sigma_{11}(t) = \dot{\epsilon}_{11} [119.180 - 0.434 \text{EXP}(-4.630t) - 118.75 \text{EXP}(-0.028t)] \quad (4.50)$$

$$\sigma_{22} = \dot{\epsilon}_{11} [11.183 - 11.183 \text{EXP}(-0.9t) + 8.031 - 8.031 \text{EXP}(-0.318t)] \quad (4.51)$$

The biaxial state of stress associated with (4.27), (4.28), and (4.29) can be represented in the Laplace domain by

$$\bar{\sigma}_{11} = [(\bar{S}\bar{E})/(1-(\nu S)^2)] \bar{\epsilon}_{11} \quad (4.52)$$

$$\bar{\epsilon}_{33} = [(-\bar{\nu}S)/(1-\bar{\nu}S)] \bar{\epsilon}_{11} \quad (4.53)$$

$$\bar{\sigma}_{22} = [\bar{\nu}S/(1-\bar{\nu}S)] (G_1) \bar{\epsilon}_{11} \quad (4.54)$$

The inversion of (4.52), (4.53), and (4.54) to the time domain gives

$$\sigma_{11}(t) = (0.03 + 3.099t) \dot{\epsilon}_{11} \quad (4.55)$$

$$\epsilon_{33}(t) = 1.225[\text{EXP}(-0.4t) - 1] \dot{\epsilon}_{11} \quad (4.56)$$

$$\sigma_{22}(t) = -14.800 \dot{\epsilon}_{11} [\text{EXP}(-0.318t) - \text{EXP}(-0.403t)] \quad (4.57)$$

Similarly, (4.30) and (4.31) associated with the case of uniaxial loading of a cylindrical specimen yields

$$\bar{\sigma}_{11} = S \bar{E} \bar{\epsilon}_{11} \quad (4.58)$$

$$\bar{\epsilon}_{22} = -\frac{\bar{\nu}S}{s^2} \dot{\epsilon}_{11} \quad (4.59)$$

The inversion of the above equations yields

$$\sigma_{11}(t) = \dot{\epsilon}_{11} [98.903 - 0.179 \text{EXP}(-4.15t) - 98.724 \text{EXP}(-0.029t)] \quad (4.60)$$

$$\epsilon_{22}(t) = -\dot{\epsilon}_{11} [1.222 (1 - \text{EXP}(-0.270t))] \quad (4.61)$$

4.6 Stress Controlled Uniaxial Loading

For a uniaxial loading of cylinder, the elastic representation is given by (4.30) and (4.31). The Laplace transforms of these equations are

$$\bar{\varepsilon}_{11} \bar{E} S = \bar{\sigma}_{11} \quad (4.62)$$

and
$$\bar{\varepsilon}_{22} = \frac{-\bar{\nu}}{\bar{E}} \frac{\dot{\sigma}_{11}}{s^2} \quad (4.63)$$

In the time domain they become

$$\varepsilon_{11}(t) = \dot{\sigma}_{11} [-0.021 + 0.347t + 0.006t^2 + 0.021 \text{ EXP}(-3.302t)] \quad (4.64)$$

$$\varepsilon_{22}(t) = \frac{1}{3} [0.292t + 0.018t^2] \cdot \dot{\varepsilon}_{11} \quad (4.65)$$

4.7 The Non-linear Viscoelastic Formulation for Apple Material

It was seen in Chapter II that the non-linear viscoelastic behavior of vegetative tissues had been approximated by linear viscoelastic constitutive equations for certain cases (Morrow and Mohsenin, 1966; Hamann, 1967, 1970). However, Chappell and Hamann (1968) have reported cases in which such an approximation was not possible. In either case, the real behavior of vegetative tissue in reality is non-linear viscoelastic.

Non-linear behavior of viscoelastic bodies is not as well understood as it is for the linear case. The first attempt in giving a mathematical formulation for non-linear viscoelastic phenomena was to represent the time derivatives of the linear operator form by convected derivatives (Oldroyd, 1950). This model was criticized by the resulting

differences when contravariant or covariant tensors are used and does not predict non-newtonian viscous flow (Fredrickson, 1964). Further modification of this formulation was proposed by the same author by including non-linear terms on the convected operator form as $\dot{\epsilon}_{ij}^*$, σ^{ij} ($i \neq j$), and $\epsilon^{*ik} \sigma_k^j$. The resulting equation would reduce to the linear operator form in cases of small strain rates. The objections raised against this formulation are related to its lack of generality as well as the covariant and contravariant effects (Fredrickson, 1964).

A further step was taken by expressing the stress tensor σ^{ij} in terms of a non-linear function of $\dot{\epsilon}_{ij}^*$ and its N-1 convected derivatives (Rivlin and Ericksen, 1955). The condition that $\sigma^{ij} = 0$ whenever $\dot{\epsilon}^{*ij} = D \dot{\epsilon}^{*ij} / Dt = 0$ was assumed in order to derive the non-linear relations. Instead of convected derivatives, one could use Jaumann derivatives (Fredrickson, 1964; Prager, 1961, and Oldroyd, 1950). The covariant and contravariant tensors are equivalent expressions in terms of Jaumann derivatives.

Another approach to describe non-linear behavior is to formulate a non-linear superposition principle (Noll, 1958). However, this new theory sometimes yields the same result as the proposed Rivlin-Ericksen model (Coleman and Noll, 1959). This theory had been followed by similar approaches (Green and Rivlin, 1960). Non-linear behavior of anisotropic fluids had been treated with a very different approach, by introducing relaxation effects (Ericksen, 1960).

Further development on non-linear viscoelastic behavior has been presented by Bychawski (1974), Lockett (1974), and Sobotka (1975). Comparison of experimental data with theoretical results was reported by Yoshiaki (1977).

A non-linear viscoelastic formulation for apple material by representing the time derivatives appearing on the hereditary integral forms by convected time derivatives is proposed in the following discussion. Although it was not used to isolate the failure parameters, it is included to stimulate the possibility of using a non-linear viscoelastic theory for apple flesh.

4.7.1 The convected derivative of a covariant strain tensor

The convected coordinate system can be understood as a reference frame which moves and deforms with the deforming body (Fredrickson, 1964). Some authors use material coordinates as a synonym of convected coordinates (Green and Adkins, 1970).

If the strain tensor is written as a covariant cartesian tensor ϵ_{ij} , its convected derivative $D \epsilon_{ij}/Dt$ can be expressed as (Fredrickson, 1964)

$$D \epsilon_{ij}/Dt = \sigma \epsilon_{ij}/\sigma t + v^k \epsilon_{ij,k} + v^{k,i} \epsilon_{kj} + v^{k,j} \epsilon_{ik} \quad (4.66)$$

where the commas in the subscripts indicate differentiation. The term v^k is a velocity along the X_1 , X_2 , and X_3 axes. The differentiations $v^{k,i}$ and $v^{k,j}$ are gradient velocities expressed as (Eringen, 1962)

$$\varepsilon_{ij}^* = (1/2) (v_{i,j} + v_{j,i}) \quad (4.67)$$

If symmetrical conditions are held in respect to the axis X_1 and $\varepsilon_{12} = \varepsilon_{21}$ $\varepsilon_{13} = \varepsilon_{31}$, equation (4.66) can be written as

$$\begin{aligned} \frac{D\varepsilon_{11}}{\partial t} &= \frac{\partial \varepsilon_{11}}{\partial t} + v^{(1)} \frac{\partial \varepsilon_{11}}{\partial t} + 2v^{(2)} \frac{\partial \varepsilon_{11}}{\partial X_2} \\ &+ 2 \frac{\partial v^{(1)}}{\partial X_1} \varepsilon_{11} + 4 \frac{\partial v^{(2)}}{\partial X_1} \varepsilon_{12} \end{aligned} \quad (4.68)$$

Recalling the definition of the infinitesimal strain tensor

$$\varepsilon_{ij} = (1/2) (\partial U_i / \partial x_j + \partial U_j / \partial x_i) \quad (4.69)$$

A strain function of time and strain rate $\varepsilon_{11}(\dot{\varepsilon}_{11}, t)$ is imposed on the linear viscoelastic model in the X_1 direction. This means that deformation should also be function of time, $U_i(X_i, t)$. The X_1 direction is the only important one due to the fact that the strain and deformation parameters are imposed in this direction.

If the deformation is considered a linear function with respect to time and X_1 coordinate, equation (4.68) reduces to

$$\frac{D\varepsilon_{11}}{Dt} = \frac{\partial \varepsilon_{11}}{\partial t} + 2 \frac{\partial v^{(1)}}{\partial X_1} \varepsilon_{11} + v^{(1)} \frac{\partial \varepsilon_{11}}{\partial X_1} \quad (4.70)$$

Once the deformation function has been determined, the non-linear viscoelastic expression for the different loading situations could be found by replacing the linear strain rate tensor ε_{ij} by its convected counterpart ε_{ij}^* , where

$$\varepsilon_{11}^* = \frac{D\varepsilon_{11}}{Dt} \quad (4.71)$$

CHAPTER V
EXPERIMENTAL PROCEDURE

5.1 General Remarks

In the first group of experiments the apple specimens were subjected to compressive loads up to failure. Failure was determined by the point on the loading curve which indicates the end of the elastic behavior. As mentioned previously, cylindrical and cubic specimens were loaded uniaxially, biaxially, or triaxially. All specimens were subjected to a uniaxial strain rate ($\dot{\epsilon}_{11}$) unless a radial stress failure occurred prior to the axial loading. Displacement and force values at failure were recorded on a strip chart recorder. The axial load was applied using an InstronTM model testing machine which had several different loading speeds, allowing a wide range of strain rates to be imposed on the specimen. The tests were divided into seven groups according to the loading conditions, and the shape and size of the specimens. Table 5.1 shows the loading conditions, shape, and dimensions of the specimens. The mean and standard deviations of the basic dimensions are given. These were calculated from ten measurements taken from each type of specimen. Twenty replications of each individual type of test were conducted. The individual stress (σ_{11})

TABLE 5.1. Tests carried on apple material. Imposed strain rates and radial stresses. Shape and dimensions of the specimens.

SPECIMENS DIMENSIONS							
TEST	$\dot{\epsilon}_{11}$ (SEC ⁻¹)	(MPa)	SPECIMEN SHAPE	L (mm)	H (mm)	D (mm)	A (mm ²)
UNIAXIAL	-0.002	0.000	CYLINDRICAL		12.22	12.58	124.29
	-0.007						
	-0.017						
	-0.035						
	-0.173						
-0.347				0.08*	0.17*	4.84*	
UNIAXIAL	-0.007	0.000	CYLINDRICAL		8.32	19.30	292.55
					12.13		
					19.17		
					26.55		
34.98				0.06*	0.08*	6.06*	
				0.12*			
				0.13*			
				0.11*			
				0.11*			
TRIAXIAL	-0.007	0.000	CYLINDRICAL		12.22	12.58	124.29
		-0.067					
		-0.138					
		-0.207					
		-0.276					
-0.345				0.08*	0.17*	4.94*	
RIGID DIE	-0.007		CYLINDRICAL		12.22	12.58	124.29
					0.03*	0.17*	4.34*
UNIAXIAL	-0.007		CUBIC	12.37			153.02
				0.09*			5.25*
BIAXIAL	-0.007		CUBIC	12.37			153.02
				0.09*			5.25*
RIGID DIE	-0.007		CUBIC	12.37			153.02
				0.09*			5.25*

(*) standard deviation

and strain (ϵ_{11}) values at failure for those replications are given in the appendices. In the second group of experiments, cylindrical specimens of apple were subjected to stress rate controlled uniaxial loading.

5.2 Apple Selection and Storage

The varieties Red Delicious, Jonathan, and McIntosh were harvested during the 1977 growing season and were stored at 0-2°C in plastic bags. They were removed from storage 24 hours before being tested.

5.3 Specimen Preparation

The specimens were prepared by driving a corkborer into the apple parallel to the stem-calyx axis. The specimen was then placed in a cylindrical hole in a plexiglass bar and the ends were cut parallel to the faces of the bar by using a sharp blade. The same procedure was used to obtain cubic specimens. In this case, a square corkborer and a square trimming hole were used.

5.4 Uniaxial Loading of Cylindrical Specimens at Different Strain Rates

Cylindrical specimens with a height of 12.20 ± 0.08 mm, a diameter of 12.58 ± 0.17 mm, and a cross-sectional area of 124.29 ± 4.84 mm² were uniaxially loaded to failure in the Instron testing machine at the following strain rates: -0.002, -0.007, -0.017, -0.035, -0.069, -0.137, and -0.347 sec⁻¹. This first group of tests is summarized in Table 5.1.

5.5 Uniaxial Loading of Cylindrical Specimens of Different Height at a Constant Strain Rate

Cylindrical specimens with a constant cross-sectional area of $292.55 \pm 6.06 \text{ mm}^2$ and heights of 8.32 ± 0.06 , 12.13 ± 0.12 , 19.17 ± 0.13 , 26.55 ± 0.16 , $34.98 \pm 0.12 \text{ mm}$ were uniaxially loaded in the Instron testing machine at a strain rate of -0.007 sec^{-1} . For these tests the deformation was obtained for each height with a constant force of 36.38 N. This was done to obtain the variation of the deformation with the height (H) at a fixed load level.

5.6 Triaxial Loading of Cylindrical Specimens at a Constant Strain Rate, and Different Radial Stresses

This group of specimens is the third row of Table 5.1. In order to impose a constant strain rate of -0.007 sec^{-1} along the X_1 axis and at the same time impose a radial stress, σ_{22} , a special apparatus was developed. Figure 5.1 shows the details of this device. The specimen is contained in a very thin wall rubber tube (6). Two aluminum rods (1 and 11) are in contact with the bottom and top of the specimens. Those aluminum rods are axially and radially perforated in order to allow any small quantity of air that might be trapped between the specimen and the rubber tube to escape. Trapped air would transmit the load applied on the outer surface of the rubber tube to the bottom and top surfaces of the specimen. This situation would create a hydrostatic stress state before the specimen was axially loaded. This test creates a radial stress, $\sigma_{22} \gtrless \sigma_{11}$.

Figure 5.1. Triaxial loading device, showing the longitudinal cross-sectional view (a) and top view (b).

Legend:

- 1 - Aluminum rod
- 2 - Brass tube
- 3 - Bolts
- 4 - Steel frame
- 5 - Rubber cork
- 6 - Rubber tube
- 7 - Specimen
- 8 - Plexiglass tube
- 9 - Brass tube
- 10 - Rubber cork
- 11 - Aluminum rod
- 12 - Opening
- 13 - Plexiglass frame
- 14 - Steel frame
- 15 - Plexiglass frame
- 16 - Plexiglass tube-frame
- 17 - Air pressure valve
- 18 - Air pressure release

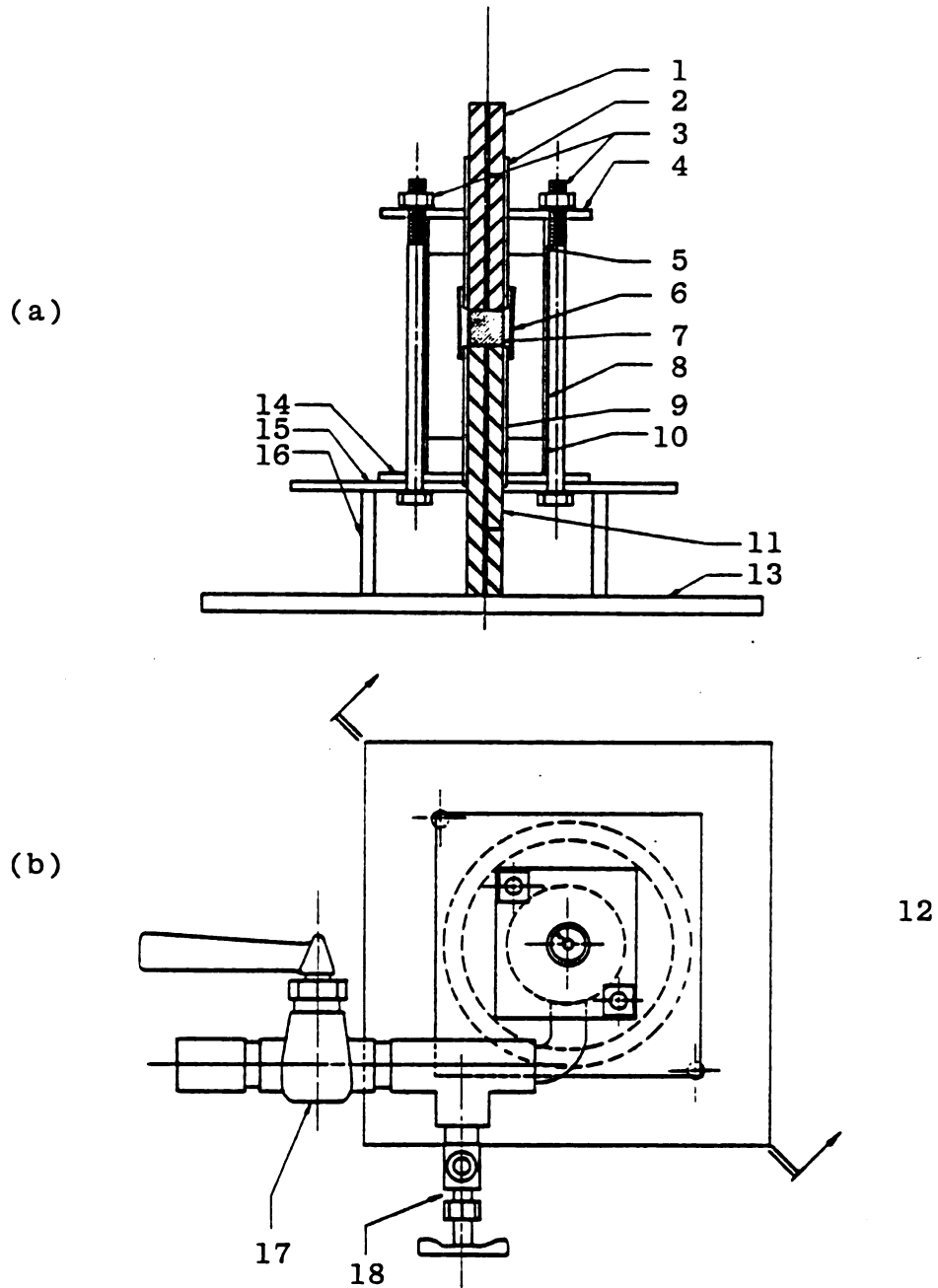


Figure 5.1. Triaxial loading device, showing the longitudinal cross-sectional view (a) and top view (b).

In a hydrostatic stress situation, the axial stress σ_{11} would be always larger than the radial stress σ_{22} (in this case equal to the hydrostatic stress).

The aluminum rods are fitted inside of two brass tubes (2 and 9) which were glued to the rubber tube. Two rubber corks (5 and 10) were inserted in the top and bottom of the plexiglass tube (8). The brass tubes (2 and 9) are fitted in the circular holes made in the rubber corks (5 and 10).

The cylindrical specimen was placed between the aluminum rods and lubricated with vaseline to avoid friction. The apparatus was placed on the load cell of the Instron testing machine, keeping the upper aluminum rod in contact with the compressive head. A strain of -0.007 sec^{-1} was imposed to the specimen through the aluminum rod. The radial stresses acting as the outer surface of the rubber membrane were created by connecting the opening (12) on the plexiglass tube to an air pressure line before the axial load was applied. The cylindrical specimens had a diameter of $12.58 \pm 0.17 \text{ mm}$, a height of $12.22 \pm 0.08 \text{ mm}$, and a cross-sectional area of $124.29 \pm 4.84 \text{ mm}^2$. The selected radial stresses were equal to 0.000, -0.069, -0.138, -0.207, and -0.345 MPa.

5.7 Rigid Die Loading of Cylindrical Apple Specimens

A rigid die as shown in Figure 5.2 was used to obtain axial deformation while constraining the sample in the radial direction. This made it possible to impose an axial strain rate, $\dot{\epsilon}_{11}$, while keeping $\epsilon_{22} = \epsilon_{33} = 0$. The specimen was placed in the cylindrical hole, topped by an aluminum rod.

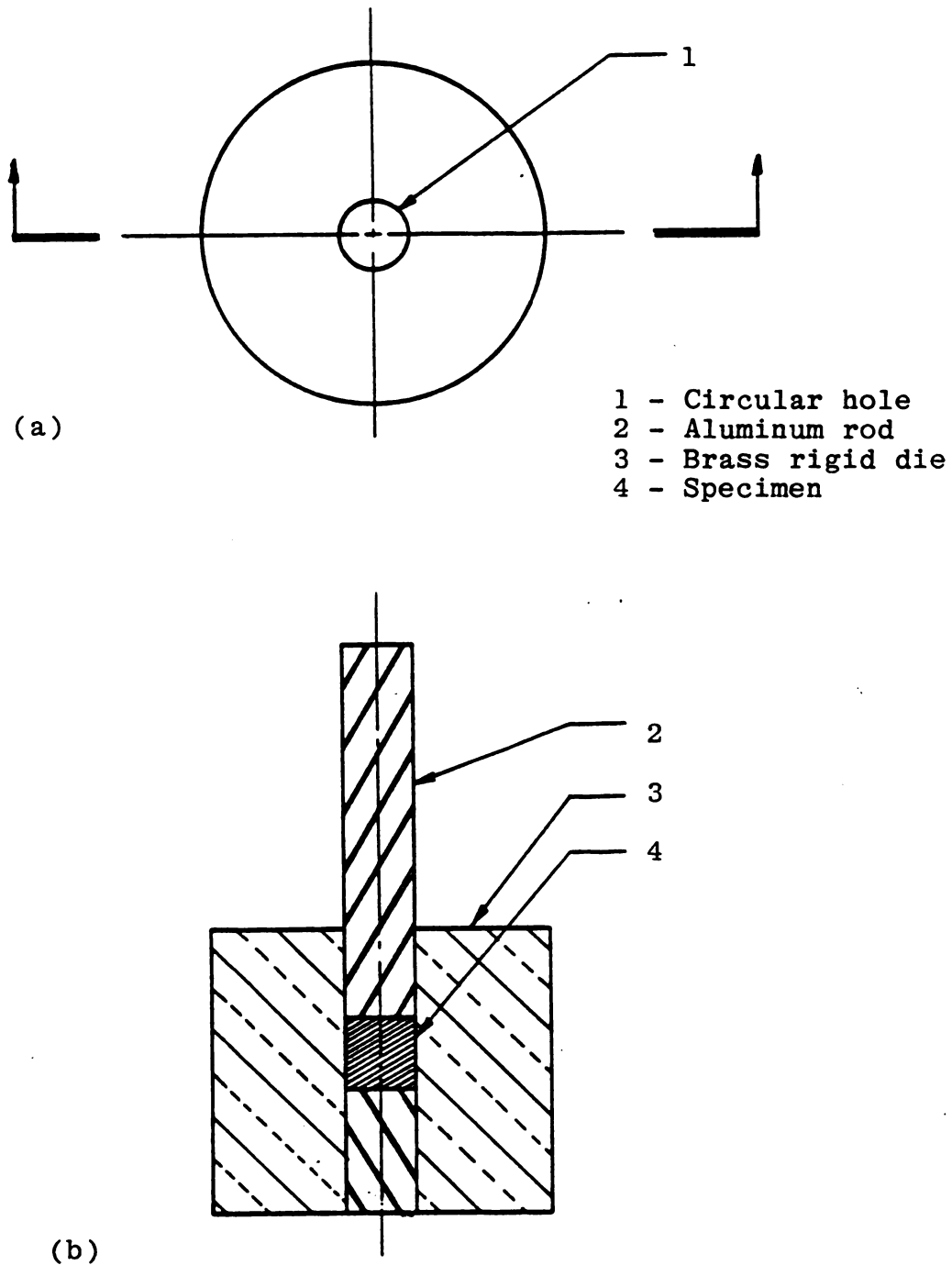


Figure 5.2. Top (a) and longitudinal cross-sectional view (b) of the device for loading of cylindrical specimens in rigid die.

The die was then placed on the load cell of the testing machine and a constant strain rate of -0.007 sec^{-1} was imposed on the specimen through the aluminum rod. The specimens used in this test had a height of $12.22 \pm 0.08 \text{ mm}$, diameter of $12.58 \pm 0.17 \text{ mm}$, and a cross-sectional area of $124.29 \pm 4.84 \text{ mm}^2$.

5.8 Uniaxial Loading of Cubic Specimens at a Constant Strain Rate

Cubic specimens having a dimension of $12.37 \pm 0.09 \text{ mm}$ and cross-sectional area of $153.02 \pm 5.25 \text{ mm}^2$ were uniaxially loaded in a testing machine under the conditions given in Table 5.1.

5.9 Biaxial Loading of Cubic Specimens at a Constant Strain Rate

In the biaxial test, a cubic specimen is loaded axially along the X_1 axis while constraining the side orthogonal to the X_1 axis ($\epsilon_{22} = 0$). The side orthogonal to the X_3 axis was free to move. The apparatus designed to allow these features is shown in Figure 5.3. The two blocks (1 and 2) kept the bars (3 and 4) at a constant distance from each other ($12.37 \pm 0.09 \text{ mm}$). The specimens had a dimension of $12.37 \pm 0.09 \text{ mm}$ and a cross-sectional area of $153.02 \pm 5.25 \text{ mm}^2$. This apparatus was then placed on load cell of the testing machine and the strain rate is imposed to the specimen through the square cross-sectional area steel bar (5) (see the sixtieth row of Table 5.1).

- 1 - Steel block
- 2 - Steel block
- 3 - Aluminum plate
- 4 - Aluminum plate
- 5 - Steel bar
- 6 - Cubic specimen

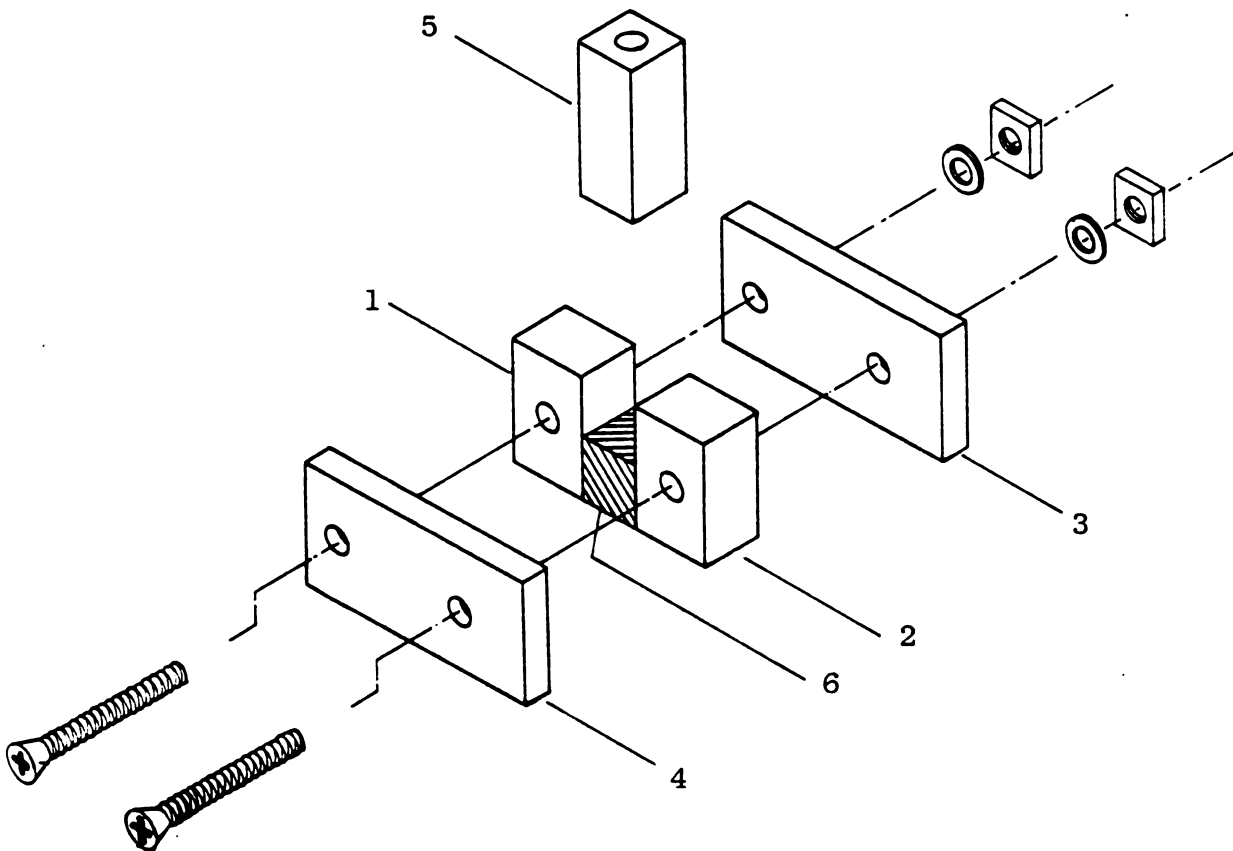


Figure 5.3. Exploded view of the device used for biaxial and rigid loading of cubic specimens.

5.10 Rigid Die Loading of Cubic Specimens

The cubic specimens used in this test had the same dimensions as the uniaxial and biaxial specimens. The apparatus described in 5.9 was used. This time, the block (2) was aligned such that a constant distance between the bars (3 and 4) was obtained. The cubic specimen was the biaxially constrained. The force orthogonal to the axis X_1 was loaded by the steel plunger, to which the strain rate of -0.007 sec^{-1} was imposed. The bottom row of the Table 5.1 summarizes the conditions of this test.

5.11 Stress Rate Controlled Loading of Cylindrical Specimens of Red Delicious

This experiment was designed to control stress and give freedom to the state of strain. Cylindrical specimens of Red Delicious with a height of 12.22 ± 0.08 mm, a diameter of 12.58 ± 0.17 mm, were uniaxially loaded to failure by controlling the stress rate. Six different stress rates were chosen, from 0.0005 MPa/sec to 0.013 MPa/sec (see Table 6.7). Figure 5.4 illustrates the apparatus designed for this test. The specimen is placed between the plate of a scale (1) and a rigid plate (2). Deformation on X_1 direction is measured by a LVDT device (3) and recorded on a strip chart recorder. The second plate of the scale supports the loading water container (4). The water reservoir (5) was kept at a constant level by the outlet (6) and inlet (7). By controlling the valve (8) it was possible to control the stress rate being applied to the apple specimen (9).

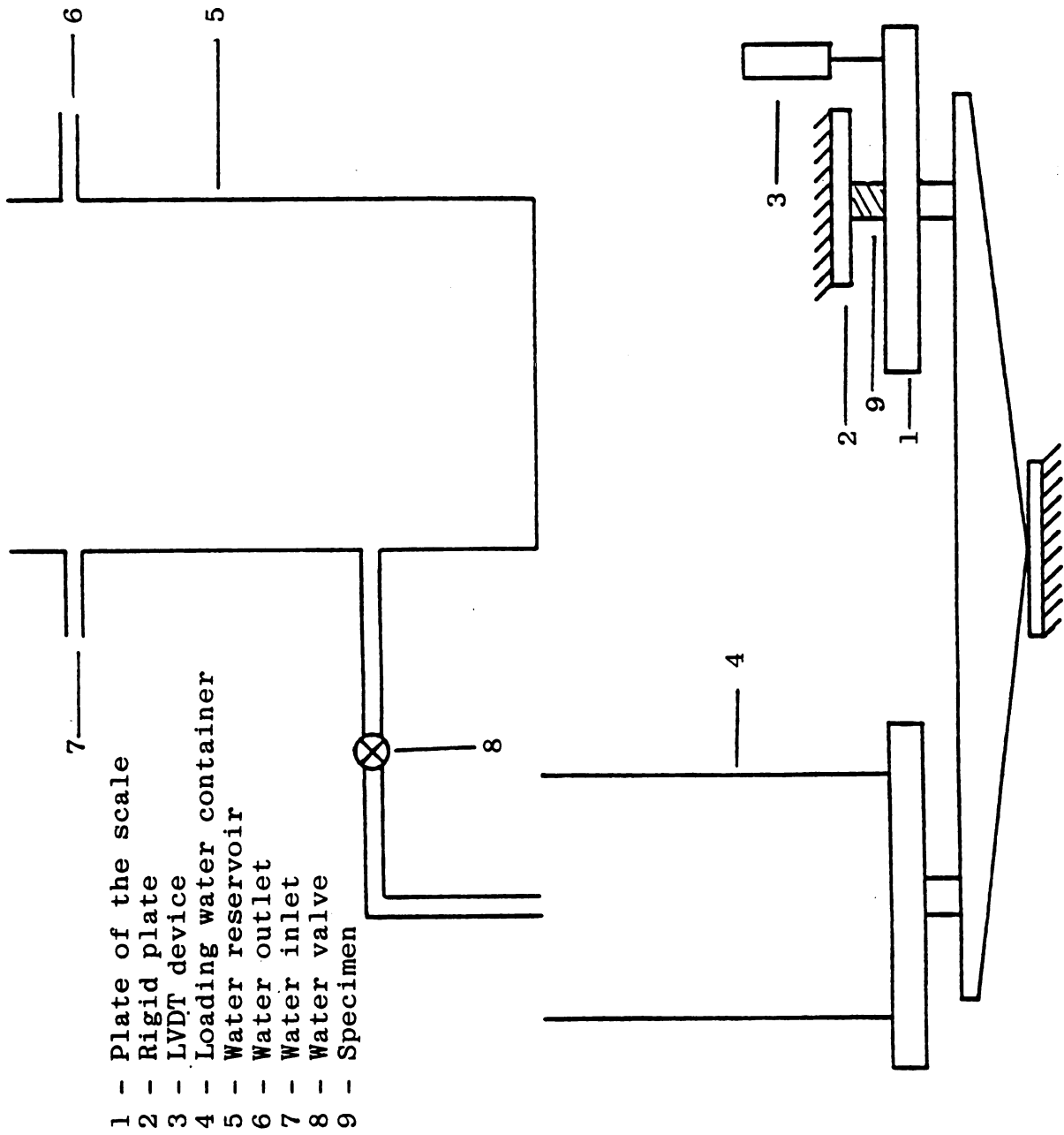


Figure 5.4. Creep loading apparatus.

CHAPTER VI

RESULTS AND DISCUSSION

6.1 General Remarks

Values of σ_{11} and ϵ_{11} at failure were experimentally obtained for all the loading cases discussed in Chapter V. In the case of triaxial loading, the values of σ_{22} were also known. Remaining parameters such as ϵ_{22} for uniaxial and triaxial tests, ϵ_{33} and σ_{22} for biaxial and σ_{22} for rigid die loading were determined using elastic and viscoelastic formulations. This allowed the experimental and theoretical values of σ_{11} to be compared. The availability of σ_{22} also made possible the calculation of τ_{\max} and ϵ_{22} which was needed for the calculation of the strain energy components.

Viscoelastic relaxation functions were not available for the McIntosh and Jonathan varieties. The functions $E(t)$, $X(t)$, $G_1(t)$, $G_2(t)$ and $\nu(t)$ determined by DeBaeremaeker, 1975, apply only to Red Delicious. However, the experimental data obtained for McIntosh and Jonathan varieties are presented in parallel with those from Red Delicious with the purpose of comparison.

6.2 Uniaxial Loading of Cylindrical Specimens at Different Strain Rates

In the uniaxial compression test of cylindrical specimens, strain rates of -0.002 sec^{-1} to -0.347 sec^{-1} were imposed. Average values and standard deviations of stress and strain to failure are shown in Table 6.1. This data is also illustrated on Figures 6.1, 6.2 and 6.3, respectively. The axial stress increases exponentially as strain rate increases while strain values at failure do not exhibit significant changes.

Figure 6.2 suggests that strain at failure can be represented by a straight line parallel to the horizontal axis. The average axial strain values for the various strain rates are $-0.11 \pm 0.008 \text{ mm/mm}$, $-0.13 \pm 0.017 \text{ mm/mm}$ and $-0.12 \pm 0.012 \text{ mm/mm}$ for Red Delicious, Jonathan and McIntosh, respectively. Standard deviations for the axial stress at failure varies from 10 to 15 percent. The standard deviation for strain at failure was about 10 percent of its average value.

The value of σ_{11} calculated using the viscoelastic formulation has the same general form as the experimental data. A constant value of σ_{11} was not obtained because the strain rate is a parameter in the viscoelastic formulation.

Lateral strain ϵ_{22} at failure was calculated from the elastic equation (4.31) and its viscoelastic counterpart (4.61). The values obtained from the elastic formulation are higher than the viscoelastic values, however both of them are relatively constant. From Table 6.2 one can see

TABLE 6.1. Uniaxial Loading of Cylindrical Apple Specimens for Different Strain Rates. Average Values and Standard Deviations of Stress, Strain and Time at Failure.

MC INTOSH			JONATHAN			RED DELICIOUS			
ϵ_{11} (sec ⁻¹)	σ_{11} (MPa)	ϵ_{11} (mm/mm)	t (sec)	σ_{11} (MPa)	ϵ_{11} (mm/mm)	t (sec)	σ_{11} (MPa)	ϵ_{11} (mm/mm)	t (sec)
-0.002	-0.18 0.02*	-0.14 0.01*	70.00 5.14*	-0.19 0.01*	-0.15 0.01*	75.00 8.37*	-0.29 0.04*	-0.12 0.02*	60.00 7.30*
-0.007	-0.24 0.02*	-0.12 0.01*	17.39 1.86*	-0.27 0.02*	-0.14 0.02*	20.29 1.69*	-0.32 0.02*	-0.11 0.01*	15.94 1.01*
-0.017	-0.23 0.04*	-0.12 0.01*	6.93 0.01*	-0.29 0.03*	-0.11 0.02*	6.35 0.93*	-0.30 0.03*	-0.12 0.01*	6.94 0.83*
-0.035	-0.26 0.03*	-0.12 0.01*	3.46 0.43*	-0.30 0.04*	-0.12 0.02*	3.46 0.46*	-0.35 0.03*	-0.11 0.01*	3.17 0.35*
-0.069	-0.26 0.02*	-0.13 0.01*	1.88 0.02*	-0.32 0.04*	-0.13 0.02*	1.88 0.35*	-0.34 0.03*	-0.12 0.01*	1.74 0.18*
-0.173	-0.28 0.03*	-0.10 0.01*	0.58 0.06*	-0.34 0.04*	-0.10 0.01*	0.58 0.09*	-0.35 0.06*	-0.10 0.01*	0.56 0.08*
-0.346	-0.27 0.02*	-0.13 0.02*	0.37 0.06*	-0.33 0.02*	-0.13 0.01*	0.37 0.04*	-0.34 0.03*	-0.12 0.01*	0.35 0.04*

(*) standard deviation.

TABLE 6.2. Uniaxial Loading of Cylindrical Specimens of Red Delicious at Different Strain Rates. Strain Energy Components Obtained from Experimental Values of σ_{11} and ϵ_{11} and Calculated Values of ϵ_{22} . Maximum Shear Stress Obtained from Experimental Data and Values of ϵ_{22} Calculated from the Elastic and Viscoelastic Theories.

ϵ_{11-1} (sec ⁻¹)	τ_{max} (MPa)	(MPa)	ϵ_{22} (mm/mm)	Us (J)	Ud (J)	U (J)	σ_{11}	ϵ_{22}	Us (J)	Ud (J)	U (J)
-0.002	0.145	-0.349	-0.042	0.069	0.002	0.067	-0.358	-0.035	0.069	0.002	0.067
-0.007	0.160	-0.320	-0.039	0.070	0.002	0.068	0.363	-0.035	0.069	0.002	0.067
-0.017	0.150	-0.349	-0.042	0.071	0.002	0.070	-0.414	-0.039	0.071	0.002	0.069
-0.035	0.175	-0.320	-0.039	0.076	0.002	0.074	-0.418	-0.036	0.076	0.002	0.074
-0.069	0.170	-0.349	-0.042	0.081	0.002	0.079	-0.426	-0.039	0.081	0.002	0.078
-0.173	0.175	-0.291	-0.035	0.070	0.002	0.068	-0.349	-0.032	0.069	0.002	0.067
-0.346	0.170	-0.349	-0.042	0.081	0.003	0.079	-0.436	-0.033	0.080	0.003	0.077

THEORY OF ELASTICITY

THEORY OF VISCOLASTICITY

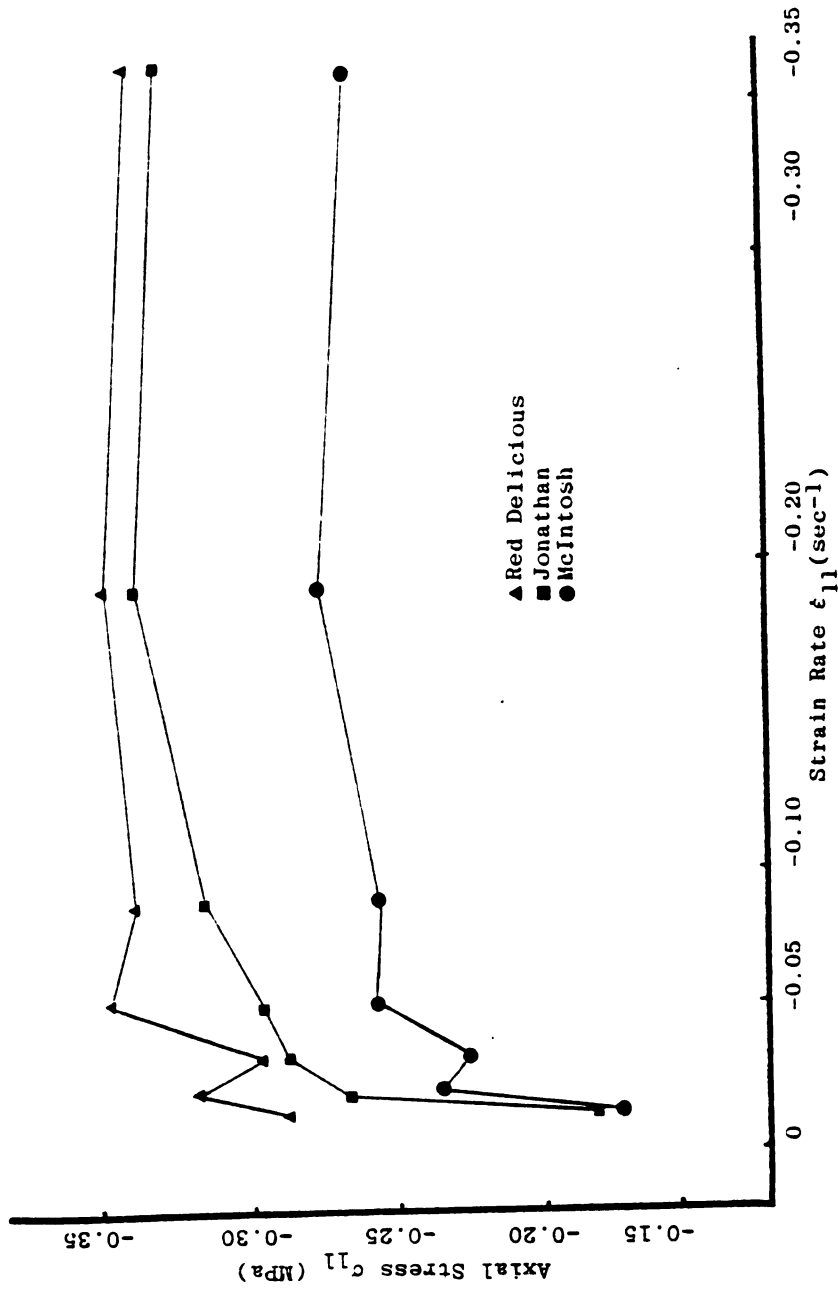


Figure 6.1. Stress at failure versus strain rate for uniaxial loading of cylindrical apple specimens.

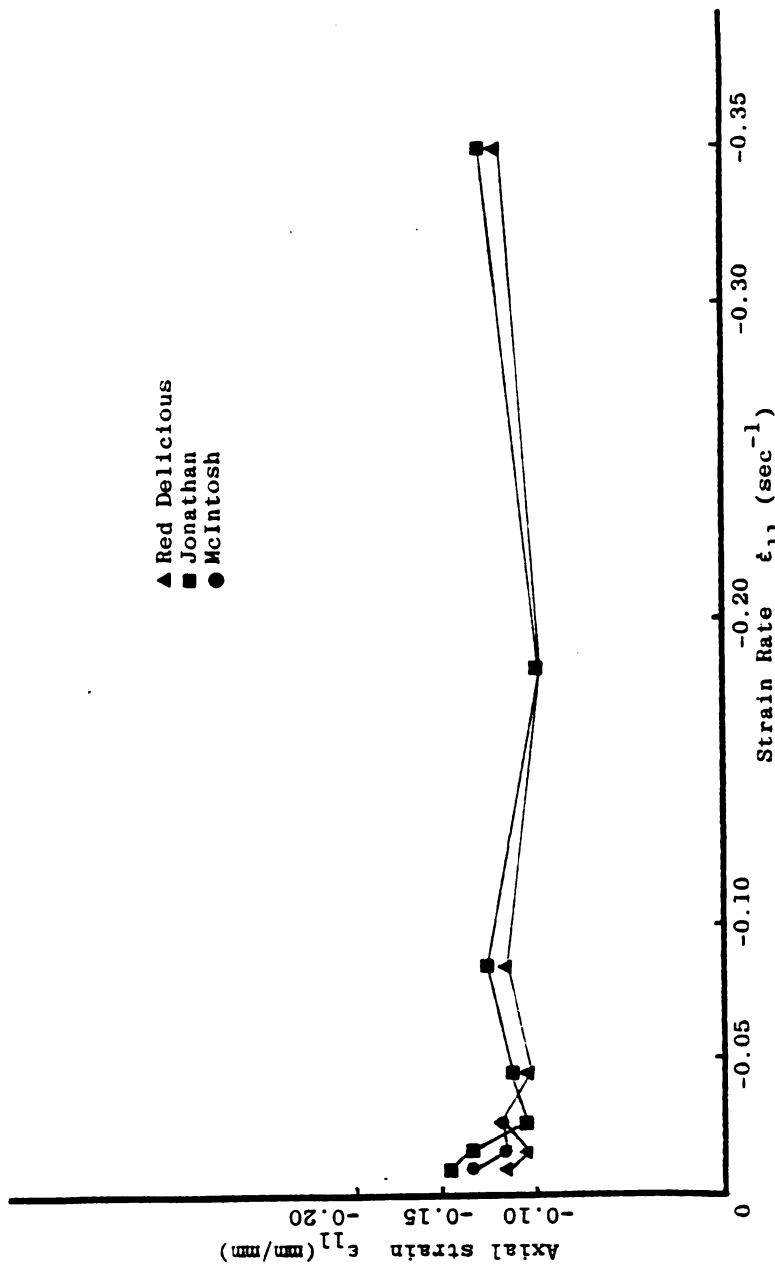


Figure 6.2. Strain at failure versus strain rate for uniaxial loading of cylindrical apple specimens.

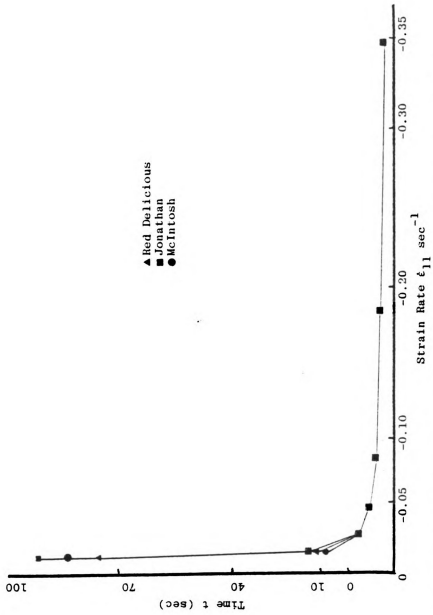


Figure 6.3. Time versus strain rate for uniaxial loading of cylindrical apple specimens.

that the values of U_d are quite constant; this seems reasonable when we consider that U_d is calculated from strain parameters. Remaining parameters, τ_{\max} , U_s , and U vary as strain rate changes. Strain at failure presents a relatively constant value as strain rate varies. From these results it appears that the axial strain is a possible failure parameter.

6.3 Triaxial Loading of Cylindrical Apple Specimens

The average values of axial stress, axial strain and time at failure as well as the values of the imposed radial stresses during the triaxial loading studies are displayed on Table 6.3 and illustrated on Figures 6.4, 6.5 and 6.6, respectively. The average normal stress σ_{11} decreases while the normal strain ϵ_{11} remains relatively constant when the radial stress increases. McIntosh and Jonathan varieties failed for a radial stress loading between -0.345 and -0.414 MPa and Red Delicious failed between -0.414 and -0.483 MPa when $\sigma_{11}=0$ MPa. This means that radial stress at failure is twice or three times larger than the axial stress at failure, which eliminates the maximum normal stress failure criteria.

Table 6.4 shows the values of the maximum shear stress calculated from experimental data as well as the strain energy components obtained from elastic and viscoelastic theory. Maximum shear stress decreases to a minimum of -0.028 MPa and increases for consecutive values of radial stress. This indicates that during a continuous variation

TABLE 6.3. Triaxial Loading of Cylindrical Apple Specimens for Different Radial stresses and Constant Strain Rate. Average values of Time, Axial Stress and Strain at Failure.

MC INTOSH				JONATHAN				RED DELICIOUS				
σ_{22}	σ_{11}	ϵ_{11}	t	σ_{11}	ϵ_{11}	t	σ_{11}	ϵ_{11}	t	σ_{11}	ϵ_{11}	tt
(MPa)	(MPa)	(mm/mm)	(sec)									
0.000	-0.24	-0.12	17.39	-0.27	-0.14	20.29	-0.32	-0.11	15.94	0.01*	0.01*	1.81*
												1.09*
-0.069	-0.23	-0.13	18.84	-0.26	-0.13	18.84	-0.30	-0.13	18.84	0.02*	0.01*	1.69*
												1.83*
-0.138	-0.22	-0.15	21.73	-0.25	-0.14	20.29	-0.26	-0.12	17.39	0.04*	0.04*	5.40*
												3.83*
-0.207	-0.22	-0.11	15.94	-0.22	-0.12	17.39	-0.26	-0.12	17.39	0.04*	0.02*	3.01*
												3.24*
-0.276	-0.18	-0.10	14.49	-0.19	-0.11	15.94	-0.22	-0.12	17.39	0.03*	0.02*	2.84*
												3.43*
-0.345	0.00	0.00	0.00	0.00	0.00	0.00	0.20	0.11	15.94	0.00	0.11	0.00
												2.63*

(*) standard deviation.

TABLE 6.4. Triaxial Loading of Cylindrical Specimens of Red Delicious at Different Radial Stress. Strain Energy Components Obtained from Experimental Values of σ_{11} and Calculated Values of ϵ_{22} . Maximum Shear Stress Obtained from Experimental Data and Values of ϵ_{22} Calculated from Elastic and Viscoelastic Theories. $E=2.909$ MPa, $\nu=0.35$.

σ_{22} (MPa)	τ_{max} (MPa)	σ_{11} (MPa)	ϵ_{22} (mm/mm)	Us (J)	Ud (J)	U (J)	σ_{11} (MPa)	ϵ_{22} (mm/mm)	Us (J)	Ud (J)	U (J)
-0.000	0.160	-0.320	-0.038	0.070	0.002	0.068	-0.369	-0.014	0.076	0.009	0.067
-0.069	0.116	-0.368	-0.036	0.074	0.004	0.070	-0.389	-0.029	0.074	0.005	0.069
-0.138	0.081	-0.446	-0.023	0.072	0.007	0.065	-0.484	-0.015	0.060	0.008	0.052
-0.207	0.027	-0.494	-0.013	0.056	0.010	0.046	-0.526	-0.004	0.061	0.013	0.048
-0.276	0.028	-0.542	-0.004	0.062	0.014	0.048	-0.568	+0.006	0.051	0.017	0.034
-0.345	0.036	-0.561	-0.009	0.041	0.019	0.022	-0.581	+0.019	0.046	0.022	0.024

THEORY OF ELASTICITY

THEORY OF VISCOELASTICITY

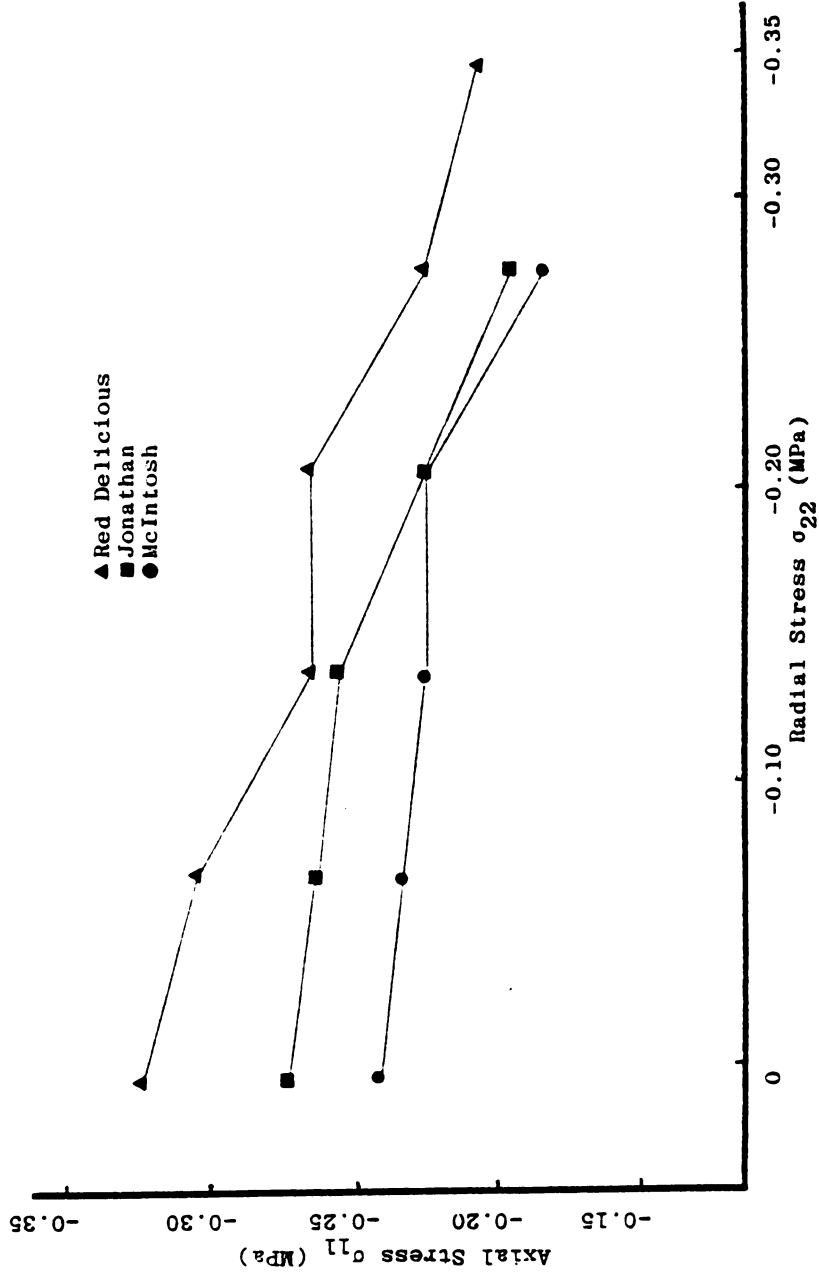


Figure 6.4. Axial stress at failure versus radial stress for triaxial loading of cylindrical apple specimens.

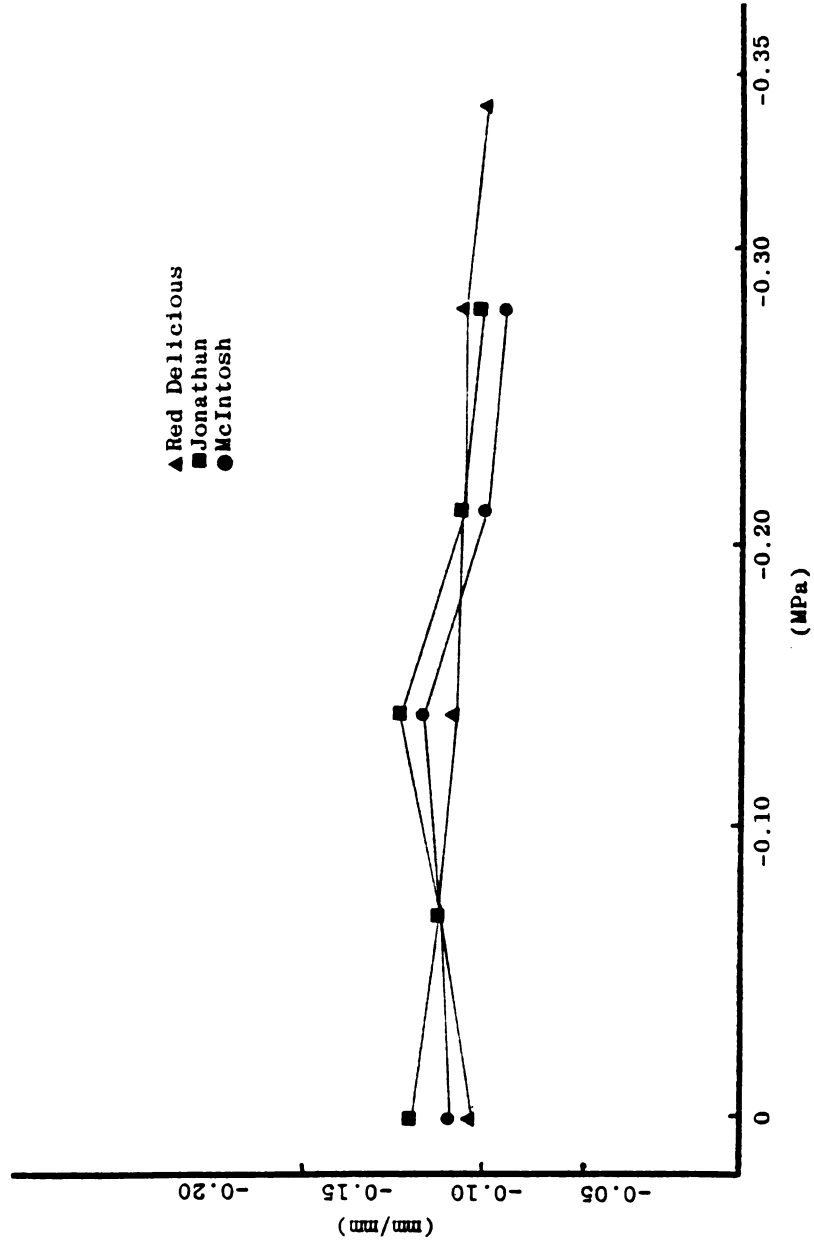


Figure 6.5. Strain at failure versus radial stress for triaxial loading of cylindrical apple specimens.

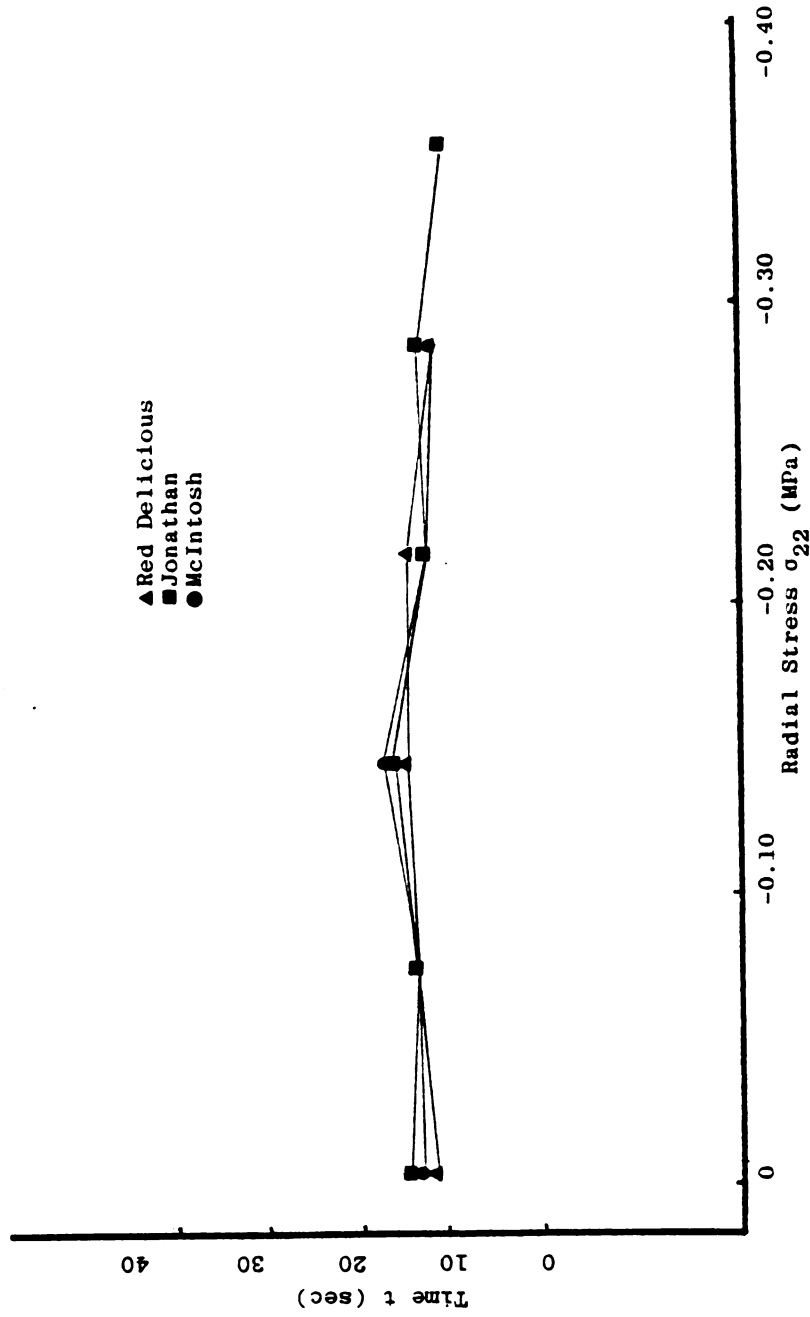


Figure 6.6. Time at failure versus radial stress for triaxial loading of cylindrical apple specimens.

of radial stress, the maximum shear stress would reach values close to zero or even possibly zero at failure. This eliminates the possibility of the apple flesh failing when the maximum shear stress exceeds a critical value.

Table 6.4 presents a relative constant value for the spherical component of the total strain energy at failure as calculated by the elastic theory. However, the viscoelastic results show a relative variation for the spherical energy component. Remaining strain energy components vary with increasing values of radial stress. Results from triaxial loading of cylindrical specimens strongly point to the conclusion that apple flesh fails when a critical value of normal strain reaches a critical value.

6.4 Uniaxial, Biaxial and Rigid Die Loading of Cubic Specimens. Uniaxial and Rigid Die Loading of Cylindrical Specimens.

Uniaxial, biaxial and rigid die loadings of cubic specimens are formulated by the elastic equations (4.25) to (4.31) and by the viscoelastic equations (4.50) to (4.57), (4.60) and (4.61), respectively. Table 6.4 gives the experimentally obtained parameters and Table 6.6 gives the calculated values for σ_{11} and the values for the remaining parameters as calculated by the above equations, in addition to maximum shear stress values. The axial normal stress varies for the different loading cases, for both the cubic and cylindrical specimens, while the axial normal strain remains relatively constant. This supports the conclusion

TABLE 6.5. Rigid Die Loading of Cylindrical (1) and Cubic (4) Specimens, Uniaxial (2) and Biaxial (3) Loadings of Cubic Specimens of Appple. Values Average and Standard Deviations of Stress, Strain and Time at Failure.

	MC INTOSH				JONATHAN				RED DELICIOUS			
	σ_{11} (MPa)	ϵ_{11} (mm/mm)	t (sec)	σ_{11} (MPa)	ϵ_{11} (mm/mm)	t (sec)	σ_{11} (MPa)	ϵ_{11} (mm/mm)	t (sec)	σ_{11} (MPa)	ϵ_{11} (mm/mm)	t (sec)
(1)	-0.36 0.06*	-0.12 0.01*	17.39 1.82*	-0.37 0.09*	-0.12 0.02*	17.39 3.21*	-0.44 0.08*	-0.11 0.01*	15.94 1.62*			
(2)	-0.27 0.02*	-0.12 0.01*	17.39 1.89*	-0.27 0.02*	-0.11 0.01*	15.94 2.16*	-0.25 0.02*	-0.11 0.02*	15.94 2.38*			
(3)	-0.27 0.03*	-0.12 0.01*	17.39 1.72*	-0.34 0.05*	-0.13 0.01*	18.84 2.26*	-0.39 0.04*	-0.12 0.01*	17.39 1.77*			
(4)	-0.35 0.08*	-0.12 0.02*	17.39 2.71*	-0.38 0.08*	-0.14 0.04*	20.29 5.94*	-0.53 0.05*	-0.12 0.02*	17.39 2.19*			

(*) standard deviation.

TABLE 6.6. Uniaxial (1), Biaxial (2) and Rigid Die Loadings (3) of Cubic Specimens. Rigid Die Loading of Cylindrical Specimens (4). Axial Stress and Strain, Lateral or Radial Stress and Strain and Energy Components Obtained from Elastic and Viscoelastic Theories.

Results from Elastic Theory						
σ_{11} (MPa)	σ_{22} (MPa)	ϵ_{22} (mm/mm)	τ_{max} (MPa)	US (J)	Ud (J)	U (J)
(1) -0.320	0.000	-0.039	0.160	0.010	0.057	0.149
(2) -0.398	-0.139	-0.065	0.126	0.017	0.067	0.084
(3) -0.560	-0.302	0.000	0.114	0.023	0.155	0.178
(4) -0.514	-0.302	0.000	0.067	0.020	0.129	0.149
Results from Viscoelastic Theory						
(1) -0.363	0.000	-0.035	0.060	0.020	0.106	0.126
(2) -0.390	-0.138	-0.056	0.162	0.012	0.012	0.070
(3) -0.536	-0.459	0.000	0.086	0.023	0.141	0.164
(4) -0.497	-0.425	0.000	0.060	0.020	0.106	0.126

TABLE 6.7 Stress Controlled Loading of Specimens of Red Delicious. Calculated Values of Strain Energy Components, Experimental Values of axial Stress, Strain and Maximum Shear Stress at Failure.

$\dot{\sigma}_{11}$ (MPa/sec)	σ_{11} (MPa)	ϵ_{11} (mm/mm)	$\epsilon_{11}(\text{calc})$ (mm/mm)	ϵ_{22} (mm/mm)	τ_{max} (Mpa)	U_s (Joules)	U_d (Joules)	U (Joules)
-0.0005	-0.391	-0.124	-0.166	0.069	0.196	0.001	0.003	0.004
-0.002	-0.355	-0.124	-0.127	0.045	0.178	0.002	0.003	0.005
-0.003	-0.322	-0.118	-0.113	0.035	0.161	0.003	0.009	0.012
-0.005	-0.230	-0.119	-0.111	0.023	0.115	0.003	0.008	0.011
-0.008	-0.182	-0.119	-0.056	0.018	0.091	0.003	0.008	0.011
-0.013	-0.139	-0.123	-0.041	0.014	0.070	0.002	0.008	0.010

TABLE 6.8. Uniaxial Loading of Cylindrical Apple Specimens, Average Values and standard deviations of deformation at $\sigma_{11} = -0.11$ Mpa.

	H(mm)	H(mm)	H(mm)	H(mm)	H(mm)
	8.32	12.13	19.17	26.55	34.98
	0.06*	0.12*	0.13*	0.16*	0.11*
Varieties	U1(mm)	U1(mm)	U1(mm)	U1(mm)	U1(mm)
Mc Intosh	-8.20	-10.75	-13.83	-16.18	-20.67
	1.54*	2.13*	2.40*	2.47*	2.46*
Jonathan	-8.31	-8.98	-12.16	-14.37	-18.75
	2.27*	1.82*	2.19*	1.77*	2.61*
Red Delicious	-6.07	-5.86	-8.66	-10.34	-13.41
	1.80*	1.57*	2.05*	1.32*	1.49*

(*) standard deviation

TABLE 6.9. Uniaxial Loading of Cylindrical Apple Specimens of Different Height. Axial Strain and Stress at $\sigma_{11} = -0.11$ MPa for McIntosh (1), Jonathan (2), and Red Delicious (3).

	H (mm)				
	8.320	12.130	19.170	26.550	34.980
	ϵ_{11}	ϵ_{11}	ϵ_{11}	ϵ_{11}	ϵ_{11}
	(mm/mm)	(mm/mm)	(mm/mm)	(mm/mm)	(mm/mm)
(1)	-0.096	-0.088	-0.072	-0.061	-0.059
(2)	-0.100	-0.074	-0.066	-0.054	-0.056
(3)	-0.070	-0.059	-0.044	-0.041	-0.038

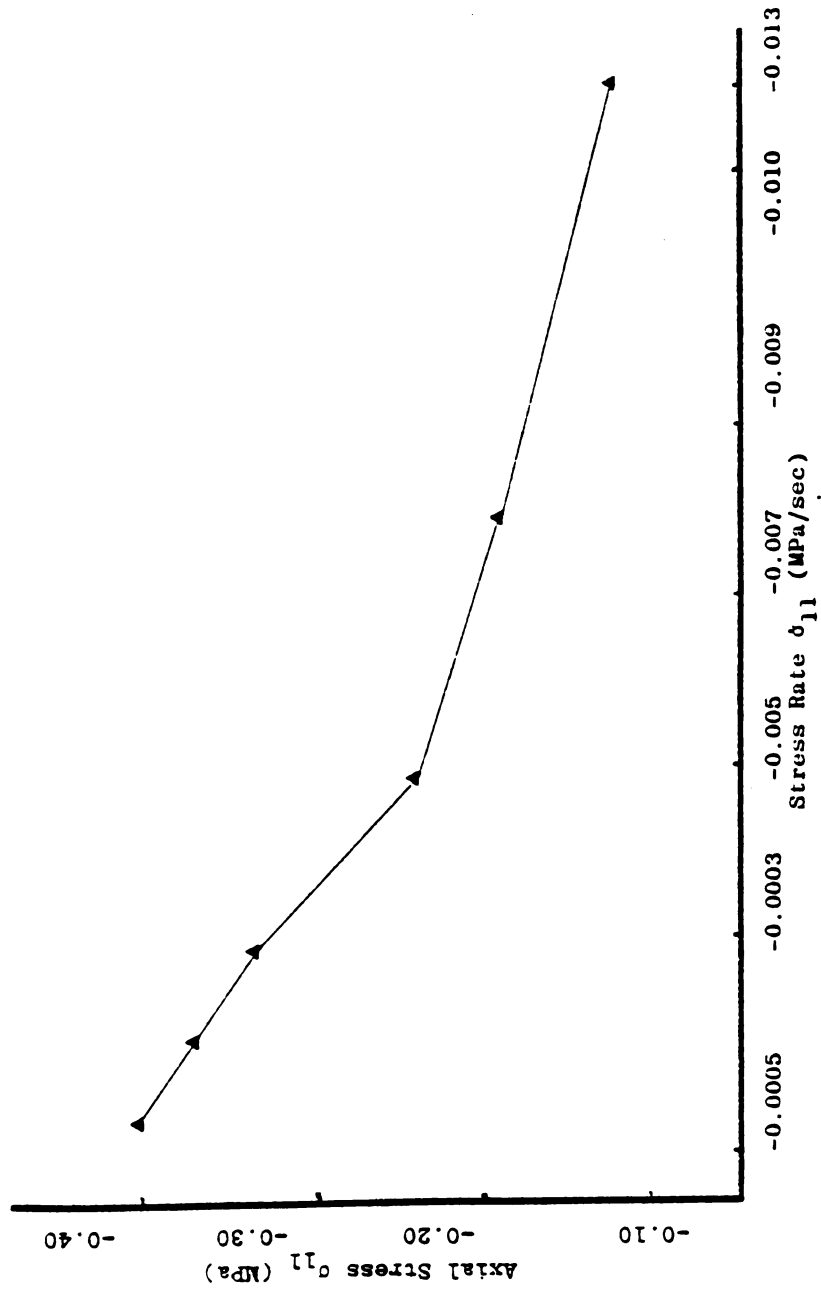


Figure 6.7. Stress at failure for controlled stress rate loading of cylindrical specimens of Red Delicious.

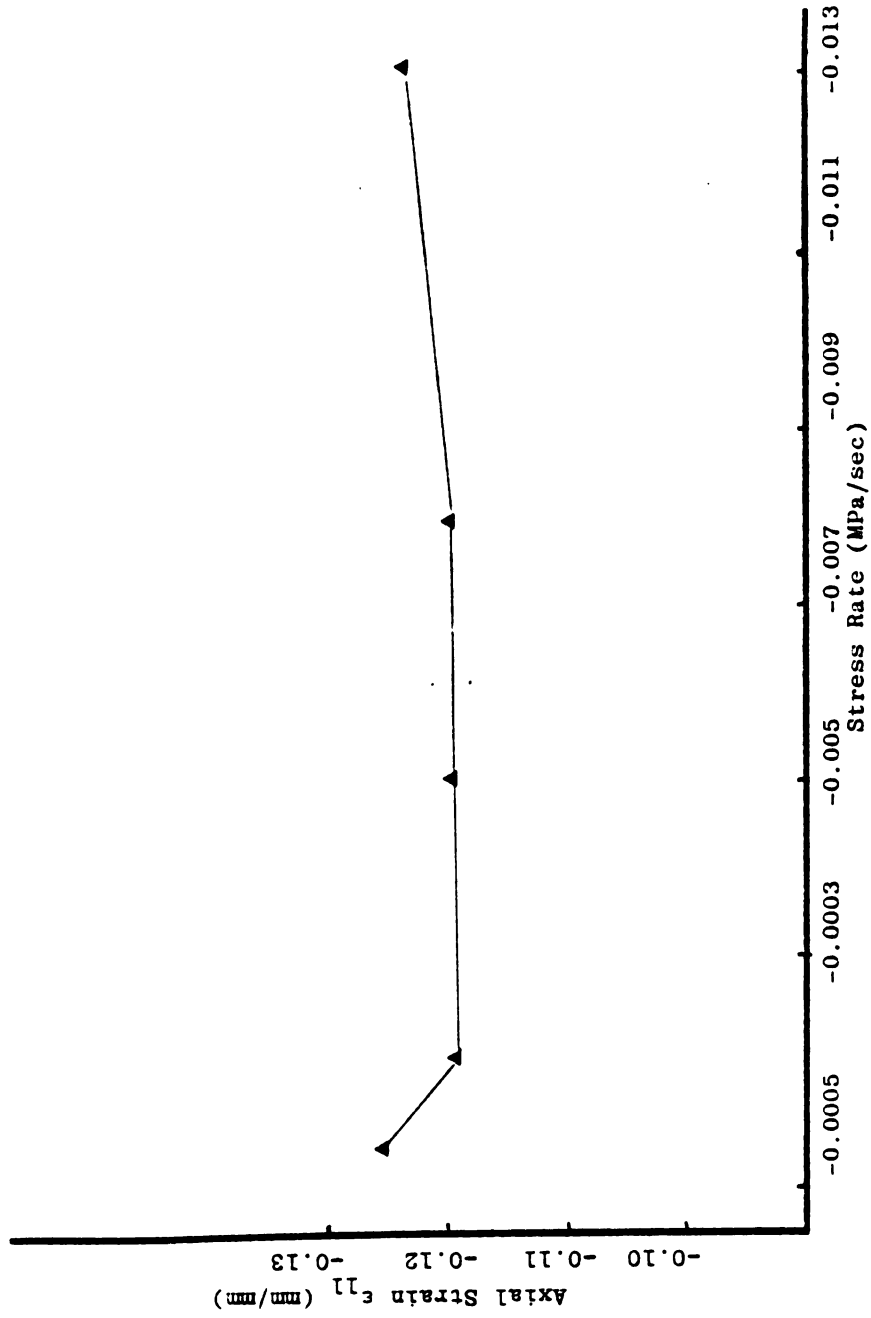


Figure 6.8. Strain at failure versus stress rate for controlled stress rate of Red Delicious.

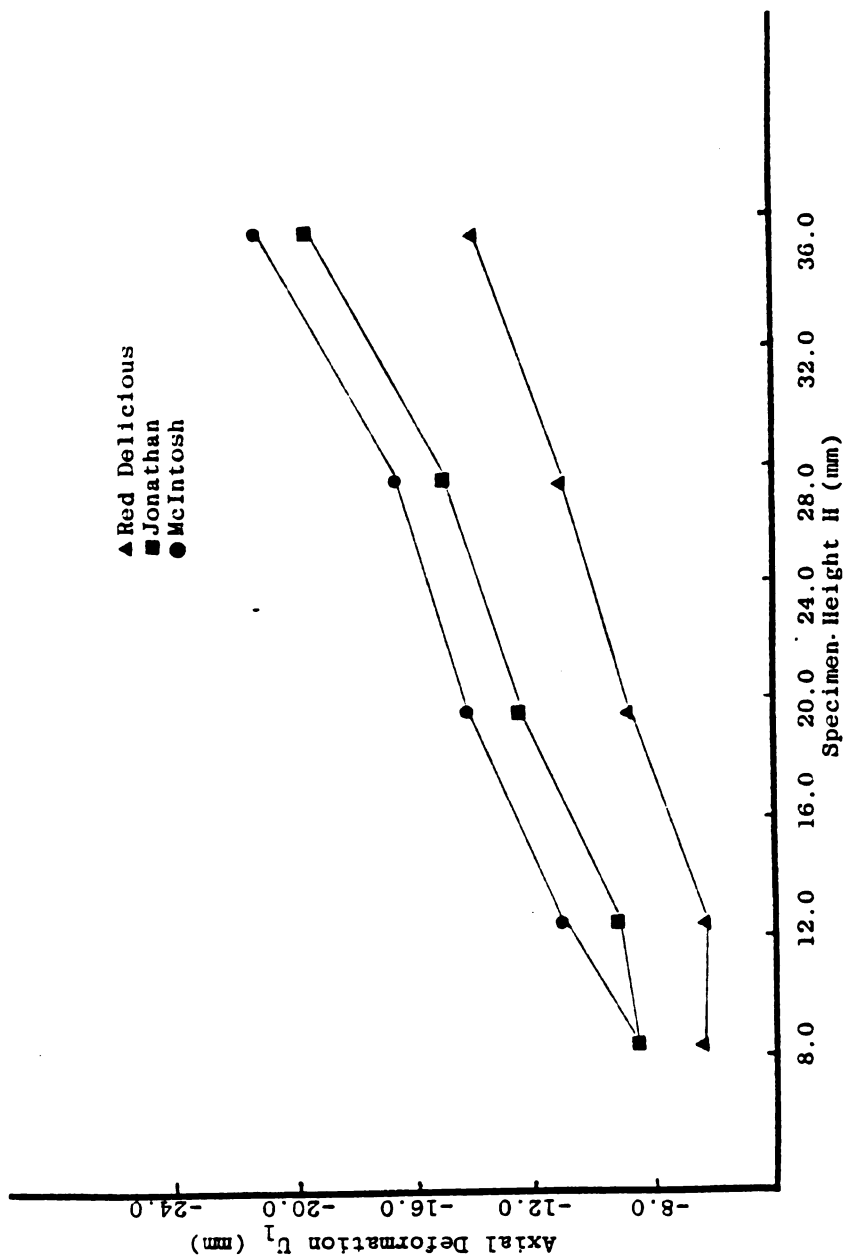


Figure 6.9. Deformation values of cylindrical apple specimens of different height at constant axial stress value during uniaxial loading.

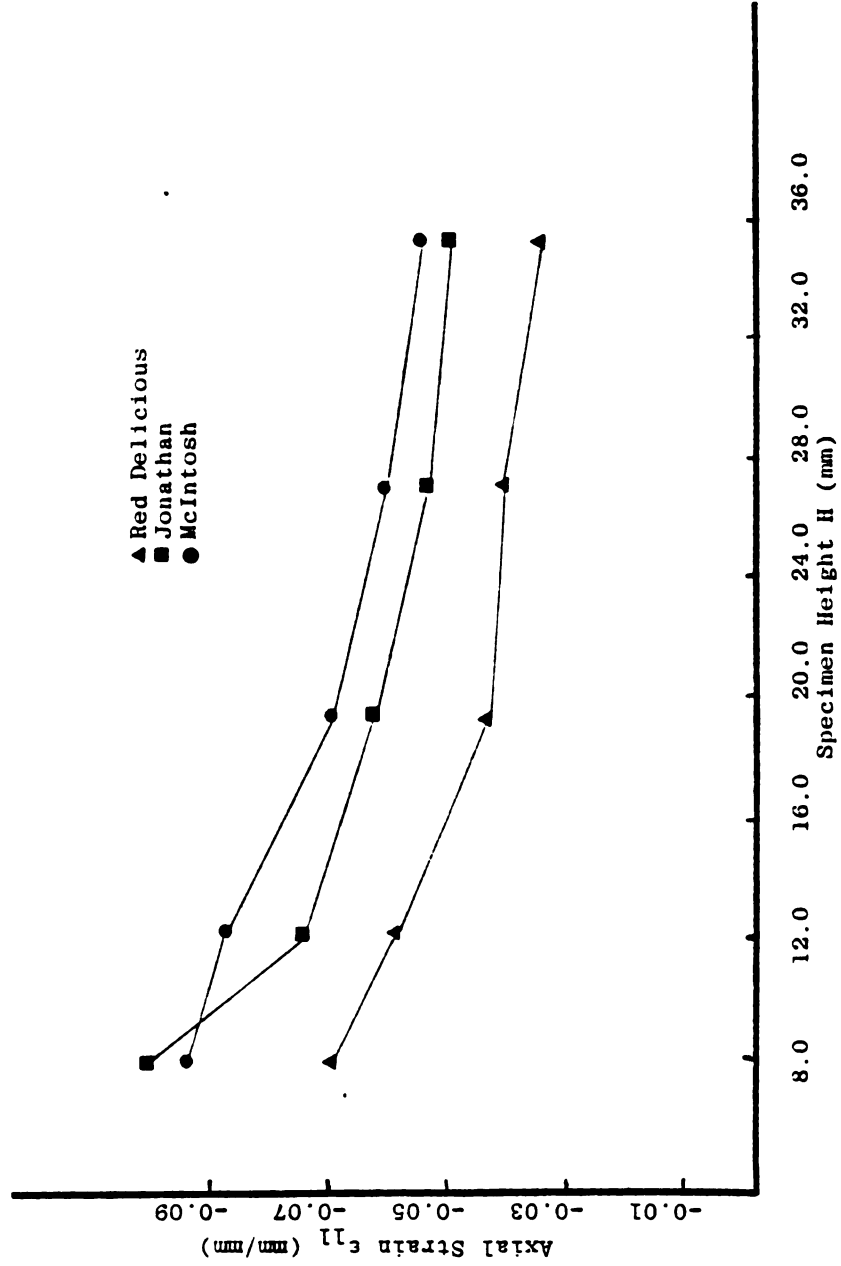


Figure 6.10. Strain values of cylindrical apple specimens of different height at constant stress values during uniaxial loading.

drawn from the experimental results presented in 6.2 and 6.3 that axial normal strain is a possible failure parameter. This group of tests discards the possibility of the maximum normal stress being considered as the failure parameter.

6.5 Stress Controlled Loading of Cylindrical Specimens of Red Delicious

Normal stress at failure decreases from -0.391 MPa to -0.139 MPa as the stress rate increases from -0.0005 MPa/sec to -0.013 MPa/sec, while the strain at failure remains relatively constant, averaging -0.12 mm/mm, Table 6.7 and Figures 6.7 and 6.8. Table 6.7 also gives the values of the maximum shear stress and strain energy components at failure. The fact that a creep failure can be induced in apple specimens is additional support to the hypothesis that apple flesh fails when normal strain reaches a critical value.

6.6 The Non-linear Viscoelastic Formulation for Apple Material

Cylindrical specimens of apples of different lengths were axially compressed. For each different length, the axial deformation $U_1(X_1, t)$ at a predetermined stress level $\sigma_{11} = -0.11$ MPa, was obtained as explained in Section 5.5. Table 6.9 shows these deformation values for each of the five lengths. These values are also illustrated on Figures 6.9 and 6.10, respectively. Ideal conditions are assumed, i.e., axial stress does not change along the X_1 coordinate

which is the same as to say that the deformation at $\sigma_{11} = -0.11$ MPa for the specimens of different height each, represents the deformation along the X_1 axis for the tallest specimen. In this case, X_1 assumes values equal to the heights of each individual specimen. Time parameter is referred to the deformation of the tallest specimen ($H = 34.98$ mm).

Data from Table 6.9 can be fitted in the following power function for McIntosh, Jonathan and Red Delicious, respectively,

$$U_1(X_1) = (-1.007 X_1 - 0.036X_1^2 + 0.007X_1^3 - 0.0004X_1^4) \quad (6.1)$$

$$U_1(X_1) = (-3.099X_1 + 0.454X_1^2 - 0.031X_1^3 + 0.001X_1^4) \quad (6.2)$$

$$U_1(X_1) = (-3.088X_1 + 0.579X_1^2 - 0.049X_1^3 + 0.002X_1^4) \quad (6.3)$$

with the following respective coefficient of determination: 0.99, 0.99 and 0.99.

If the deformation rate of -0.085 mm/sec is imposed at $X_1 = 34.98$ mm (top of the specimen) and time $t = 15.84$ sec at $\sigma_{11} = -0.11$ MPa are computed, equation 6.1 can be rewritten as:

$$U_1(X_1, t) = (-0.195X_1 + 0.036 X_1^2 - 0.003X_1^3 + 0.0001X_1^4)t \quad (6.4)$$

With the deformation function written in terms of spatial and time coordinates the elements of equation (4.70) can be determined as:

$$\epsilon_{11}(X_1, t) = (-0.195 + 0.072X_1 - 0.009X_1^2 + 0.0004X_1^3)t \quad (6.5)$$

$$\frac{\partial \epsilon_{11}}{\partial t} = (-0.195 + 0.072X_1 - 0.009X_1^2 + 0.0004X_1^3) \quad (6.6)$$

$$v^{(1)} = (-0.195X_1 + 0.036X_1^2 - 0.003X_1^3 + 0.0001X_1^4) \quad (6.7)$$

$$\frac{\partial \epsilon_{11}}{\partial X_1} = (0.072 - 0.018X_1 + 0.0012X_1^2)t \quad (6.8)$$

$$\frac{\partial v^{(1)}}{\partial X_1} = (-0.195 + 0.072X_1 - 0.009X_1^2 + 0.0004X_1^3) \quad (6.9)$$

From equations (4.66), (6.1), (6.2), (6.3), (6.4), (6.5), (6.6), (6.7), (6.8), and (6.9), the convected axial strain rate can be written as:

$$\begin{aligned} \frac{D\epsilon_{11}}{Dt} = & (-0.195 + 0.072X_1 - 0.009X_1^2 + 0.0004X_1^3) \\ & + 2(-0.195 - 0.072X_1 - 0.009X_1^2 + 0.0004X_1^3)^2 \\ & + (-0.195 + 0.036X_1^2 - 0.003X_1^3 + 0.0001X_1^4) \\ & \cdot (0.072 - 0.018X_1 + 0.0012X_1^2)t \end{aligned} \quad (6.10)$$

Equation (6.4) should be rewritten if the specimen has a total height different from 34.98 mm and it is subjected to a deformation ratio different from -0.085 mm/sec. Equation (6.5) describes the variation of strain along the X_1 coordinate and according to time. Equation (6.10) is the convected strain rate to be substituted on linear viscoelastic equations.

The introduction of the spatial coordinate in the visco-elastic equations enables one to relate the strain and strain rate parameters to a fixed point in the body being loaded.

A valid question could be raised against such experimental procedure. By loading different sizes of specimens, contact stress is developed on the surface being loaded. If only the taller specimens were tested and the deformations were obtained at several axial positions, the question raised could be neglected. A quite useful technique to circumvent this problem would be to mark several points along the height of the specimen and to record the positions of the points by taking pictures during several steps of the loading procedure. Further analysis of those pictures would yield the data to describe the deformation function. Another second question is related to the Poisson's ratio effect. If lateral deformation is measured, the chosen stress level could be found to be slightly different for each specimen.

Equation 6.5 indicates that strain is larger for higher values of X_1 . In other words, strain is higher at the top of the specimen. If normal strain is the failure parameter, failure should start on the surface where the load is being applied. Figure 6.10 illustrates the variations of axial strain for different specimen height.

6.7 Summary

Experimental results from uniaxial, biaxial, triaxial, rigid die and creep loading were used to study the parameters

involved in the failure phenomena of apple material. Elastic and viscoelastic formulations were used to calculate the parameters not experimentally obtained.

From the parameters considered -- maximum normal stress, maximum shear stress, maximum normal strain and strain energy components -- the maximum normal strain was found to be the most likely factor producing a failure in apple flesh.

A non-linear viscoelastic formulation has been proposed, based on the model described by Oldroyd (1950) and Fredrickson (1964). Such modeling procedure consists in obtaining the deformation vector as a function of time and space from which the convected strain rate tensor was obtained. The substitution of the strain rate tensor from linear viscoelastic equations by the convected strain rate tensor completes the non-linear viscoelastic formulation.

CHAPTER VII
SUMMARY AND CONCLUSIONS

A failure criteria for apple flesh was presented. A new experimental technique has been developed in order to apply biaxial and triaxial loadings on apple specimens. Uniaxial loading of apple specimens showed that normal stress at failure varies with strain rate while the normal strain turned to be relatively constant. This eliminates the possibility of considering normal stress as failure parameter. Triaxial loading of cylindrical specimens also indicates a constant value for normal strain at different levels of cylindrical stress. This experiment also showed significant variations of shear stress and normal stress at failure, including failure of the specimens at zero level of shear stress, which eliminates the maximum shear stress as a failure criteria.

Uniaxial, biaxial, and rigid die loadings of cubic and cylindrical specimens indicated that normal strain at failure remained relatively constant for these different loading cases, meanwhile the normal stress at failure varied. This group of experiments also eliminates the maximum normal stress as a failure criteria. Stress controlled uniaxial loading shows decreasing values of normal stress

at failure and constant values for normal strain at different stress rate values. This test also eliminates the maximum normal stress failure criteria.

Calculated values of total strain energy and its spherical and deviatoric components, obtained from viscoelastic and elastic equations showed significant variations.

A non-linear viscoelastic constitutive equation, based on the substitution of the strain rate tensor by a convected strain (Oldroyd, 1950) was proposed. For this accomplishment a deformation function in terms of time and space had been obtained. This resulted in a time and space dependent strain and strain rate tensors.

The following conclusions can be drawn from this study:

1. Apple tissue fails when a normal strain exceeds a limiting value. The average normal strain values at failure for all the tests conducted was 0.116 0.007 mm/mm for Red Delicious, 0.126 0.014 mm/mm for Jonathan and 0.122 0.013 mm/mm for McIntosh.
2. There exist a noticeable difference in the mechanical behavior of the three apple varieties tested.
3. The developed experimental procedure yields reliable data.
4. The proposed non-linear viscoelastic constitutive equation can be considered as a preliminary step toward more complete formulations.

CHAPTER VIII
SUGGESTIONS FOR FUTURE RESEARCH

In spite of positive conclusions concerning the failure of apple material that has been reached, certain points still remain unclear.

The present work shows a visible difference on the mechanical behavior of the varieties tested. It was seen that viscoelastic functions are available only for Red Delicious (DeBaerdemaeker, 1975). The determination of the time dependent functions $G_1(t)$, $G_2(t)$, $E(t)$ and $\nu(t)$ for varieties of economical importance would provide a better understanding of their mechanical behavior.

The strain level at failure possibly varies with the physiological state of the apple tissue. This includes ripening, time and conditions of storage, as well as water potential level. DeBaerdemaeker (1975) reported that the failure of cylindrical apple specimens under compressive uniaxial loads varies from -0.49 MPa at the beginning of the storage period up to -0.34 MPa after four months of storage. This information can be useful in determining the best physiological state for mechanical handling of apples. In other words, a certain amount of bruise damage can be expected for different stages of maturation, water

potential level and time of storage. These factors should be included in future experimental works.

Apple material has been considered homogeneous within the same experimental specimen. For the time being this assumption can be considered satisfactory, however the variation of mechanical properties inside of the fruit should be investigated. This topic should encompass the development of a more realistic shape for the apple fruit. The average size and shape for a specific variety should be determined. Now the whole fruit is divided into elements and for each element specific mechanical properties are allotted. This finite element model would yield the strain level distribution in the fruit. This concept will guide the handling of whole fruits since bruise could now be predicted and located.

The present experimental technique has proved to be successful and viscoelastic theory supports the interpretation of experimental data. The concept of strain failure can be extended to remaining vegetative material.

Suggestions to improve the non-linear viscoelastic formulation have already been presented in Section 6.7.

REFERENCES

REFERENCES

- Akyurt, M., 1969. Constitutive relations for Plant Materials. Unpublished Ph.D. thesis. Purdue University.
- Apaclla, R., 1973. Stress analysis in agricultural products using finite element method. Unpublished technical research report. Agricultural Engineering Department, Michigan State University.
- Bishop, A. W. and D. J. Henkel, 1962. The Measurement of Soil Properties in the Triaxial Test. Second edition. Edward Arnold, Ltd., London.
- Brusewitz, G. H., 1969. Consideration of plant materials as an interacting continuum. Unpublished Ph.D. thesis. Agricultural Engineering Department, Michigan State University.
- Bychawski, Z., 1975. Analysis of features and properties of physical non-linearities in viscoelastic behavior: Mechanics of viscoelastic media and bodies. Symposium Gothenburg/Sweden, September 2-6, 1974. Editor Jan Hult. Springer-Verlag, Berlin.
- Chappell, T. W. and D. D. Hamann, 1968. Poisson's ratio and Young's modulus for apple flesh under compressive loading. Transactions of the ASAE, 11(5):608-610.
- Chen, P. and R. B. Fridley, 1972. Analytical method for determining viscoelastic constants of agricultural products. Transactions of the ASAE, 15(6):1103-1106.
- Chen, P., H. E. Studer and S. T. Lam, 1975. A bulk compressibility tester for agricultural products. ASAE paper no. 75-5533.
- Clevenger, J. T. and D. D. Hamann, 1968. The behavior of apple skin under tensile loading. Transactions of the ASAE, 11(1):34-37.
- Christensen, R. M., 1971. Theory of Viscoelasticity. Academic Press, New York.
- Christensen, R. M., 1968. On obtaining solutions in non-linear viscoelasticity. J. App. Mech., March, pp. 129-133.

- Coleman, B. D. and W. Noll, 1959. Helical flow of general fluids. *J. Appl. Phys.*, 30(1959), 1508.
- Davis, D. C. and G. L. Rehkugler, 1971. A theoretical and experimental analysis of the apple-limb impact problem. *Transactions of the ASAE*, 14(2):234-239.
- DeBaerdemaeker, J. G., 1975. Experimental and numerical techniques related to the stress analysis of apple under static load. Unpublished Ph.D. thesis. Agricultural Engineering Department, Michigan State University.
- Diener, R. G., R. E. Adams, M. Ingle, K. C. Elliott, P. E. Nesselroad, and S. H. Blizzard, 1977. Bruise energy of peaches and apples. ASAE paper no. 77-1029.
- De Tar, W. R., C. G. Haugh, and J. F. Hamilton, 1971. Vibrational analysis of a non-uniform, viscoelastic beam for an agricultural application. ASAE paper no. 71-691.
- DeBaerdemaeker, J., L. J. Segerlind, H. Murase, and G. E. Merva, 1978. Water potential effect on tensile and compressive failure of apple and potato tissue. ASAE paper no. 78-3057.
- Ericksen, J. L., 1960. *Viscoelasticity, Phenomenological Aspects.* ed. J. T. Bergen. Academic Press, New York.
- Eringen, A. C., 1962. *Nonlinear Theory of Continuous Media.* McGraw-Hill Book Company, New York.
- Eringen, A. C. and S. L. Koh, 1963. On the foundations of non-linear-thermo-viscoelasticity. *Int. J. Engineering Science.* Vol. I, pp. 199-229.
- Finney, E. E., 1963. The viscoelastic behavior of the potato, *Solanum tuberosum*, under quasi-static loading. Unpublished Ph. D. thesis. Agricultural Engineering Department, Michigan State University.
- Finney, E. E. and C. W. Hall, 1967. Elastic properties of potatoes. *Transactions of the ASAE*, 10(10):4-8.
- Fletcher, S. W., N. N. Mohsenin, J. R. Hammerle, and L. D. Tukey, 1965. Mechanical behavior of selected fruits and vegetables under fast rates of loading. *Transactions of the ASAE*, 8(3):324-326, 331.
- Fluck, R. C. and E. M. Ahmed, 1972. Impact testing of fruits and vegetables. ASAE paper no. 72-306.

- Fridley, R. B., H. Goehlich, L. L. Claypool, and P. A. Adrian, 1964. Factors affecting impact injury to mechanically harvested fruits. Transactions of the ASAE, 7(4):409-411.
- Fridley, R. B. and P. A. Adrian, 1966. Mechanical properties of peaches, pears, apricots, and apples. Transactions of the ASAE, 9(1):135-142.
- Fridley, R. B., R. A. Bradley, L. W. Rumsey, and P. A. Adrian, 1968. Some aspects of elastic behavior of selected fruits. Transactions of the ASAE, 11(1):46-49.
- Fredrickson, A. G., 1964. Principles and Applications of Rheology. Prentice-Hall, Inc., Englewood Cliffs, NJ.
- Flugee, W., 1975. Viscoelasticity. Second edition. Springer-Verlag, Berlin.
- Fodor, G., 1965. Laplace Transform in Engineering. Akademiai Kiado. Publishing House of the Hungarian Academy of Sciences, Budapest.
- Gustafson, R. J., 1974. Continuum theory for gas-solid-liquid media. Unpublished Ph.D. thesis. Agricultural Engineering Department, Michigan State University.
- Green, A. E. and R. S. Rivlin, 1957. The mechanics of non-linear materials with memory. Arch. Rational Mechanical Analysis, Anal. 1, 1-21.
- Green, A. E. and J. E. Adkins, 1970. Large Elastic Deformations. Second edition. Clarendon Press, Oxford.
- Hall, L. D., C. G. Maple, and B. Vinograde, 1959. Introduction to the Laplace Transform. Appleton-Century-Crofts, Inc., New York.
- Hamann, D. D., 1967. Some dynamic mechanical properties of apple fruits and their use in the solution of an impacting contact problem of a spherical fruit. Unpublished Ph.D. thesis. Virginia Polytechnic Institute, Blacksburg, VA.
- Hamann, D. D., 1970. Analysis of stress during impact of fruit considered to be viscoelastic. Transactions of the ASAE, 13(6):893-899.
- Hammerle, J. R. and N. N. Mohsenin, 1966. Some dynamic aspects of fruit impacting hard and soft materials. Transactions of the ASAE, 9(4):484-488.
- Hammerle, J. R. and N. N. Mohsenin, 1970. Tensile relaxation modulus of corn horny endosperm as a function of time, temperature and moisture content. Transactions of the ASAE, 13(3):372-375.

- Hammerle, J. R. and W. F. McClure, 1971. The determination of Poisson's ratio by compression tests of cylindrical specimens. *Journal of Texture Studies*, 2:31-49.
- Hammerle, J. R., M. V. N. Rao, and D. D. Hamann, 1971. Comparison of static creep and relaxation rate sensitive and frequency sensitive loading for axial compression. ASAE paper no. 71-801.
- Hill, R., 1964. *The Mathematical Theory of Plasticity*. Oxford University Press, London.
- Horsfield, B. L., R. B. Fridley, and L. L. Claypool, 1972. Application of theory of elasticity to design of fruit harvesting and handling equipment for minimum bruising. *Transactions of the ASAE*, 15:746-750.
- Hoffman, O. and G. Sachs, 1953. *Introduction to the Theory of Plasticity for Engineers*. McGraw-Hill Book Company, Inc., New York.
- Holcomb, D. P., J. R. Cooke, and P. L. Hartman, 1977. A study of electrical, thermal, and mechanical properties of apples in relation to bruise detection. ASAE paper no. 77-3512.
- Huff, E. E., 1967. Tensile properties of Kennebec potatoes. *Transactions of the ASAE*, 10(3):414-419.
- Hughes, H. and L. J. Segerlind, 1972. A rapid mechanical method for determining Poisson's ratio in biological materials. ASAE paper no. 71-310.
- Juvinall, R. C., 1967. *Stress, Strain, and Strength*. McGraw-Hill Book Company, Inc., New York.
- Little, R. W., 1973. *Elasticity*. Prentice-Hall, Inc., Englewood Cliffs, NJ.
- Lockett, F. J., 1975. Assessment of linearity and characterization of non-linear behavior. *Mechanics of viscoelastic media and bodies*. Symposium Gothenburg/Sweden, September 2-6, 1974. Editor Jan Hult. Springer-Verlag, Berlin.
- Malvern, L. E., 1969. *Introduction to the Mechanics of Continuous Medium*. Prentice-Hall, Inc., Englewood Cliffs, NJ.
- Marin, J., 1953. *Metals Engineering Design Handbook*. ASME publication, McGraw-Hill Book Co., New York.
- Marin, J., 1962. *Mechanical Behavior of Engineering Materials*. Prentice-Hall, Inc., Englewood Cliffs, NJ.

- Mattus, G. E., L. E. Scott, and L. L. Claypool, 1960. Brown spot bruises of Bartlett pears. Proc. Am. Soc. Hort. Sci., Vol. 75, pp. 100-105.
- Mendelson, A., 1965. Plasticity: Theory and Application. The MacMillan Company, New York. Collier-MacMillan, Ltd., London.
- Miles, J. A., 1971. The development of a failure criterion for apple flesh. Unpublished Ph.D. thesis. Department of Agricultural Engineering, Cornell University.
- Mohsenin, N. N. and H. Gohlich, 1962. Techniques for determination of mechanical properties of fruits and vegetables related to design and development of harvesting and processing machinery. Journal of Agricultural Engineering Research, 7(4):300-315.
- Mohsenin, N. N., H. E. Cooper and L. D. Tukey, 1963. Engineering approach to evaluating textural factors in fruits and vegetables. Transactions of the ASAE, 6(2):85-88.
- Mohsenin, N. N., 1970. Physical Properties of Plant and Animal Materials. Gordon and Breach Science Publishers, New York.
- Mohsenin, N. N., 1971. Mechanical properties of fruits and vegetables. Review of a decade of research, applications, and future needs. ASAE paper no. 71-849.
- Mohsenin, N. N., H. E. Cooper, J. R. Hammerle, S. W. Fletcher, and L. D. Tukey, 1965. Readiness for harvest of apple as affected by physical and mechanical properties of the fruit. Pennsylvania Agricultural Experiment Station, Bulletin No. 721.
- Morrow, C. T., 1965. Viscoelasticity in a selected agricultural product. Unpublished M.S. thesis. Pennsylvania State University.
- Morrow, C. T. and N. N. Mohsenin, 1966. Consideration of selected agricultural products as viscoelastic materials. Journal of Food Science, 31(5):686-698.
- Morrow, C. T. and N. N. Mohsenin, 1968. Dynamic viscoelastic characterization of solid food materials. Journal of Food Science, 33(6):646-651.
- Morrow, C. T., D. D. Hamann, N. N. Mohsenin, and E. E. Finney, 1971. Mechanical characterization of red delicious apples. ASAE paper no. 71-372.

- Murase, H., 1977. Elastic stress-strain constitutive equations for vegetable material. Unpublished Ph.D. thesis. Agricultural Engineering Department, Michigan State University.
- Nadai, A., 1931. Plasticity. McGraw-Hill Book Company, Inc., New York.
- Nadai, A., 1950. Theory of Flow and Fracture of Solids. Volumes I and II. McGraw-Hill Book Company, Inc., New York.
- Nelson, C. W. and N. N. Mohsenin, 1968. Maximum allowable static and dynamic loads and effect of temperature for mechanical injury of apples. Journal of Agricultural Engineering Research, 13(4):305-317.
- Oldroyd, J. G., 1950. The motion of an elastico-viscous liquid contained between coaxial cylinders. I. Quart. J. Mech. Appl. Math., 4, Pt. 3 (1950), 271.
- Park, D., 1963. The resistance of potato to mechanical damage caused by impact loading. Journal of Agricultural Engineering Research, 8(3):173-177.
- Peterson, C. L. and C. W. Hall, 1973. Consideration of the Russett Burbank potato as a thermorheological simple material. ASAE paper no. 73-303.
- Prager, W., 1942. Theory of Plasticity. Advanced Instruction in Mechanics, Brown University. Providence, RI.
- Prager, W., 1959. An Introduction to Plasticity. Addison-Wesley Publishing Company, Inc., London.
- Prager, W., 1961. Introduction to Mechanics of Continua. Chicago: Ginn, 1961.
- Rivlin, R. W. and J. L. Ericksen, 1955. Stress-deformation relations for isotropic materials. J. Rat'l. Mech. Anal., 4(1955), 323.
- Rivlin, R. W., 1975. On the foundations of the theory of non-linear viscoelasticity. Mechanics of viscoelastic media and bodies. Symposium Gothenburg/Sweden, September 2-6, 1974. Editor Jan Hult. Springer-Verlag, Berlin.
- Rumsey, T. R. and R. B. Fridley, 1974. Analysis of viscoelastic contact stresses in agricultural products using finite element method. ASAE paper no. 74-3513.
- Seeley, F. B. and J. S. Smith, 1967. Advanced Mechanics of Materials. John Wiley & Sons, Inc., New York.

- Sherif, S. M., 1976. The quasi-static contact problem for nearly-incompressible agricultural products. Unpublished Ph.D. thesis. Agricultural Engineering Department, Michigan State University.
- Sherif, S. M., L. J. Segerlind, and T. S. Frame, 1976. An equation for the modulus of elasticity of radially compressed cylinder. Transactions of the ASAE (to be published).
- Simpson, J. B. and G. E. Rehkugler, 1972. Forces and apple damage during impact. ASAE paper no. 72-307 MI-H.
- Snobar, B. A., 1976. Engineering parameters related to the hardness of carrots. Unpublished Ph.D. thesis. Agricultural Engineering Department, Michigan State University.
- Sharma, M. G. and N. N. Mohsenin, 1970. Mechanics of deformation of fruits subjected to hydrostatic pressure. Journal of Agricultural Engineering Research, 15(1):65-74.
- Sobotka, Z., 1975. Non-linear constitutive equations of viscoelastic bodies. Mechanics of viscoelastic media and bodies. Symposium Gothenburg/Sweden, September 2-6, 1974. Editor Jan Hult. Springer-Verlag, Berlin.
- Stuart, H. A., 1956. Die Physik Der Hochpolymeren. Theorie und Molekulare Deutung Technologischer Eigenschaften Von Hochpolymeren Werkstoffen. Springer-Verlag, Berlin. Gottingen-Heilderberg.
- Terzaghi, K., and R. B. Peck, 1967. Soil Mechanics in Engineering Practice. Second edition. John Wiley & Sons, Inc., New York.
- Thomas, T. Y., 1961. Plastic Flow and Fracture in Solids. Academic Press, New York.
- Timbers, G. E., L. M. Staley, and E. L. Watson, 1966. Some mechanical and rheological properties of the Netted Gem potato. Canadian Journal of Agricultural Engineering, February.
- Timoshenko, S. P. and J. N. Goodier, 1970. Theory of Elasticity. McGraw-Hill Book Company, New York.
- Van Lancker, J. V., L. Kermis, J. DeBruyn, F. DeSmet, G. Ottermans, and A. Calus, 1977. Mechanical behavior and compression tests on apples (Golden Delicious). Landbouwtijdschrift, 10(1977), Nr. 1.
- Wang, J. K. and H. S. Chang, 1970. Mechanical properties of papaya and their dependence on maturity. ASAE paper no. 69-389.

- Weber, T. D., 1975. Hypothese des variables internes et viscoelasticite non-lineaire: Etude du cas particulier d'une seule variable interne tensorielle. Mechanics of viscoelastic media and bodies. Symposium Gothenburg/Sweden, September 2-6, 1974. Editor Jan Hult. Springer-Verlag, Berlin.
- White, R. K. and N. N. Mohsenin, 1967. Apparatus for determination of bulk modulus of compressibility of materials. Transactions of the ASAE, 10(5):670-671.
- Wright, F. S. and W. E. Splinter, 1968. Mechanical behavior of sweet potatoes under slow loading and impact loading. Transactions of the ASAE, 11(6):765-770.
- Yoshiaki, I. and J. L. White, 1977. Investigation on failure during elongation flow of polymer melts. Journal of Non-newtonian fluid Mechanics, 2(1977)281-298.
- Zoerb, G. C., 1958. Mechanical and rheological properties of grain. Unpublished Ph.D. thesis. Agricultural Engineering Department, Michigan State University.

APPENDICES

TABLE A1. STRESS, STRAIN AND TIME AT FAILURE FOR UNIAXIAL LOADING OF CYLINDRICAL SPECIMENS OF APPLE. $\dot{\epsilon}_{11} = -0.002 \text{ SEC}^{-1}$.

MC INTOSH			JONATHAN			RED DELICIOUS		
σ_{11} (MPa)	ϵ_{11} (mm/mm)	t (sec)	σ_{11} (MPa)	ϵ_{11} (mm/mm)	t (sec)	σ_{11} (MPa)	ϵ_{11} (mm/mm)	t (sec)
-0.21	-0.127	63.79	-0.16	-0.137	68.69	-0.25	-0.091	43.90
-0.19	-0.132	66.24	-0.23	-0.159	79.73	-0.31	-0.127	63.83
-0.18	-0.130	65.01	-0.17	-0.142	71.15	-0.30	-0.132	66.28
-0.20	-0.147	73.60	-0.23	-0.161	80.96	-0.30	-0.117	58.92
-0.20	-0.147	73.60	-0.16	-0.152	76.05	-0.29	-0.111	55.97
-0.17	-0.137	68.69	-0.16	-0.161	80.96	-0.27	-0.120	63.30
-0.20	-0.142	71.15	-0.15	-0.147	73.60	-0.29	-0.116	58.19
-0.15	-0.137	68.69	-0.14	-0.166	83.41	-0.31	-0.120	60.39
-0.17	-0.147	73.60	-0.14	-0.176	98.32	-0.22	-0.114	57.44
-0.13	-0.137	68.69	-0.21	-0.181	90.77	-0.23	-0.114	57.44
-0.17	-0.137	68.69	-0.26	-0.161	80.96	-0.27	-0.115	57.93
-0.17	-0.152	76.05	-0.22	-0.157	78.51	-0.26	-0.131	65.79
-0.18	-0.142	71.15	-0.22	-0.132	66.24	-0.29	-0.122	61.37
-0.15	-0.142	71.15	-0.24	-0.152	76.05	-0.21	-0.126	63.33
-0.17	-0.127	63.79	-0.18	-0.147	73.60	-0.26	-0.120	60.14
-0.16	-0.142	71.15	-0.21	-0.157	78.51	-0.27	-0.125	62.60
-0.18	-0.157	78.51	-0.15	-0.127	63.79	-0.33	-0.135	67.51
-0.15	-0.157	78.51	-0.21	-0.142	71.15	-0.37	-0.137	68.74
-0.17	-0.137	68.69	-0.14	-0.137	68.69	-0.41	-0.152	75.10
-0.16	-0.134	67.47	-0.17	-0.157	78.51	-0.27	-0.117	58.92

TABLE A2. STRESS, STRAIN AND TIME AT FAILURE FOR UNIAXIAL LOADING OF CYLINDRICAL SPECIMENS OF APPLE. $\dot{\epsilon}_{11} = -0.007 \text{ SEC}^{-1}$.

MC INTOSH			JONATHAN			RED DELICIOUS		
σ_{11} (MPa)	ϵ_{11} (mm/mm)	t (sec)	σ_{11} (MPa)	ϵ_{11} (mm/mm)	t (sec)	σ_{11} (MPa)	ϵ_{11} (mm/mm)	t (sec)
-0.25	-0.123	17.96	-0.27	-0.115	16.77	-0.29	-0.111	15.17
-0.25	-0.123	17.96	-0.30	-0.148	21.56	-0.29	-0.107	15.57
-0.24	-0.148	21.56	-0.26	-0.144	20.96	-0.33	-0.128	18.56
-0.24	-0.123	17.96	-0.27	-0.144	20.96	-0.33	-0.107	15.57
-0.24	-0.111	16.17	-0.25	-0.136	19.76	-0.30	-0.115	16.77
-0.25	-0.136	19.76	-0.27	-0.148	21.56	-0.31	-0.115	16.77
-0.24	-0.144	20.96	-0.24	-0.136	19.76	-0.31	-0.107	15.57
-0.25	-0.119	17.37	-0.26	-0.144	20.96	-0.33	-0.123	17.96
-0.23	-0.136	19.76	-0.26	-0.140	20.36	-0.34	-0.107	15.57
-0.25	-0.136	19.76	-0.28	-0.132	19.16	-0.34	-0.111	16.17
-0.20	-0.136	19.76	-0.24	-0.111	16.17	-0.29	-0.107	15.57
-0.18	-0.103	14.97	-0.26	-0.140	20.36	-0.29	-0.111	16.17
-0.19	-0.103	14.97	-0.25	-0.123	17.96	-0.33	-0.115	16.77
-0.24	-0.123	17.96	-0.28	-0.132	19.16	-0.33	-0.107	15.57
-0.23	-0.111	16.17	-0.25	-0.119	17.37	-0.30	-0.115	16.77
-0.22	-0.123	17.96	-0.28	-0.157	22.76	-0.31	-0.107	15.57
-0.22	-0.123	17.96	-0.26	-0.132	19.16	-0.31	-0.123	17.96
-0.24	-0.119	17.37	-0.31	-0.144	20.96	-0.33	-0.119	17.37
-0.23	-0.111	16.17	-0.27	-0.132	19.16	-0.34	-0.115	16.77
-0.23	-0.107	15.57	-0.23	-0.123	17.96	-0.34	-0.099	14.37

TABLE A3. STRESS, STRAIN AND TIME AT FAILURE FOR UNIAXIAL LOADING OF CYLINDRICAL SPECIMENS OF APPLE. $\dot{\epsilon}_{11} = -0.017 \text{ SEC}^{-1}$.

MC INTOSH			JONATHAN			RED DELICIOUS		
σ_{11} (MPa)	ϵ_{11} (mm/mm)	t (sec)	σ_{11} (MPa)	ϵ_{11} (mm/mm)	t (sec)	σ_{11} (MPa)	ϵ_{11} (mm/mm)	t (sec)
-0.22	-0.121	7.03	-0.30	-0.121	7.03	-0.28	-0.106	6.15
-0.19	-0.131	7.62	-0.28	-0.101	5.86	-0.31	-0.106	6.15
-0.22	-0.116	6.74	-0.30	-0.091	5.27	-0.31	-0.116	6.74
-0.24	-0.126	7.33	-0.26	-0.101	5.86	-0.28	-0.086	4.98
-0.18	-0.101	5.86	-0.28	-0.111	6.45	-0.29	-0.101	5.86
-0.22	-0.111	6.45	-0.28	-0.142	9.21	-0.25	-0.101	5.86
-0.26	-0.106	6.15	-0.26	-0.106	6.15	-0.30	-0.131	7.62
-0.20	-0.111	6.45	-0.28	-0.131	7.62	-0.29	-0.142	8.21
-0.20	-0.131	7.62	-0.26	-0.101	5.86	-0.28	-0.137	7.91
-0.26	-0.106	6.15	-0.32	-0.121	7.03	-0.27	-0.101	5.86
-0.25	-0.111	6.45	-0.28	-0.101	5.86	-0.30	-0.121	7.03
-0.18	-0.111	6.45	-0.29	-0.101	5.86	-0.30	-0.126	7.33
-0.18	-0.126	7.33	-0.26	-0.142	8.21	-0.25	-0.126	7.33
-0.14	-0.142	8.21	-0.26	-0.106	6.15	-0.25	-0.116	6.74
-0.18	-0.111	6.45	-0.28	-0.121	7.03	-0.25	-0.121	7.03
-0.29	-0.116	6.74	-0.30	-0.111	6.45	-0.28	-0.106	6.15
-0.28	-0.121	7.03	-0.31	-0.101	5.86	-0.28	-0.101	5.86
-0.25	-0.152	8.79	-0.24	-0.076	4.39	-0.36	-0.121	7.03
-0.27	-0.123	7.15	-0.26	-0.101	5.86	-0.36	-0.126	7.33
-0.26	-0.126	7.33	-0.36	-0.111	6.45	-0.37	-0.106	6.15

TABLE A4. STRESS, STRAIN AND TIME AT FAILURE FOR UNIAXIAL LOADING OF CYLINDRICAL SPECIMENS OF APPLE. $\dot{\epsilon}_{11} = -0.035 \text{ SEC}^{-1}$.

MC INTOSH			JONATHAN			RED DELICIOUS		
σ_{11} (MPa)	ϵ_{11} (mm/mm)	t (sec)	σ_{11} (MPa)	ϵ_{11} (mm/mm)	t (sec)	σ_{11} (MPa)	ϵ_{11} (mm/mm)	t (sec)
-0.26	-0.138	3.99	-0.28	-0.138	3.99	-0.32	-0.099	2.85
-0.29	-0.138	3.99	-0.30	-0.099	2.85	-0.33	-0.109	3.14
-0.28	-0.109	3.14	-0.31	-0.089	2.57	-0.37	-0.109	3.14
-0.31	-0.128	3.71	-0.36	-0.109	3.14	-0.35	-0.118	3.42
-0.29	-0.138	3.99	-0.35	-0.109	3.14	-0.36	-0.099	2.85
-0.29	-0.118	3.42	-0.39	-0.118	3.42	-0.26	-0.118	3.42
-0.25	-0.128	3.71	-0.29	-0.109	3.14	-0.34	-0.109	3.14
-0.29	-0.138	3.99	-0.25	-0.109	3.14	-0.35	-0.109	3.14
-0.27	-0.128	3.71	-0.25	-0.118	3.42	-0.36	-0.089	2.57
-0.26	-0.128	3.71	-0.29	-0.128	3.71	-0.35	-0.099	2.85
-0.27	-0.128	3.71	-0.25	-0.118	3.42	-0.29	-0.099	2.85
-0.28	-0.138	3.99	-0.26	-0.109	3.14	-0.33	-0.128	3.71
-0.22	-0.109	3.14	-0.28	-0.138	3.99	-0.34	-0.109	3.14
-0.23	-0.109	3.14	-0.24	-0.158	4.57	-0.33	-0.099	2.85
-0.23	-0.109	3.14	-0.29	-0.118	3.42	-0.34	-0.109	3.14
-0.18	-0.148	4.28	-0.31	-0.118	3.42	-0.34	-0.099	2.85
-0.22	-0.109	3.14	-0.32	-0.118	3.42	-0.37	-0.099	2.85
-0.22	-0.109	3.14	-0.30	-0.128	3.71	-0.37	-0.111	3.19
-0.23	-0.099	2.85	-0.26	-0.138	3.99	-0.37	-0.138	3.99
-0.23	-0.109	3.14	-0.27	-0.118	3.42	-0.37	-0.099	2.85

TABLE A5. STRESS, STRAIN AND TIME AT FAILURE FOR UNIAXIAL LOADING OF CYLINDRICAL SPECIMENS OF APPLE. $\dot{\epsilon}_{11} = -0.069 \text{ SEC}^{-1}$

MC INTOSH			JONATHAN			RED DELICIOUS		
σ_{11} (MPa)	ϵ_{11} (mm/mm)	t (sec)	σ_{11} (MPa)	ϵ_{11} (mm/mm)	t (sec)	σ_{11} (MPa)	ϵ_{11} (mm/mm)	t (sec)
-0.28	-0.124	1.79	-0.29	-0.165	2.39	-0.34	-0.082	1.19
-0.25	-0.165	2.39	-0.39	-0.165	2.39	-0.34	-0.124	1.79
-0.29	-0.144	2.09	-0.34	-0.144	2.09	-0.35	-0.124	1.79
-0.27	-0.144	2.09	-0.28	-0.144	2.09	-0.29	-0.144	2.09
-0.29	-0.144	2.09	-0.27	-0.124	1.79	-0.33	-0.124	1.79
-0.29	-0.124	1.79	-0.38	-0.186	2.68	-0.41	-0.124	1.79
-0.24	-0.124	1.79	-0.33	-0.082	1.19	-0.34	-0.103	1.49
-0.27	-0.124	1.79	-0.31	-0.103	1.49	-0.31	-0.124	1.79
-0.24	-0.124	1.79	-0.40	-0.144	2.09	-0.32	-0.103	1.49
-0.25	-0.144	2.09	-0.33	-0.124	1.79	-0.32	-0.124	1.79
-0.27	-0.124	1.79	-0.32	-0.124	1.79	-0.30	-0.124	1.79
-0.26	-0.103	1.49	-0.34	-0.165	2.39	-0.34	-0.115	1.67
-0.25	-0.124	1.79	-0.31	-0.144	2.09	-0.26	-0.124	1.79
-0.25	-0.124	1.79	-0.31	-0.124	1.79	-0.33	-0.103	1.49
-0.27	-0.124	1.79	-0.27	-0.103	1.49	-0.34	-0.124	1.79
-0.24	-0.124	1.79	-0.31	-0.124	1.79	-0.38	-0.124	1.79
-0.24	-0.124	1.79	-0.28	-0.144	2.09	-0.37	-0.124	1.79
-0.25	-0.124	1.79	-0.26	-0.124	1.79	-0.37	-0.124	1.79
-0.24	-0.103	1.49	-0.30	-0.124	1.79	-0.37	-0.124	1.79
-0.24	-0.124	1.79	-0.30	-0.124	1.79	-0.38	-0.124	1.79

TABLE A6. STRESS, STRAIN AND TIME AT FAILURE FOR UNIAXIAL LOADING OF CYLINDRICAL SPECIMENS OF APPLE. $\dot{\epsilon}_{11} = -0.173 \text{ SEC}^{-1}$

MC INTOSH			JONATHAN			RED DELICIOUS		
σ_{11} (MPa)	ϵ_{11} (mm/mm)	t (sec)	σ_{11} (MPa)	ϵ_{11} (mm/mm)	t (sec)	σ_{11} (MPa)	ϵ_{11} (mm/mm)	t (sec)
-0.24	-0.090	0.52	-0.34	-0.099	0.57	-0.37	-0.090	0.52
-0.23	-0.099	0.57	-0.33	-0.090	0.52	-0.41	-0.090	0.52
-0.25	-0.090	0.52	-0.36	-0.126	0.73	-0.43	-0.099	0.57
-0.28	-0.081	0.47	-0.32	-0.090	0.52	-0.43	-0.090	0.52
-0.23	-0.090	0.52	-0.28	-0.090	0.52	-0.41	-0.108	0.62
-0.28	-0.081	0.47	-0.28	-0.081	0.47	-0.43	-0.108	0.62
-0.30	-0.090	0.52	-0.28	-0.090	0.52	-0.28	-0.081	0.47
-0.26	-0.090	0.52	-0.37	-0.090	0.52	-0.26	-0.072	0.41
-0.26	-0.099	0.57	-0.41	-0.126	0.73	-0.28	-0.072	0.41
-0.34	-0.099	0.57	-0.37	-0.081	0.47	-0.30	-0.105	0.60
-0.32	-0.099	0.57	-0.37	-0.117	0.68	-0.28	-0.090	0.52
-0.32	-0.090	0.52	-0.31	-0.099	0.57	-0.28	-0.099	0.57
-0.29	-0.090	0.52	-0.32	-0.099	0.57	-0.28	-0.099	0.57
-0.30	-0.099	0.57	-0.30	-0.099	0.57	-0.34	-0.081	0.47
-0.30	-0.108	0.62	-0.31	-0.099	0.57	-0.33	-0.099	0.57
-0.28	-0.099	0.57	-0.34	-0.108	0.62	-0.34	-0.099	0.57
-0.24	-0.108	0.62	-0.32	-0.099	0.57	-0.32	-0.108	0.62
-0.27	-0.090	0.52	-0.36	-0.099	0.57	-0.37	-0.099	0.57
-0.25	-0.108	0.62	-0.37	-0.090	0.52	-0.36	-0.099	0.57
-0.28	-0.099	0.57	-0.34	-0.108	0.62	-0.36	-0.094	0.54

TABLE A7. STRESS, STRAIN AND TIME AT FAILURE FOR UNIAXIAL LOADING OF CYLINDRICAL SPECIMENS OF APPLE. $\dot{\epsilon}_{11} = -0.345 \text{ SEC}^{-1}$

MC INTOSH			JONATHAN			RED DELICIOUS		
σ_{11}	ϵ_{11}	t	σ_{11}	ϵ_{11}	t	σ_{11}	ϵ_{11}	t
(MPa)	(mm/mm)	(sec)	(MPa)	(mm/mm)	(sec)	(MPa)	(mm/mm)	(sec)
-0.27	-0.067	0.19	-0.30	-0.134	0.39	-0.37	-0.134	0.39
-0.28	-0.134	0.39	-0.32	-0.134	0.39	-0.37	-0.112	0.32
-0.24	-0.112	0.32	-0.34	-0.134	0.39	-0.37	-0.134	0.39
-0.26	-0.134	0.39	-0.34	-0.134	0.39	-0.37	-0.112	0.32
-0.24	-0.134	0.39	-0.28	-0.125	0.36	-0.41	-0.134	0.39
-0.23	-0.112	0.32	-0.29	-0.112	0.32	-0.37	-0.112	0.32
-0.26	-0.134	0.39	-0.30	-0.157	0.45	-0.36	-0.112	0.32
-0.26	-0.112	0.32	-0.30	-0.112	0.32	-0.34	-0.094	0.27
-0.28	-0.134	0.39	-0.33	-0.134	0.39	-0.34	-0.112	0.32
-0.28	-0.157	0.45	-0.34	-0.157	0.45	-0.34	-0.134	0.39
-0.26	-0.134	0.39	-0.32	-0.134	0.39	-0.32	-0.112	0.32
-0.26	-0.157	0.45	-0.34	-0.125	0.36	-0.32	-0.112	0.32
-0.30	-0.134	0.39	-0.34	-0.112	0.32	-0.32	-0.134	0.39
-0.28	-0.157	0.45	-0.30	-0.134	0.39	-0.32	-0.112	0.32
-0.26	-0.134	0.39	-0.33	-0.112	0.32	-0.32	-0.112	0.32
-0.30	-0.134	0.39	-0.33	-0.112	0.32	-0.32	-0.112	0.32
-0.28	-0.134	0.39	-0.30	-0.134	0.39	-0.30	-0.112	0.32
-0.28	-0.134	0.39	-0.37	-0.134	0.39	-0.32	-0.134	0.39
-0.28	-0.112	0.32	-0.34	-0.134	0.39	-0.30	-0.089	0.26
-0.26	-0.134	0.39	-0.37	-0.134	0.39	-0.32	-0.134	0.39

TABLE A8. STRESS, STRAIN AND TIME AT FAILURE FOR TRIAXIAL LOADING OF CYLINDRICAL SPECIMENS OF APPLE. $\dot{\epsilon}_{11} = -0.007 \text{ SEC}^{-1}$, $\sigma_{22} = 0.000 \text{ MPa}$.

MC INTOSH			JONATHAN			RED DELICIOUS		
σ_{11}	ϵ_{11}	t	σ_{11}	ϵ_{11}	t	σ_{11}	ϵ_{11}	t
(MPa)	(mm/mm)	(sec)	(MPa)	(mm/mm)	(sec)	(MPa)	(mm/mm)	(sec)
-0.25	-0.123	17.96	-0.27	-0.115	16.77	-0.29	-0.111	16.17
-0.25	-0.123	17.96	-0.30	-0.148	21.56	-0.29	-0.107	15.57
-0.24	-0.148	21.56	-0.26	-0.144	20.96	-0.33	-0.128	13.56
-0.23	-0.123	17.96	-0.27	-0.144	20.96	-0.33	-0.107	15.57
-0.24	-0.111	16.17	-0.24	-0.136	19.76	-0.30	-0.115	16.77
-0.25	-0.136	19.76	-0.26	-0.148	21.56	-0.31	-0.115	16.77
-0.24	-0.144	20.96	-0.24	-0.136	19.76	-0.31	-0.107	15.57
-0.25	-0.119	17.37	-0.26	-0.144	20.96	-0.33	-0.123	17.96
-0.23	-0.136	19.76	-0.26	-0.140	20.36	-0.34	-0.107	15.57
-0.25	-0.136	19.76	-0.28	-0.132	19.16	-0.34	-0.111	16.17
-0.24	-0.123	17.96	-0.24	-0.111	16.17	-0.29	-0.107	15.57
-0.19	-0.103	14.97	-0.26	-0.140	20.36	-0.29	-0.111	16.17
-0.24	-0.103	14.97	-0.25	-0.123	17.96	-0.33	-0.115	16.77
-0.23	-0.123	17.96	-0.28	-0.132	19.16	-0.33	-0.107	15.57
-0.22	-0.111	16.17	-0.25	-0.119	17.37	-0.30	-0.115	16.77
-0.25	-0.123	17.96	-0.28	-0.157	22.76	-0.31	-0.107	15.57
-0.24	-0.123	17.96	-0.26	-0.132	19.16	-0.31	-0.123	17.96
-0.23	-0.119	17.37	-0.30	-0.144	20.96	-0.33	-0.119	17.37
-0.23	-0.111	16.17	-0.27	-0.132	19.16	-0.34	-0.115	16.77
-0.23	-0.107	15.57	-0.23	-0.123	17.96	-0.34	-0.099	14.37

TABLE A9. STRESS, STRAIN AND TIME AT FAILURE FOR TRIAXIAL LOADING OF CYLINDRICAL SPECIMENS OF APPLE. $\dot{\epsilon}_{11} = -0.007 \text{ SEC}^{-1}$ $\sigma_{22} = -0.069 \text{ MPa}$.

MC INTOSH			JONATHAN			RED DELICIOUS		
σ_{11} (MPa)	ϵ_{11} (mm/mm)	t (sec)	σ_{11} (MPa)	ϵ_{11} (mm/mm)	t (sec)	σ_{11} (MPa)	ϵ_{11} (mm/mm)	t (sec)
-0.21	-0.115	16.77	-0.26	-0.115	16.77	-0.30	-0.157	22.75
-0.26	-0.136	19.76	-0.28	-0.115	16.77	-0.34	-0.148	21.56
-0.24	-0.148	21.56	-0.26	-0.115	16.77	-0.35	-0.144	20.96
-0.26	-0.140	20.36	-0.27	-0.115	16.77	-0.29	-0.115	16.77
-0.26	-0.132	19.16	-0.25	-0.115	16.77	-0.26	-0.115	16.77
-0.24	-0.144	20.96	-0.21	-0.103	14.97	-0.30	-0.132	19.16
-0.22	-0.132	19.16	-0.28	-0.136	19.76	-0.27	-0.144	20.96
-0.24	-0.132	19.16	-0.30	-0.144	20.96	-0.22	-0.103	14.97
-0.25	-0.123	17.96	-0.26	-0.132	19.16	-0.39	-0.169	24.95
-0.22	-0.123	17.96	-0.27	-0.103	14.97	-0.34	-0.140	20.36
-0.25	-0.123	17.96	-0.23	-0.132	19.16	-0.30	-0.123	17.96
-0.17	-0.103	14.97	-0.25	-0.144	20.96	-0.27	-0.123	17.96
-0.23	-0.123	17.96	-0.22	-0.123	17.96	-0.24	-0.095	13.77
-0.23	-0.132	19.16	-0.27	-0.132	19.16	-0.31	-0.115	16.77
-0.19	-0.103	14.97	-0.26	-0.148	21.56	-0.31	-0.119	17.37
-0.24	-0.115	16.77	-0.24	-0.115	16.77	-0.29	-0.128	18.56
-0.22	-0.115	16.77	-0.28	-0.123	17.96	-0.31	-0.123	17.96
-0.25	-0.157	22.76	-0.23	-0.132	19.16	-0.26	-0.119	17.37
-0.20	-0.107	15.57	-0.25	-0.123	17.96	-0.24	-0.107	15.57
-0.22	-0.115	16.77	-0.21	-0.132	19.16	-0.28	-0.115	16.77

TABLE A10. STRESS, STRAIN AND TIME AT FAILURE FOR TRIAXIAL LOADING OF CYLINDRICAL SPECIMENS OF APPLE. $\dot{\epsilon}_{11} = -0.007 \text{ SEC}^{-1}$ $\sigma_{22} = -0.138 \text{ MPa}$.

MC INTOSH			JONATHAN			RED DELICIOUS		
σ_{11} (MPa)	ϵ_{11} (mm/mm)	t (sec)	σ_{11} (MPa)	ϵ_{11} (mm/mm)	t (sec)	σ_{11} (MPa)	ϵ_{11} (mm/mm)	t (sec)
-0.26	-0.140	20.36	-0.24	-0.123	17.96	-0.18	-0.103	14.97
-0.29	-0.152	22.16	-0.22	-0.107	15.57	-0.20	-0.140	20.36
-0.17	-0.136	19.76	-0.27	-0.132	19.16	-0.35	-0.165	23.95
-0.15	-0.103	14.97	-0.22	-0.144	20.96	-0.26	-0.115	16.77
-0.18	-0.140	20.36	-0.23	-0.123	17.96	-0.30	-0.165	23.95
-0.13	-0.111	16.17	-0.29	-0.123	17.96	-0.22	-0.107	15.57
-0.22	-0.119	17.37	-0.29	-0.107	15.57	-0.33	-0.150	21.26
-0.20	-0.123	17.96	-0.28	-0.132	19.16	-0.26	-0.128	18.56
-0.20	-0.123	17.96	-0.26	-0.123	17.96	-0.25	-0.107	15.57
-0.22	-0.132	19.16	-0.28	-0.136	19.76	-0.27	-0.123	17.96
-0.23	-0.123	17.96	-0.28	-0.095	13.77	-0.25	-0.128	18.56
-0.25	-0.132	19.16	-0.25	-0.132	19.16	-0.28	-0.123	17.96
-0.25	-0.132	19.16	-0.26	-0.140	20.36	-0.25	-0.123	17.96
-0.26	-0.132	19.16	-0.25	-0.148	21.56	-0.28	-0.165	23.95
-0.24	-0.165	23.95	-0.22	-0.173	25.15	-0.22	-0.123	17.96
-0.22	-0.136	19.76	-0.25	-0.132	19.16	-0.34	-0.195	26.95
-0.22	-0.123	17.96	-0.26	-0.165	23.95	-0.29	-0.165	23.95
-0.20	-0.152	22.16	-0.25	-0.157	22.76	-0.28	-0.132	19.16
-0.15	-0.243	35.34	-0.12	-0.247	35.93	-0.12	-0.074	10.79
-0.15	-0.165	23.95	-0.22	-0.165	23.95	-0.24	-0.140	20.36

TABLE A11. STRESS, STRAIN AND TIME AT FAILURE FOR TRIAXIAL LOADING OF CYLINDRICAL SPECIMENS OF APPLE. $\epsilon_{11} = -0.007 \text{ SEC}^{-1}$ $\sigma_{22} = -0.207 \text{ MPa}$.

MC INTOSH			JONATHAN			RED DELICIOUS		
σ_{11} (MPa)	ϵ_{11} (mm/mm)	t (sec)	σ_{11} (MPa)	ϵ_{11} (mm/mm)	t (sec)	σ_{11} (MPa)	ϵ_{11} (mm/mm)	t (sec)
-0.21	-0.123	17.96	-0.24	-0.132	19.16	-0.17	-0.090	13.17
-0.13	-0.078	11.38	-0.22	-0.103	14.97	-0.27	-0.134	19.46
-0.18	-0.090	13.17	-0.27	-0.123	17.96	-0.27	-0.119	17.37
-0.18	-0.090	13.17	-0.20	-0.144	20.96	-0.28	-0.144	20.96
-0.22	-0.107	15.57	-0.17	-0.107	15.57	-0.25	-0.123	17.96
-0.23	-0.132	19.16	-0.22	-0.103	14.97	-0.27	-0.107	15.57
-0.20	-0.103	14.97	-0.24	-0.144	20.96	-0.30	-0.136	19.76
-0.20	-0.103	14.97	-0.29	-0.132	19.16	-0.15	-0.070	10.18
-0.20	-0.103	14.97	-0.17	-0.128	18.56	-0.29	-0.132	19.16
-0.18	-0.107	15.57	-0.20	-0.123	17.96	-0.28	-0.144	20.96
-0.22	-0.111	16.17	-0.24	-0.157	22.76	-0.27	-0.119	17.37
-0.20	-0.095	13.77	-0.18	-0.095	13.77	-0.20	-0.107	15.57
-0.20	-0.099	14.37	-0.18	-0.107	15.57	-0.16	-0.074	10.78
-0.20	-0.095	13.77	-0.18	-0.132	19.16	-0.28	-0.148	21.56
-0.21	-0.107	15.57	-0.17	-0.082	11.97	-0.30	-0.134	19.46
-0.30	-0.144	20.96	-0.17	-0.082	11.97	-0.29	-0.140	20.36
-0.30	-0.144	20.96	-0.25	-0.099	14.37	-0.29	-0.136	19.76
-0.23	-0.111	16.17	-0.20	-0.095	13.77	-0.26	-0.103	14.97
-0.25	-0.132	19.16	-0.22	-0.099	14.37	-0.26	-0.107	15.57
-0.22	-0.101	14.67	-0.24	-0.107	15.57	-0.23	-0.136	19.76

TABLE A12. STRESS, STRAIN AND TIME AT FAILURE FOR TRIAXIAL LOADING OF CYLINDRICAL SPECIMENS OF APPLE. $\epsilon_{11} = -0.007 \text{ SEC}^{-1}$ $\sigma_{22} = -0.276 \text{ MPa}$.

MC INTOSH			JONATHAN			RED DELICIOUS		
σ_{11} (MPa)	ϵ_{11} (mm/mm)	t (sec)	σ_{11} (MPa)	ϵ_{11} (mm/mm)	t (sec)	σ_{11} (MPa)	ϵ_{11} (mm/mm)	t (sec)
-0.18	-0.144	20.96	-0.12	-0.123	17.96	-0.17	-0.070	10.18
-0.18	-0.080	11.68	-0.16	-0.115	16.77	-0.18	-0.086	12.57
-0.18	-0.119	17.37	-0.12	-0.082	11.97	-0.13	-0.057	8.38
-0.18	-0.082	11.97	-0.18	-0.123	17.96	-0.28	-0.123	17.96
-0.23	-0.095	13.77	-0.19	-0.095	13.77	-0.17	-0.074	10.78
-0.14	-0.095	13.77	-0.16	-0.115	16.77	-0.15	-0.066	9.58
-0.14	-0.086	12.57	-0.23	-0.074	10.78	-0.22	-0.095	13.77
-0.18	-0.107	15.57	-0.20	-0.090	13.17	-0.30	-0.123	17.96
-0.17	-0.092	13.47	-0.22	-0.115	16.77	-0.27	-0.115	16.77
-0.13	-0.074	10.78	-0.17	-0.115	16.77	-0.31	-0.128	18.56
-0.18	-0.095	13.77	-0.17	-0.115	16.77	-0.28	-0.115	16.77
-0.17	-0.099	14.37	-0.20	-0.099	14.37	-0.26	-0.111	16.17
-0.21	-0.080	11.68	-0.23	-0.107	15.57	-0.28	-0.128	18.56
-0.23	-0.111	16.17	-0.23	-0.107	15.57	-0.17	-0.074	10.78
-0.21	-0.074	10.78	-0.19	-0.115	16.77	-0.23	-0.103	14.97
-0.19	-0.103	14.97	-0.17	-0.103	14.97	-0.26	-0.123	17.96
-0.22	-0.123	17.96	-0.20	-0.103	14.97	-0.20	-0.099	14.37
-0.17	-0.097	14.07	-0.18	-0.173	25.15	-0.21	-0.099	14.37
-0.14	-0.095	13.77	-0.18	-0.123	17.96	-0.13	-0.061	8.98
-0.18	-0.103	14.97	-0.15	-0.107	15.57	-0.15	-0.074	10.78

TABLE A13. STRESS, STRAIN AND TIME AT FAILURE FOR TRIAXIAL LOADING OF CYLINDRICAL SPECIMENS OF APPLE. $\dot{\epsilon}_{11} = -0.007 \text{ SEC}^{-1}$ $\sigma_{22} = -0.395 \text{ MPa}$.

MC INTOSH			JONATHAN			RED DELICIOUS		
σ_{11}	ϵ_{11}	t	σ_{11}	ϵ_{11}	t	σ_{11}	ϵ_{11}	t
(MPa)	(mm/mm)	(sec)	(MPa)	(mm/mm)	(sec)	(MPa)	(mm/mm)	(sec)
0.00	0.000	0.00	0.00	0.000	0.00	-0.15	-0.059	8.68
0.00	0.000	0.00	0.00	0.000	0.00	-0.16	-0.066	9.58
0.00	0.000	0.00	0.00	0.000	0.00	-0.09	-0.066	9.58
0.00	0.000	0.00	0.00	0.000	0.00	-0.15	-0.078	11.38
0.00	0.000	0.00	0.00	0.000	0.00	-0.15	-0.070	10.18
0.00	0.000	0.00	0.00	0.000	0.00	-0.22	-0.082	11.97
0.00	0.000	0.00	0.00	0.000	0.00	-0.25	-0.082	11.97
0.00	0.000	0.00	0.00	0.000	0.00	-0.30	-0.103	14.97
0.00	0.000	0.00	0.00	0.000	0.00	-0.22	-0.082	11.97
0.00	0.000	0.00	0.00	0.000	0.00	-0.22	-0.095	13.77
0.00	0.000	0.00	0.00	0.000	0.00	-0.25	-0.115	16.77
0.00	0.000	0.00	0.00	0.000	0.00	-0.22	-0.082	11.97
0.00	0.000	0.00	0.00	0.000	0.00	-0.26	-0.103	14.97
0.00	0.000	0.00	0.00	0.000	0.00	-0.11	-0.086	12.57
0.00	0.000	0.00	0.00	0.000	0.00	-0.22	-0.107	15.57
0.00	0.000	0.00	0.00	0.000	0.00	-0.26	-0.107	15.57
0.00	0.000	0.00	0.00	0.000	0.00	-0.19	-0.082	11.97
0.00	0.000	0.00	0.00	0.000	0.00	-0.22	-0.082	11.97
0.00	0.000	0.00	0.00	0.000	0.00	-0.18	-0.066	9.58
0.00	0.000	0.00	0.00	0.000	0.00	-0.11	-0.041	5.98

TABLE A14. STRESS, STRAIN AND TIME AT FAILURE FOR LOADING IN RIGID DIE OF CYINDRICAL APPLE SPECIMENS. $\dot{\epsilon}_{11} = -0.007 \text{ SEC}^{-1}$.

MC INTOSH			JONATHAN			RED DELICIOUS		
σ_{11}	ϵ_{11}	t	σ_{11}	ϵ_{11}	t	σ_{11}	ϵ_{11}	t
(MPa)	(mm/mm)	(sec)	(MPa)	(mm/mm)	(sec)	(MPa)	(mm/mm)	(sec)
-0.24	-0.103	14.97	-0.32	-0.134	19.46	-0.41	-0.111	16.17
-0.36	-0.111	16.17	-0.42	-0.107	15.57	-0.33	-0.086	12.57
-0.28	-0.099	14.37	-0.35	-0.105	15.27	-0.40	-0.092	13.47
-0.25	-0.136	19.76	-0.49	-0.119	17.37	-0.42	-0.111	16.17
-0.32	-0.128	18.56	-0.28	-0.144	20.96	-0.57	-0.103	14.97
-0.30	-0.103	14.97	-0.41	-0.157	22.76	-0.44	-0.099	14.37
-0.36	-0.119	17.37	-0.66	-0.165	23.95	-0.36	-0.086	12.57
-0.34	-0.099	14.37	-0.40	-0.140	20.36	-0.36	-0.115	16.77
-0.37	-0.119	17.37	-0.27	-0.103	14.97	-0.34	-0.101	14.67
-0.36	-0.115	16.77	-0.49	-0.144	20.96	-0.23	-0.113	16.47
-0.43	-0.107	15.57	-0.26	-0.103	14.97	-0.42	-0.107	15.57
-0.50	-0.144	20.96	-0.30	-0.095	13.77	-0.44	-0.119	17.37
-0.32	-0.111	16.17	-0.50	-0.148	21.56	-0.53	-0.128	18.56
-0.37	-0.115	16.77	-0.31	-0.099	14.37	-0.45	-0.117	17.07
-0.37	-0.111	16.17	-0.28	-0.099	14.37	-0.57	-0.103	14.97
-0.47	-0.140	20.36	-0.34	-0.107	15.57	-0.47	-0.111	16.17
-0.40	-0.119	17.37	-0.37	-0.095	13.77	-0.55	-0.109	15.87
-0.36	-0.123	17.96	-0.34	-0.099	14.37	-0.49	-0.128	18.56
-0.40	-0.111	16.17	-0.32	-0.115	16.77	-0.56	-0.111	16.17
-0.34	-0.111	16.17	-0.29	-0.123	17.96	-0.44	-0.103	14.97

TABLE A15. STRESS, STRAIN AND TIME AT FAILURE FOR UNIAXIAL LOADING OF CUBIC APPLE SPECIMENS. $\dot{\epsilon}_{11} = -0.007 \text{ SEC}^{-1}$.

MC INTOSH			JONATHAN			RED DELICIOUS		
σ_{11} (MPa)	ϵ_{11} (mm/mm)	t (sec)	σ_{11} (MPa)	ϵ_{11} (mm/mm)	t (sec)	σ_{11} (MPa)	ϵ_{11} (mm/mm)	t (sec)
-0.27	-0.115	16.77	-0.29	-0.113	16.47	-0.27	-0.123	17.96
-0.26	-0.123	17.96	-0.24	-0.099	14.37	-0.27	-0.123	17.96
-0.27	-0.123	17.96	-0.24	-0.115	16.77	-0.25	-0.111	16.17
-0.25	-0.121	17.67	-0.24	-0.092	13.47	-0.22	-0.097	14.07
-0.26	-0.115	16.77	-0.25	-0.082	11.97	-0.26	-0.070	10.18
-0.25	-0.123	17.96	-0.26	-0.123	17.96	-0.25	-0.099	14.37
-0.25	-0.090	13.17	-0.30	-0.095	13.77	-0.25	-0.128	18.56
-0.25	-0.121	17.67	-0.26	-0.107	15.57	-0.25	-0.107	15.57
-0.25	-0.111	16.17	-0.28	-0.090	13.17	-0.29	-0.111	16.17
-0.23	-0.115	16.77	-0.33	-0.111	16.17	-0.26	-0.109	15.87
-0.26	-0.111	16.17	-0.26	-0.119	17.37	-0.24	-0.128	18.56
-0.30	-0.136	19.76	-0.26	-0.119	17.37	-0.27	-0.111	16.17
-0.29	-0.123	17.96	-0.26	-0.123	17.96	-0.27	-0.119	17.37
-0.30	-0.136	19.76	-0.25	-0.082	11.97	-0.23	-0.119	17.37
-0.26	-0.144	20.96	-0.23	-0.097	14.07	-0.26	-0.123	17.96
-0.26	-0.134	19.46	-0.23	-0.132	19.16	-0.25	-0.103	14.97
-0.29	-0.144	20.96	-0.25	-0.090	13.17	-0.21	-0.132	19.16
-0.29	-0.103	14.97	-0.28	-0.086	12.57	-0.19	-0.074	10.78
-0.25	-0.128	18.56	-0.29	-0.095	13.77	-0.23	-0.095	13.77
-0.26	-0.132	19.16	-0.28	-0.115	15.77	-0.26	-0.103	14.97

TABLE A16. STRESS, STRAIN AND TIME AT FAILURE FOR BIAxIAL LOADING OF CUBIC APPLE SPECIMENS. $\dot{\epsilon}_{11} = -0.007 \text{ SEC}^{-1}$.

MC INTOSH			JONATHAN			RED DELICIOUS		
σ_{11} (MPa)	ϵ_{11} (mm/mm)	t (sec)	σ_{11} (MPa)	ϵ_{11} (mm/mm)	t (sec)	σ_{11} (MPa)	ϵ_{11} (mm/mm)	t (sec)
-0.24	-0.128	18.56	-0.33	-0.144	20.96	-0.40	-0.136	19.76
-0.29	-0.123	17.96	-0.37	-0.126	18.26	-0.36	-0.132	19.16
-0.25	-0.117	17.07	-0.37	-0.132	19.16	-0.36	-0.119	17.37
-0.22	-0.107	15.57	-0.31	-0.123	17.96	-0.43	-0.119	17.37
-0.30	-0.119	17.37	-0.34	-0.140	20.36	-0.36	-0.107	15.57
-0.25	-0.099	14.37	-0.30	-0.123	17.96	-0.39	-0.111	16.17
-0.28	-0.103	14.97	-0.34	-0.119	17.37	-0.33	-0.123	17.96
-0.23	-0.115	16.77	-0.37	-0.144	20.96	-0.43	-0.119	17.37
-0.28	-0.103	14.97	-0.34	-0.119	17.37	-0.43	-0.119	17.37
-0.29	-0.140	20.36	-0.44	-0.152	22.16	-0.40	-0.128	18.56
-0.29	-0.136	19.76	-0.31	-0.140	20.36	-0.40	-0.119	17.37
-0.27	-0.111	16.17	-0.42	-0.144	20.96	-0.33	-0.115	16.77
-0.26	-0.119	17.37	-0.42	-0.161	23.36	-0.33	-0.095	13.77
-0.34	-0.115	16.77	-0.33	-0.103	14.97	-0.41	-0.123	17.96
-0.26	-0.090	13.17	-0.29	-0.111	16.17	-0.34	-0.136	19.76
-0.24	-0.115	16.77	-0.26	-0.111	16.17	-0.38	-0.111	16.17
-0.23	-0.115	16.77	-0.29	-0.107	15.57	-0.49	-0.128	18.56
-0.23	-0.115	16.77	-0.30	-0.123	17.96	-0.36	-0.111	16.17
-0.26	-0.123	17.96	-0.34	-0.132	19.16	-0.34	-0.132	19.16
-0.23	-0.103	14.97	-0.31	-0.113	16.47	-0.41	-0.152	22.16

TABLE A17. STRESS, STRAIN AND TIME AT FAILURE FOR LOADING IN RIGID DIE OF CUBIC APPLE SPECIMENS. $\dot{\epsilon}_{11} = -0.007 \text{ SEC}^{-1}$.

MC INTOSH			JONATHAN			RED DELICIOUS		
σ_{11} (MPa)	ϵ_{11} (mm/mm)	t (sec)	σ_{11} (MPa)	ϵ_{11} (mm/mm)	t (sec)	σ_{11} (MPa)	ϵ_{11} (mm/mm)	t (sec)
-0.26	-0.097	14.07	-0.37	-0.123	17.96	-0.46	-0.095	13.77
-0.29	-0.111	16.17	-0.47	-0.185	26.95	-0.50	-0.103	14.97
-0.29	-0.103	14.97	-0.29	-0.115	16.77	-0.50	-0.119	17.37
-0.26	-0.111	16.17	-0.58	-0.165	23.95	-0.51	-0.115	16.77
-0.27	-0.099	14.37	-0.54	-0.165	23.95	-0.52	-0.148	21.56
-0.36	-0.115	16.77	-0.38	-0.115	16.77	-0.53	-0.128	18.56
-0.34	-0.140	20.36	-0.34	-0.144	20.96	-0.63	-0.123	17.96
-0.29	-0.107	15.57	-0.34	-0.281	40.73	-0.52	-0.103	14.97
-0.34	-0.115	16.77	-0.37	-0.169	24.55	-0.54	-0.107	13.57
-0.23	-0.119	17.37	-0.34	-0.115	16.77	-0.63	-0.128	18.56
-0.34	-0.119	17.37	-0.34	-0.115	16.77	-0.63	-0.128	18.56
-0.30	-0.107	15.57	-0.43	-0.144	20.96	-0.52	-0.103	14.97
-0.33	-0.123	17.96	-0.46	-0.165	23.95	-0.58	-0.128	18.56
-0.38	-0.119	17.37	-0.34	-0.123	17.96	-0.45	-0.152	22.16
-0.39	-0.140	20.36	-0.36	-0.132	19.16	-0.50	-0.132	19.16
-0.55	-0.161	23.36	-0.29	-0.111	16.17	-0.53	-0.128	18.56
-0.31	-0.115	16.77	-0.38	-0.115	16.77	-0.53	-0.128	18.56
-0.49	-0.144	20.96	-0.34	-0.123	17.96	-0.55	-0.111	16.17
-0.49	-0.165	23.95	-0.34	-0.111	16.17	-0.50	-0.136	19.76
-0.33	-0.132	19.16	-0.31	-0.082	11.97	-0.45	-0.136	19.76

TABLE A18. UNIAXIAL COMPRESSION OF CYLINDRICAL SPECIMENS OF MC INTOSH. AXIAL DEFORMATION VALUES AT $\sigma_{11} = -0.11 \text{ MPa}$ FOR FIVE SPECIMEN HEIGHT. $\dot{\epsilon}_{11} = -0.007 \text{ SEC}^{-1}$

8.32		12.13		19.17		26.55		34.98	
0.06*		0.12*		0.13*		0.16*		0.11*	
U1		U1		U1		U1		U1	
(mm)		(mm)		(mm)		(mm)		(mm)	
- 6.60	-10.16	-13.71	-13.71	-15.74					
- 7.62	- 8.12	-14.22	-16.76	-17.27					
- 8.12	- 8.12	-11.68	-14.22	-18.79					
-11.68	- 7.62	-12.70	-12.19	-19.81					
- 8.63	- 8.63	-15.74	-18.28	-24.89					
- 9.65	-11.17	-11.17	-19.30	-20.32					
- 8.12	-10.92	-12.70	-18.28	-18.28					
- 9.65	- 9.65	-18.79	-22.86	-19.30					
- 7.62	-13.20	-13.71	-16.76	-20.82					
- 9.65	-12.70	-11.17	-15.24	-26.92					
- 6.60	-14.22	-13.20	-17.27	-21.84					
- 7.11	-10.66	-13.20	-13.71	-19.81					
-10.16	- 9.14	-12.44	-14.22	-20.82					
- 8.12	-11.68	-12.70	-14.22	-21.32					
- 6.60	-14.22	-13.20	-13.71	-21.33					
- 8.63	- 7.62	-11.17	-17.78	-21.84					
- 5.58	-12.19	-15.74	-16.25	-20.32					
- 9.65	-10.16	-20.32	-15.24	-22.35					
- 7.11	-13.20	-15.24	-16.76	-22.35					
- 7.62	-11.68	-13.71	-16.76	-20.32					

(*) standard deviation

TABLE A19. UNIAXIAL COMPRESSION OF CYLINDRICAL SPECIMENS OF JONATHAN. AXIAL DEFORMATION VALUES AT $\sigma_{11} = -0.11 \text{ MPa}$ FOR FIVE SPECIMEN HEIGHT. $\dot{\epsilon}_{11} = -0.007 \text{ SEC}^{-1}$

8.32		12.13		19.17		26.55		34.98	
0.06*		0.12*		0.13*		0.16*		0.11*	
U1 (mm)		U1 (mm)		U1 (mm)		U1 (mm)		U1 (mm)	
- 9.90	- 7.11	- 8.12	- 15.49	- 13.20	- 21.84	- 7.11	- 8.89	- 15.49	- 13.20
- 7.11	- 8.89	- 15.49	- 13.20	- 21.84	- 7.11	- 12.19	- 13.71	- 16.76	- 7.62
- 12.19	- 12.19	- 7.11	- 12.19	- 17.27	- 7.62	- 13.20	- 9.65	- 14.22	- 17.27
- 7.62	- 7.11	- 12.19	- 12.19	- 17.27	- 13.20	- 13.20	- 8.63	- 14.22	- 20.32
- 13.20	- 9.65	- 14.22	- 9.65	- 14.22	- 8.63	- 13.71	- 13.71	- 12.70	- 14.22
- 13.20	- 8.63	- 12.70	- 12.70	- 13.20	- 7.62	- 10.16	- 10.16	- 12.70	- 19.30
- 8.63	- 13.71	- 12.70	- 12.70	- 14.73	- 7.62	- 9.14	- 9.14	- 11.17	- 23.87
- 7.62	- 10.16	- 12.70	- 12.70	- 14.73	- 7.11	- 9.14	- 9.14	- 10.92	- 20.82
- 7.11	- 9.14	- 11.17	- 10.92	- 12.19	- 5.58	- 8.63	- 13.20	- 11.68	- 17.27
- 5.58	- 9.14	- 10.92	- 13.20	- 11.68	- 5.58	- 7.11	- 13.20	- 15.24	- 21.84
- 5.58	- 8.63	- 13.20	- 13.20	- 15.24	- 9.65	- 7.11	- 14.73	- 12.70	- 17.52
- 9.65	- 7.11	- 13.20	- 14.73	- 12.70	- 7.11	- 7.11	- 11.17	- 12.19	- 18.79
- 7.11	- 7.11	- 14.73	- 11.17	- 12.19	- 6.60	- 8.12	- 9.65	- 16.25	- 17.27
- 6.60	- 8.12	- 11.17	- 9.65	- 16.25	- 8.12	- 8.12	- 10.66	- 13.71	- 19.30
- 8.12	- 8.12	- 9.65	- 16.25	- 13.71	- 7.11	- 8.63	- 12.70	- 12.70	- 15.74
- 7.11	- 8.63	- 10.66	- 13.71	- 12.70	- 8.12	- 10.16	- 10.16	- 17.27	- 15.24
- 8.12	- 10.16	- 12.70	- 12.70	- 17.27	- 6.60	- 6.60	- 10.16	- 13.71	- 15.24
- 6.60	- 6.60	- 10.16	- 17.27	- 13.71	- 8.63	- 10.16	- 12.19	- 13.71	- 15.24
- 8.63	- 10.16	- 12.19	- 13.71	- 15.24	- 6.60	- 12.19	- 11.17	- 13.74	- 21.84
- 6.60	- 12.19	- 11.17	- 13.74	- 21.84					

(*) standard deviation

TABLE A20. UNIAXIAL COMPRESSION OF CYLINDRICAL SPECIMENS OF RED DELICIOUS. AXIAL DEFORMATION VALUES AT $\sigma_{11} = -0.11 \text{ MPa}$ FOR FIVE SPECIMEN HEIGHT. $\dot{\epsilon}_{11} = -0.007 \text{ SEC}^{-1}$.

8.32		12.13		19.17		26.55		34.98	
0.06*		0.12*		0.13*		0.16*		0.11*	
U1		U1		U1		U1		U1	
(mm)		(mm)		(mm)		(mm)		(mm)	
- 7.11	- 5.84	- 7.11	- 5.84	- 7.11	- 5.84	- 12.70	- 5.84	- 15.24	- 5.84
- 5.58	- 5.58	- 10.16	- 5.58	- 10.16	- 5.58	- 9.14	- 5.58	- 13.71	- 5.58
- 5.08	- 5.08	- 7.11	- 5.08	- 7.11	- 5.08	- 10.66	- 5.08	- 12.19	- 5.08
- 6.09	- 3.55	- 7.11	- 3.55	- 7.11	- 3.55	- 12.19	- 3.55	- 14.73	- 3.55
- 10.66	- 7.62	- 7.11	- 7.62	- 7.11	- 7.62	- 10.66	- 7.62	- 14.73	- 7.62
- 5.58	- 7.62	- 8.63	- 7.62	- 8.63	- 7.62	- 11.17	- 7.62	- 11.68	- 7.62
- 5.58	- 4.06	- 8.12	- 4.06	- 8.12	- 4.06	- 11.17	- 4.06	- 12.19	- 4.06
- 6.09	- 4.57	- 8.12	- 4.57	- 8.12	- 4.57	- 10.16	- 4.57	- 13.71	- 4.57
- 5.08	- 8.12	- 9.14	- 8.12	- 9.14	- 8.12	- 8.63	- 8.12	- 12.70	- 8.12
- 5.08	- 4.06	- 6.09	- 4.06	- 6.09	- 4.06	- 9.65	- 4.06	- 12.19	- 4.06
- 5.58	- 5.08	- 8.63	- 5.08	- 8.63	- 5.08	- 12.19	- 5.08	- 14.22	- 5.08
- 4.06	- 4.57	- 13.20	- 4.57	- 13.20	- 4.57	- 12.19	- 4.57	- 13.20	- 4.57
- 8.12	- 8.12	- 9.65	- 8.12	- 9.65	- 8.12	- 10.16	- 8.12	- 13.71	- 8.12
- 5.58	- 7.62	- 9.14	- 7.62	- 9.14	- 7.62	- 12.70	- 7.62	- 17.78	- 7.62
- 5.08	- 6.60	- 9.65	- 6.60	- 9.65	- 6.60	- 10.16	- 6.60	- 13.20	- 6.60
- 8.12	- 4.57	- 7.62	- 8.12	- 7.62	- 8.12	- 8.63	- 7.62	- 11.17	- 8.12
- 4.57	- 5.08	- 5.58	- 4.57	- 5.58	- 4.57	- 9.14	- 4.57	- 13.71	- 4.57
- 4.06	- 6.60	- 12.19	- 6.60	- 12.19	- 6.60	- 9.14	- 6.60	- 12.70	- 6.60
- 5.08	- 10.66	- 12.19	- 5.08	- 12.19	- 5.08	- 9.14	- 5.08	- 12.19	- 5.08
- 5.08	- 6.35	- 8.63	- 5.08	- 8.63	- 5.08	- 9.14	- 5.08	- 13.20	- 5.08

(*) standard deviation

MICHIGAN STATE UNIVERSITY LIBRARIES



3 1293 03056 2965